SANDIA REPORT

SAND2019-0499

Unlimited Release
Printed January 2019

Evaluation of Multi-Inverter Anti-Islanding with Grid Support and Ride-Through and Investigation of Island Detection Alternatives

Michael Ropp, Scott Perlenfein, Dustin Schutz, Chris Mouw, Jason C. Neely, Sigifredo Gonzalez, Lee Rashkin

Prepared by
Sandia National Laboratories
Albuquerque, New Mexico 87185 and Livermore, California 94550

Sandia National Laboratories is a multimission laboratory managed and operated by National Technology & Engineering Solutions of Sandia, LLC, a wholly owned subsidiary of Honeywell International, Inc., for the U.S. Department of Energy's National Nuclear Security Administration under contract DE-NA0003525

Issued by Sandia National Laboratories, operated for the United States Department of Energy by Sandia Corporation.

Available to DOE and DOE contractors from
U.S. Department of Energy
Office of Scientific and Technical Information
P.O. Box 62
Oak Ridge, TN 37831

Telephone: (865) 576-8401
Facsimile: (865) 576-5728
E-Mail: reports@adonis.osti.gov
Online ordering: http://www.osti.gov/bridge

Available to the public from
U.S. Department of Commerce
National Technical Information Service
5285 Port Royal Rd.
Springfield, VA 22161

Telephone: (800) 553-6847
Facsimile: (703) 605-6900
E-Mail: orders@ntis.fedworld.gov
Online order: http://www.ntis.gov/help/ordermethods.asp?loc=7-4-0#online

SAND2018-xxxxx
Printed December 2018

Evaluation of Multi-Inverter Anti-Islanding with Grid Support and Ride-Through and Investigation of Island Detection Alternatives

Michael Ropp, Scott Perlenfein, Dustin Schutz, Chris Mouw
Northern Plains Power Technologies
807 32nd Avenue
Brookings, SD 57006-4716

Jason C. Neely, Lee J. Rashkin
Electrical Sciences and Experiments

Sigifredo Gonzalez
Photovoltaic and Distributed Systems Integration

Sandia National Laboratories
P.O. Box 5800
Albuquerque, New Mexico 87185-MS1033

Abstract

As utility interconnected photovoltaic systems (PV) become integrated into the electrical power system (EPS) at an increasing rate, utilities and regulators have become concerned about the potential for increased voltage and frequency deviations as well as EPS reliability and resiliency. These concerns have initiated the need to amend the utility interconnection standard to allow advanced inverter control functionalities that provide: (1) reactive power control for voltage support, (2) real (active) power control for frequency support and (3) voltage and frequency ride-through for bulk system support. The new real and reactive power modulation are intended to reduce EPS voltage and frequency deviations by mimicking the droop and excitation controls of conventional generation. The new ride-through capabilities are needed to prevent a large quantity of generation from autonomously de-energizing or disconnecting in response to a voltage or frequency deviation. These changes, however, may have the potential to interfere with autonomous anti-islanding, especially when multiple inverters from different vendors are co-located on one bus. This report presents results from an investigation of multi-inverter autonomous anti-islanding with advanced functions, and the development of a means to mitigate adverse interaction between the two.

ACKNOWLEDGMENTS

Sandia National Laboratories acknowledges the support of the U.S. Department of Energy Solar Energy Program that sponsored this work. The authors express gratitude to the following persons for their valuable support, discussions, guidance and technical input.

Jay Johnson, Department 6112

Robert Broderick, Department 6112

Abraham Ellis, Manager Department 6112

Charles Hanley, Senior Manager 6100

Steven Glover, Manager Department 1353

CONTENTS

FIGURES

TABLES

NOMENCLATURE

AC	Alternating Current
AI	Anti-Islanding
CC	Collaborative Controls
dB	decibel
DC	Direct Current
DER	Distributed Energy Resource
DETL	Distributed Energy Technology Laboratory
DOE	Department of Energy
DUT	Device Under Test
EPS	Electrical Power System
FRT	Frequency Ride Through
GSF	Grid Support Function
MPPT	Maximum Power Point Tracking
NDZ	Non-Detection Zone
NPPT	Northern Plains Power Technologies
O/UF	Over/Under Frequency
O/UV	Over/Under Voltage
PCC	Point of Common Coupling
PLL	Phase-Locked Loop
PV	Photovoltaic or Photovoltaics
RLC load	A load containing a resistor, an inductor and a capacitor
RoCoF	Rate of Change of Frequency (i.e., df/dt)
ROT	Run-On Time
RT	Ride Through
SPOV	Self-Protection Over Voltage
SFS	Sandia Frequency Shift
SNL	Sandia National Laboratories
var	Volt-Ampere reactive[a]
VRT	Voltage Ride Through

[a] The spelling of "var" officially sanctioned by the IEEE is all lower-case.

W	Watt

1. INTRODUCTION

In this chapter essential background is provided as well as information on the structure of the project, layout of this report, and outcomes of the research.

1.1. Background

1.1.1. The Emerging Role of PV

Historically, PV power plants were relatively small, and their numbers on utility circuits were low enough that any impacts of PV plants tended to be lost in the variability of the load. For this reason, and because most of these plants were connected to distribution circuits, utilities tended to regard PV basically as a negative load. The only special requirements were that PV not support an island for longer than 2 sec, that the quality of power being delivered be in compliance with the requirements in standards such as IEEE 1547 and IEEE 519, and that the PV source stop delivering power if the voltage or frequency deviated outside of narrowly-defined windows.

Today, this situation is rapidly changing. PV plants as large as 5 MW are widespread on distribution feeders, larger plants are appearing on sub-transmission systems, and some regions have seen enough PV deployed on feeders that at times portions of the distribution system are sourcing power back to the transmission system. The "negative load" treatment is clearly not appropriate in this case. In fact, as more distributed renewable generation is incorporated into the grid, well-regulated conventional generation will be displaced by stochastic energy sources, and this situation could contribute to voltage and frequency regulation difficulties [1]-[3]. In response, IEEE 1547-2018 [4] now requires that PV plants have the capability to act more like generation assets, meaning that they can, when required by the system operator, participate in voltage and frequency regulation, grid stability maintenance, and other protective and security protocols. To that end, inverter manufacturers have been incorporating functions collectively known as "grid support functions," "advanced inverter functions," or "smart inverter functions." The term "grid support functions" (GSFs) will be used here as it is less generic than the others. GSFs will allow PV to play a more active role in the grid and thus increase the value of PV, but there is also a concern that GSFs could impede the ability of distribution-connected inverters to detect and prevent unintentional islanding. This concern arises because most active anti-islanding functions rely on exacerbating abnormal grid conditions, whereas GSFs are designed to reduce the impact of abnormal grid conditions. For example, if a low frequency is detected, it is difficult for the inverter to determine whether the low frequency indicates a system-level condition that should be ridden through, or a local condition that indicates an island and necessitates a shutdown. The purpose of this study is to investigate and quantify the potential impact of GSFs on islanding detection, and to explore a potential means for mitigating the interaction between the two.

1.1.2. Grid Support Functions

There are two primary GSFs that are studied in this work: volt-var and frequency-watt [1], [2], [5].

1.1.2.1. Volt-var

The main parameters for the volt-var control that can be set are the four voltages V_1, V_2, V_3 and V_4 and corresponding four reactive power quantities Q_1, Q_2, Q_3 and Q_4. A plot of the volt-var characteristic used to control the inverter's reactive power is shown in Figure 1 for the expected operating condition $Q_2 = Q_3 = 0$ and $Q_{max} = Q_1 = -Q_4$. IEC standard 61850-90-7 [5] defines "VV11" as volt-var control in watt priority mode, and "VV12" is volt-var control in var priority mode. If the inverter is in watt-priority mode, Q_{max} and depending on the irradiance conditions, Q_{max} may not be constant ($Q_{max} < Q_1$) because it may be limited by the capability of the inverter. In other words, in watt priority mode, $Q_{\max}$ would be whatever capability the inverter has "left over" after the real power has been taken into account, and is given by:

$$Q_{\max}(t_k) = \sqrt{S_{rated}^2 - (P(t_k))^2} \tag{1}$$

where S_{rated} is the inverter's rated apparent power capability and $P(t_k)$ is the real power being produced at the k^{th} discrete time interval.

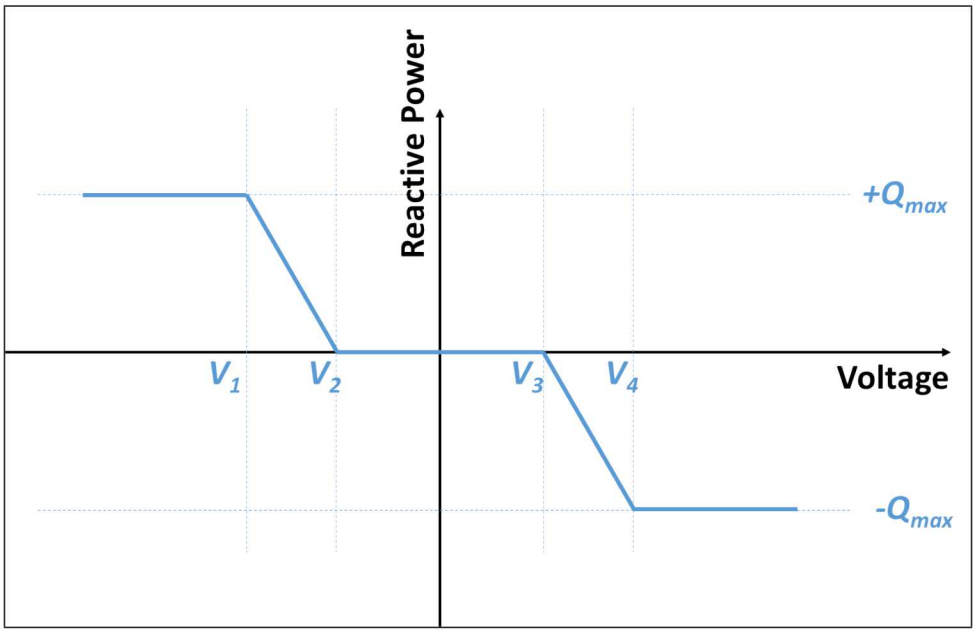

Figure 1. Plot of the volt-var characteristic used in this work

1.1.2.2. Frequency-watt

A plot of the frequency-watt characteristic used to control the inverter's output power is shown in Figure 2. This is a general characteristic that covers both upward and downward frequency support. Upward frequency support requires the inverter to source additional power in response to a sagging grid frequency, which requires either that the PV plant be operated below its maximum power point (i.e., the plant is pre-curtailed), or that the plant include energy storage.

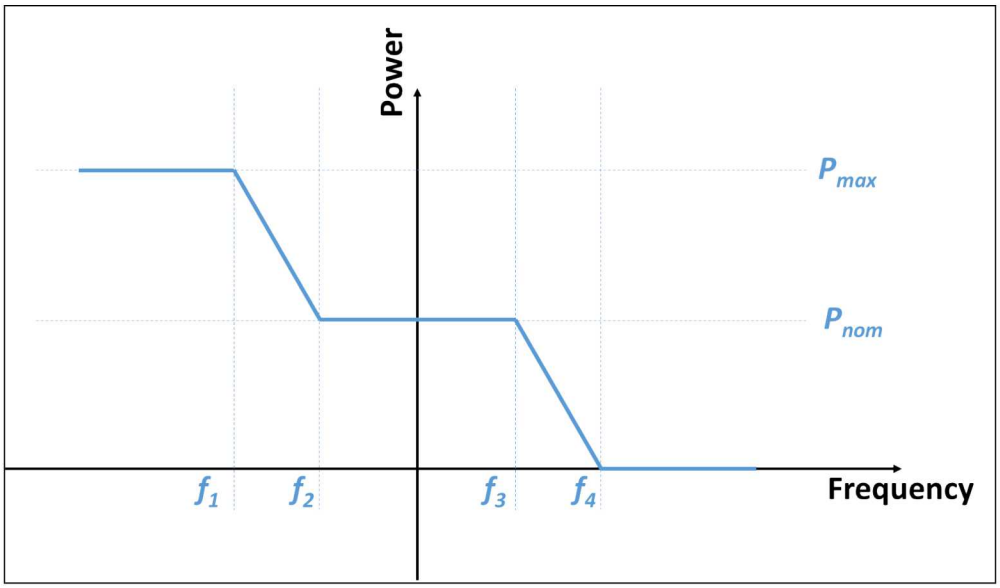

Figure 2. Plot of the frequency-watt characteristic used in this work

1.1.3. The IEEE 1547.1 Anti-Islanding Test

Most modern PV inverters are designed to pass the IEEE 1547.1 anti-islanding test and are certified as being able to pass that test under Underwriters' Laboratories UL-1741. This test is a single-inverter test using a resonant resistive, inductive, and capacitive (RLC) load with a quality factor of 1.0, and the standard requires that under these circumstances the inverter be able to detect and cease to energize an unintentional island within 2 sec [4]. The test includes the matched-load case in which generation matches load power at rated voltage, and in this case the magnitude and frequency of the voltage measured at the point of common coupling do not change when disconnected from the utility.

However, in the real world, many deviations from the conditions of this anti-islanding test are encountered. One increasingly common deviation is that islands in the field would rarely contain only a single inverter. Most PV installations will contain more than one inverter (in fact, for AC arrays or plants using string inverters, there may be hundreds of inverters), and a distribution feeder with a high penetration of PV may be hosting many inverters from several different manufacturers. That last variable is of particular concern, because in the United States the means by which manufacturers detect and prevent unintentional islands are not standardized; manufacturers typically use proprietary means of passing the IEEE 1547.1 test. Note that IEEE 1547 requires that a distributed generator detect and cease to energize an island within 2 sec under all circumstances, regardless of the number of distributed generators or the loading conditions. If several manufacturers' products are contained within an island, these proprietary means of safely de-energizing the island could in some cases be incompatible with each other, and the time to de-energize, also known as the "clearing time" or "run-on time" (ROT), may be longer for some combinations of distributed energy resources (DERs) than others.

1.1.4. Categorization and description of anti-islanding methods

For this work, anti-islanding methods used in inverters were separated into eight groups, defined as follows.

- AI Group 1: Inverters in this group use an output perturbation in positive-sequence fundamental frequency or phase that is specifically for the purpose of island detection, and that grows continuously in magnitude as frequency error increases in a direction that increases the frequency error (i.e., positive feedback on frequency error), up to the frequency trip limits, and includes no dead zone. In other words, Group 1 inverters use positive feedback on frequency or phase to create instability when the island forms. The output perturbation may be pulsed or continuous, but the key is the positive feedback; the magnitude of the perturbation must continuously increase with increasing frequency error as long as the inverter is within the frequency trip bands.
- AI Group 2A: These inverters are similar to Group 1 in that the inverter produces a pulsed or non-pulsed output perturbation in positive-sequence fundamental frequency or phase that is specifically for island detection and grows with frequency in a direction that increases the frequency error (i.e., positive feedback on frequency error), but not continuously to the trip bands. Inverters in Group 2A may have a stepped or otherwise discontinuous function of frequency, or a saturation limit that is reached prior to the frequency trip thresholds. However, because the impact of a dead zone (a hysteresis band centered around 60 Hz in which the anti-islanding perturbation is not produced) is a special case, *inverters with a dead zone centered on the nominal frequency are specifically excluded from Group 2A*.
- AI Group 2B: This group has any or all of the properties of Group 2A, but with a dead zone centered around 60 Hz in which the active anti-islanding does not act.
- AI Group 2C: This group has any or all of the properties of either Group 1 or Group 2A, except that the positive feedback on frequency error is *unidirectional*; that is, the positive feedback is in the same direction regardless of the algebraic sign of the frequency error.
- AI Group 3: This group produces an output perturbation in positive-sequence fundamental frequency or phase, the magnitude of which does NOT grow with increasing frequency error or is NOT specifically designed for island detection.
- AI Group 4: Inverters in this group produce an output perturbation at a harmonic (not fundamental) frequency that is specifically for detecting an island. Typically, these are independent of frequency error, but they do not have to be.
- AI Group 5: Inverters in this group rely on passive methods only (such as Rate of Change of Frequency [RoCoF] or vector shift) or advanced signal processing of voltage or current measurements to detect island formation. (A method that actively drives the voltage or frequency of an island to the respective trip limits and then relies on the passive trip does not fall into Group 5.)

- AI Group 6: Inverters in this group manipulate the negative sequence current for the purpose of island detection, and typically apply positive feedback to that negative-sequence perturbation. This may be achieved by several means, including altering individual phase current magnitudes or dithering the phase angle separation between the three output current phases.

The work reported here focuses on inverters representing Groups 2A and 3, and in part of the work, Group 6 is also represented. These inverters were selected primarily because they were the units available at the time this work was done, and partly because Groups 2A and 3 represent two of the most commonly-used techniques in industry.

1.2. R&D Approach

The work reported here consists of two main parts. Part I was a simulation study of the impact of GSFs on islanding detection. The inverter used in Part I, called "Inverter A," is a single-phase, 3 kW device using Group 3, and optionally Group 6, islanding detection. In Part I of this work, only Group 3 was used. Inverter A was tested in a three-phase system by using three units connected in delta. The three inverters are independently controlled. The GSFs studied were volt-var with watt priority (VV11), and frequency-watt (FW21). The settings used for these curves are given in Table 1.

Table 1. Volt-var and frequency-watt settings.

Point		Voltage	var
Volt-Var	V1	0.8 pu	+100% var
	V1	0.9 pu	0% var
	V3	1.1 pu	0% var
	V4	1.2 pu	-100% var
Point		**Frequency**	**Watt**
Freq-Watt	f1	60.5 Hz	+100% Watt
	f2	n/a	n/a
	f3	n/a	n/a
	f4	62 Hz	0% Watt

Part II was a simulation study of the impact of GSFs and ride-throughs (RTs) on islanding detection effectiveness when the distributed generation consisted of two types of inverters: the three units of Inverter A connected in delta with both Group 3 and 6 elements active, and one unit of "Inverter B," which is a 50 kW, three-phase inverter using a Group 2A islanding detection method. Part II thus examines a mixture of Groups 2A and 3, but the Group 2A inverter is dominant because of its much larger size.

For both Inverter A and Inverter B, Sandia National Laboratories and Northern Plains Power Technologies (NPPT) collaborated closely with the inverter manufacturers to develop highly detailed and well-validated models of the inverters. The models were validated against both

manufacturer data and expectations, and against test results obtained with these inverters in Sandia's Distributed Energy Technology Laboratory (DETL).

In both parts of the work, the first step was to run batches of simulations with no GSFs active, to establish a baseline. In these baseline simulations, the load real and reactive power were swept over fairly wide ranges. For each individual loading condition, the run-on time (ROT) was recorded. Then for each batch, the maximum ROT observed over that batch and the overall size and shape of any regions of elevated ROTs, including any observed nondetection zone (NDZ), was recorded. This entire process was then repeated with the GSFs active, to determine the impact of activating GSFs on the ROTs or NDZ. Comparison batches without GSFs were obtained at three different irradiance levels (33%, 66%, and 100%). In Part II, simulations were also run with two different sets of relay settings: IEEE 1547-2003 defaults, and IEEE 1547A settings.

An additional variable was explored in Part II: simulations were run with and without a mitigation measure known as Collaborative Controls (CC). The CC takes advantage of the fact that islanding detection must act rather quickly, but in most cases GSFs respond much more slowly. A filter is used to separate the fast (high-frequency) response of islanding detection from the slower (lower-frequency) response of the GSFs, to remove the interference between these functions. The CC filter is described in more detail in [6]-[8], and the reader is referred to those publications for more details on the implementation and laboratory testing of the CC. The objective of this portion of the study was to determine whether the use of the CC could restore islanding detection performance in cases in which such performance was adversely impacted by the addition of the GSFs.

3. PART I: IMPACT OF GRID SUPPORT FUNCTIONS ON IMPEDANCE-DETECTION BASED (GROUP 3) ANTI-ISLANDING

3.1. Introduction

In Part I of this work, the validated model of Inverter A was used in a simulation study to quantify the impact of grid support functions on islanding detection effectiveness. Inverter A uses an anti-islanding method that falls within the general family of impedance detection-based methods without positive feedback, and thus falls within Group 3. The primary intent of this work was to examine the impact on Group 3 islanding detection of the addition volt-var (VV11) and frequency-watt (FW21) GSFs.

3.2. Procedure

Simulations were run in a three-phase testbed using constant-impedance loads connected in grounded-Y. Inverter A is a 3 kW single-phase device, so three units were used. They were connected in delta in Part I, and were interfaced to the testbed feeder through a YG:yg distribution transformer. The inverters use Group 3 anti-islanding. Simulation batches were run without any of the GSFs to establish an anti-islanding baseline, and then with GSFs enabled, to see what impact adding them would have. For each simulation, the load power and the island VAr balance (P and Q mismatch within the island) were swept over ranges, and the run-on times (ROTs) at each load P vs. ΔQ pair were recorded and plotted. Simulations were run at three irradiance levels: 0.33 kW/m^2, 0.66 kW/m^2, and 1 kW/m^2. The irradiance was the same for all three inverters' arrays.

The length of these simulations is such that the longest ROT that can be detected is 5 sec. This was chosen because the nature of this system is such that if detection does not occur within that time, it is because the system has reached a sufficiently stable state that it will probably never detect. Thus, in the results that follow, a 5 sec ROT may be regarded as an indefinite ROT.

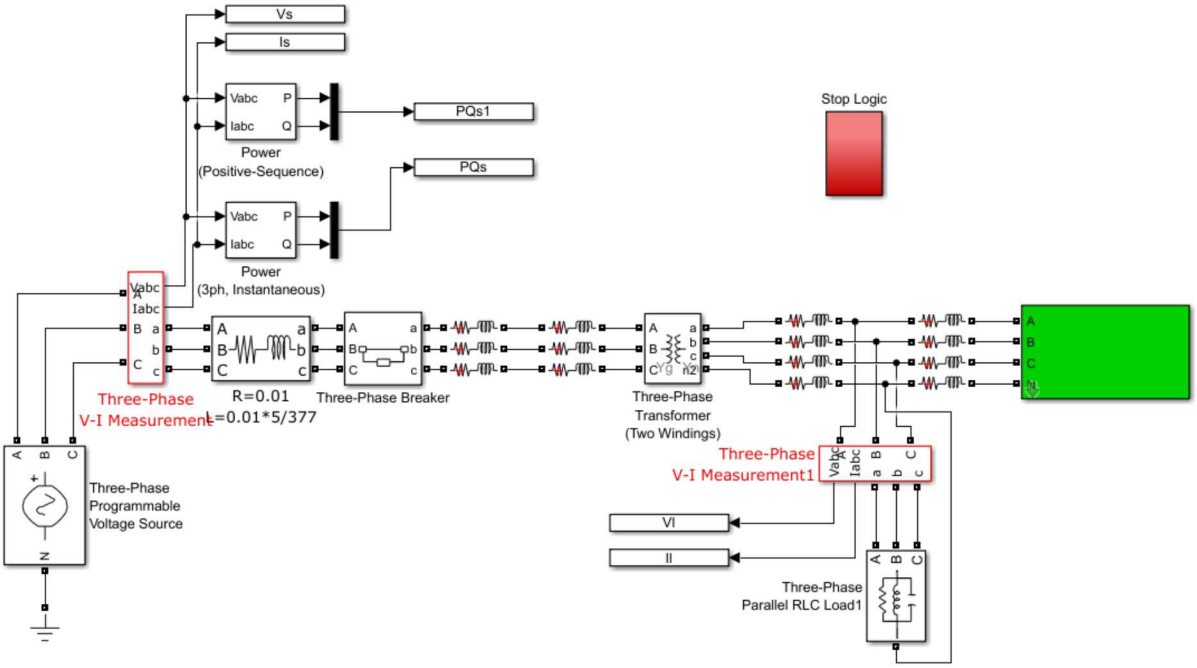

Figure 3. Testbed setup for islanding three units of Inverter A in delta. Line impedances are included on the 12.47 kV and 480 V sides of the YG:yg GSU transformer. The load is connected in wye.

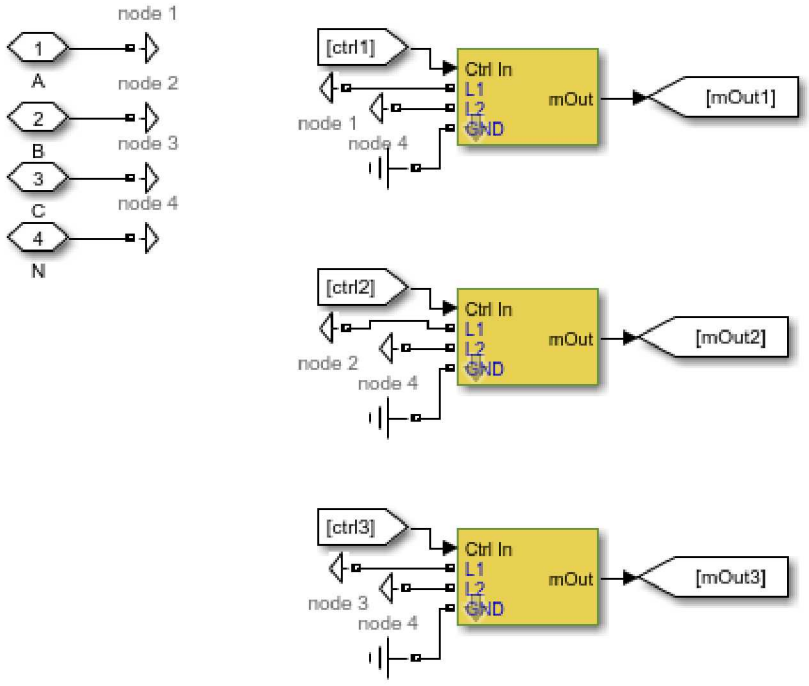

Figure 4. Contents of the green inverter block in Figure 3. The three units of Inverter A are isolated by a 480V:480V Yg-Yg tx and connected line to ground (wye)

3.3. Results

3.3.1. Thirty-three Percent Irradiance

Figure 5 shows two surface plots of the ROT versus watt and var mismatch, for the case of 33% irradiance. In each, the ROT is shown on the z-axis with surface color also varying with ROT; watt and var mismatch are shown on the x and y axes respectively. Figure 6 shows the color map (an x-y plane view) of the same results as in Figure 5. In each Figure, the plots on the left are for the case with GSFs disabled, and the plots on the right were for GSFs enabled.

At first, the results of these tests were somewhat startling. The GSF-disabled plots on the left in Figure 5 and Figure 6 show a relatively large NDZ, with a fairly broad range of indefinite ROTs indicating stable islands. However, when the GSFs are activated, the ROTs are reduced in essentially all cases, and the large region of elevated ROTs in the left-hand plots are gone, replaced by a few individual isolated elevated points, none of which indicates an ROT greater than 2 seconds. In other words, addition of the GSFs significantly *improved* the performance of the Group 3 AI. The reasons are discussed in the Discussion section below.

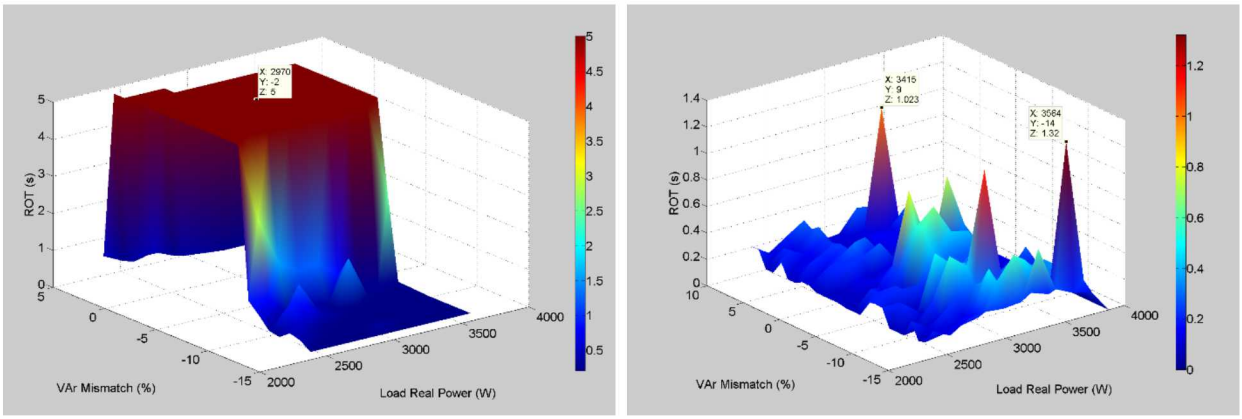

Figure 5. Results for 33% irradiance, surface plot view. Left: GSFs off. Right: GSFs on.

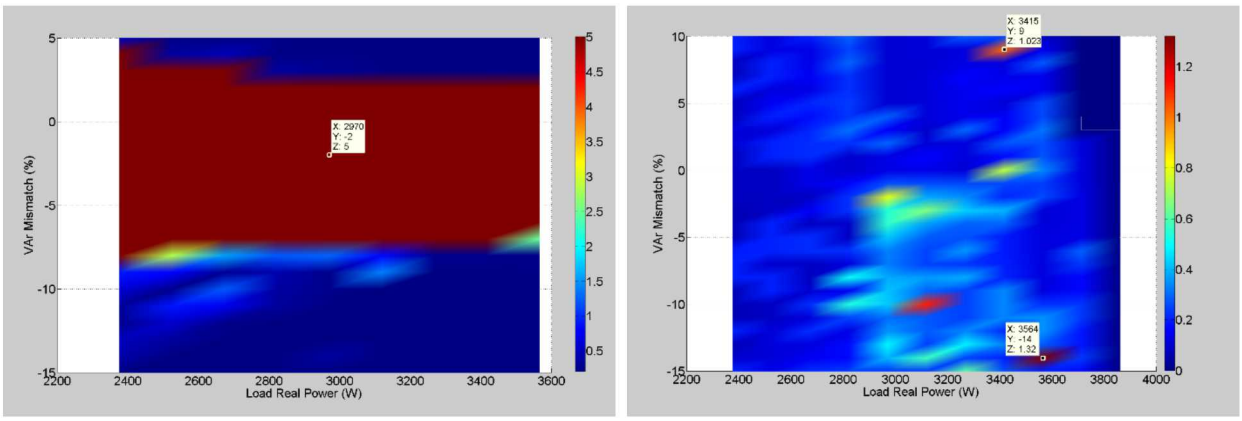

Figure 6. X-Y plane view of the same results as in Figure 5.

3.3.2. Sixty-six Percent Irradiance

Figure 7 shows two surface plots of the ROT versus watt and var mismatch, for the case of 66% irradiance, and Figure 8 shows an x-y plane view of the same results as in Figure 7. In each Figure, the plot on the left shows results with GSFs disabled, and the plot on the right is with GSFs enabled. The results are similar to the 33% irradiance case in that the activation of the GSFs significantly improved the ability of the inverter to detect islands, and ROTs dropped in nearly all cases. Note that the size of the NDZ in the no-GSF case is somewhat smaller at the higher irradiance level.

3.3.3. One-hundred Percent Irradiance

Figure 9 shows two surface plots of the ROT versus watt and var mismatch, for the case of 100% irradiance, and Figure 10 shows an x-y plane view of the same results as in Figure 9. Again, the left-hand plots are with GSFs disabled and the right-hand plots are with GSFs enabled. The results are consistent with the previous two scenarios; activation of the GSFs has reduced the size of the NDZ. However, two interesting trends are apparent. One is that the NDZ in the no-

GSF case is smaller for 100% irradiance than for 66%. The other is that the amount of improvement obtained by activating the GSFs is smaller, as indicated by the fact that the NDZ with the GSFs active is closer in size to the no-GSF NDZ than was the case at either of the lower irradiance levels.

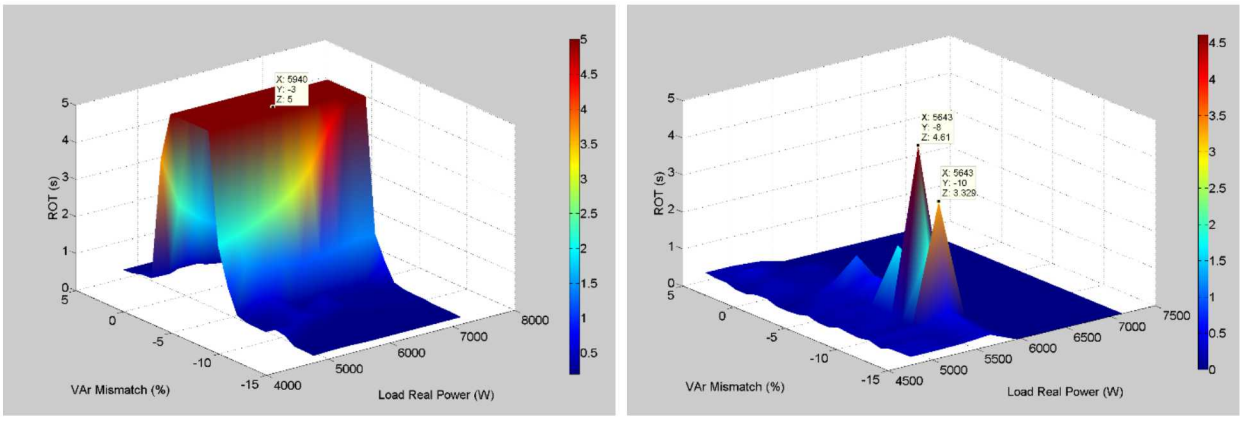

Figure 7. ROTs vs. P and Q mismatch for 66% irradiance. Left: no GSFs. Right: GSFs active.

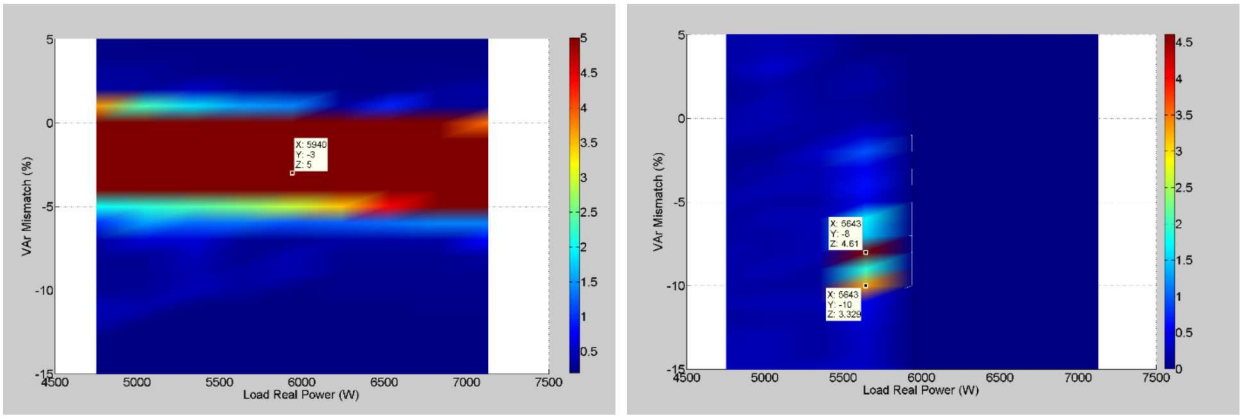

Figure 8. X-Y plane view of the results in Figure 7.

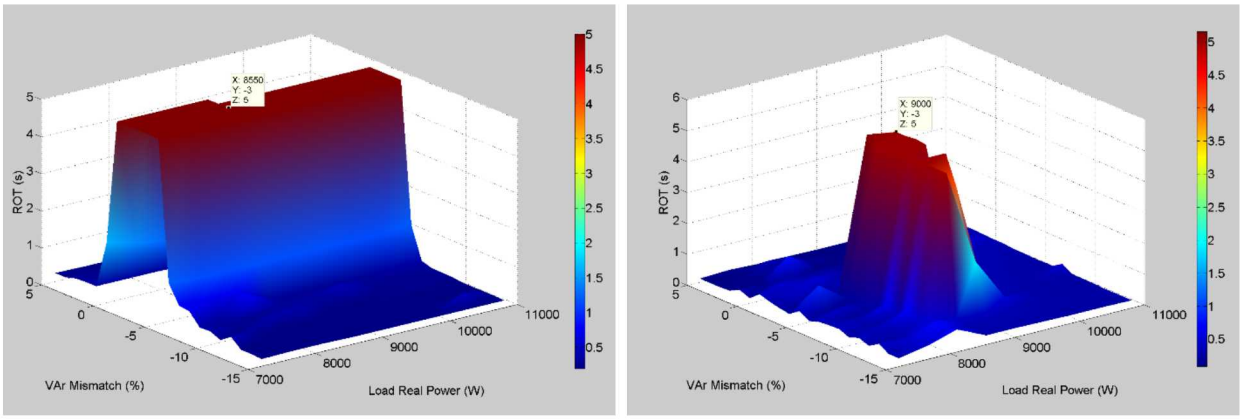

Figure 9. ROTs vs. P and Q mismatch for 100% irradiance. Left: no GSFs. Right: GSFs active.

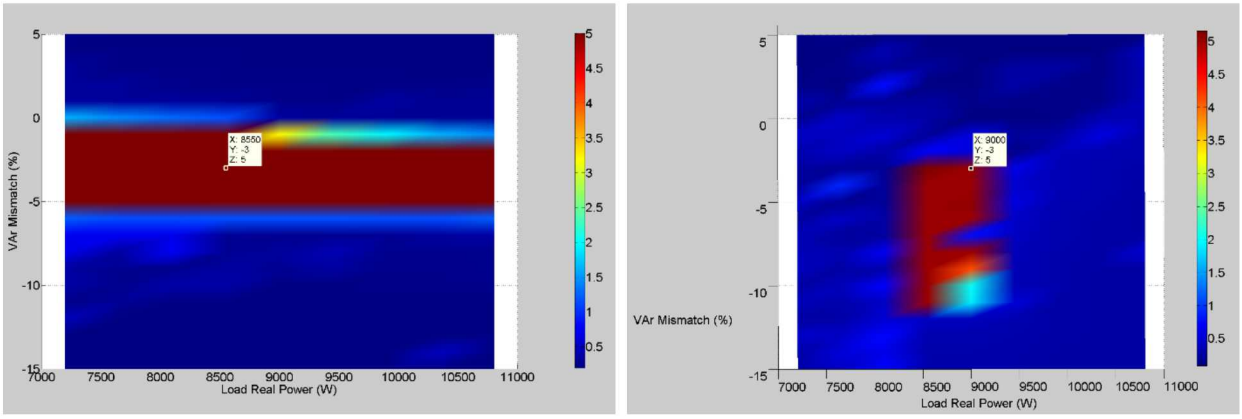

Figure 10. X-Y plane view of Figure 9.

3.4. Discussion

It was expected that ROTs for an impedance-detection method in a single inverter case would be minimally impacted by the presence of GSFs. Impedance detection (Group 3), particularly the pulse-based variety, actively disrupts the island's ability to come to a steady state, and unless something in the implementation of the GSFs causes the impedance detection pulse to change in magnitude or duration, that disruption of the steady state should persist even when GSFs are active. It would also be a fairly simple matter to have the impedance detection pulse "ride on top of" the output variations required by the GSFs.

However, the simulation results for Inverter A were significantly different than expected. First, in the baseline case with no GSFs, a fairly large NDZ was observed. It is believed that the primary reason for this lies in the fact that the output perturbation used by Inverter A was not synchronized between the three single-phase inverters. This reduces the correlation between each inverter's impedance-detection output variation and the resulting change in voltage, leading to a lessened ability of the inverters to see island formation. The fact that the inverters were connected in delta, but the load was in grounded-wye, would also play a role in reducing the correlation of each inverter's output current to its terminal voltage.

The other result observed here that was a bit surprising was that the addition of the GSFs actually *improved* the islanding detection effectiveness of the Group 3 inverters. It is believed that this improvement occurs because when the system is islanded there is coupling between V and Q and between f and P that does not normally occur in inverter controls, and that in this case acted to de-stabilize islands. To understand this situation, see Figure 11, which shows a reference model illustrating the coupling. Consider an island that is initially slightly deficient in watts but well-balanced in vars. When the island forms, the voltage falls because of the real power deficit. The volt-var functions become active, and the inverter begins to source vars to attempt to support the voltage. This may partially correct the low voltage, but the island will now be var-rich. The inverter's phased locked loop (PLL) will start to change the frequency to the value at which the load var demand and inverter var characteristics cross, but there may not be an operating point at

which the load's var demand and the PV's volt-var curve are both satisfied. Thus, the system begins "hunting" and cannot reach a stable steady state within the allowable voltage and frequency bounds. Similar situations will occur for islands that are slightly power-rich, or slightly var-rich. In a var-deficit island, one would expect less of an impact of this cross-coupling because of the asymmetry of the frequency-watt function.

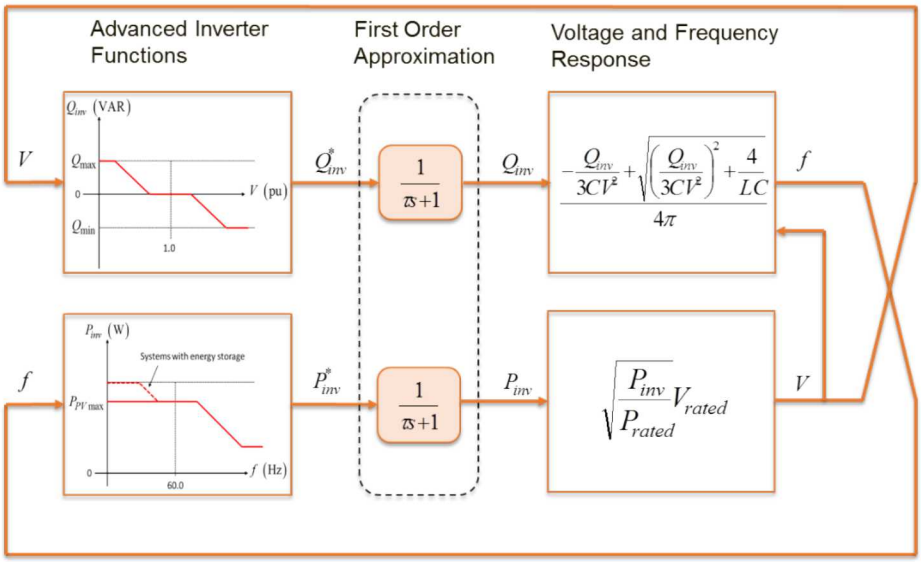

Figure 11. Reference model showing the closed-loop relationship between GSF functions and RLC load.

4. PART II: IMPACT OF GRID SUPPORT FUNCTIONS, RIDE THROUGHS AND IRRADIANCE ON GROUP 2A AND GROUP 3/6 ISLANDING DETECTION

4.1. Introduction

In Part II of this work, three units of a single-phase inverter referred to as "Inverter A" were used. Inverter A is rated at 3 kW per phase (total of 9 kW) and, in this experiment, used a combination of Group 3 and Group 6 anti-islanding techniques. The three units of Inverter A were placed into an island with Inverter B, which is a 50 kW, three-phase, transformer-isolated inverter using Group 2A anti-islanding. The purpose of the simulations was to investigate the impact of GSFs (VV11 and FW21) on island detection effectiveness, in the presence of dissimilar inverters.[b] Tests were conducted with and without GSFs, and also with collaborative controls (CC) to determine whether the CC could restore effectiveness in cases in which islanding detection effectiveness decreased. Tests were conducted at the same three irradiance levels (33%, 66%, and 100%) as in Part I. The GSF settings used are those given in Table 1.

The test apparatus simulated for this work is shown in Figure 12 and Figure 13. In this work, the three units of Inverter A were connected line-ground (wye) via a YG:yg transformer. They are independently controlled. Inverter B was connected directly to the 480 V bus. The RLC load was connected in delta.

[b] In actuality, because Inverter B represents almost 85% of the total generation in the island, the responses seen in Part II of this work are dominated by Inverter B and its Group 2A anti-islanding.

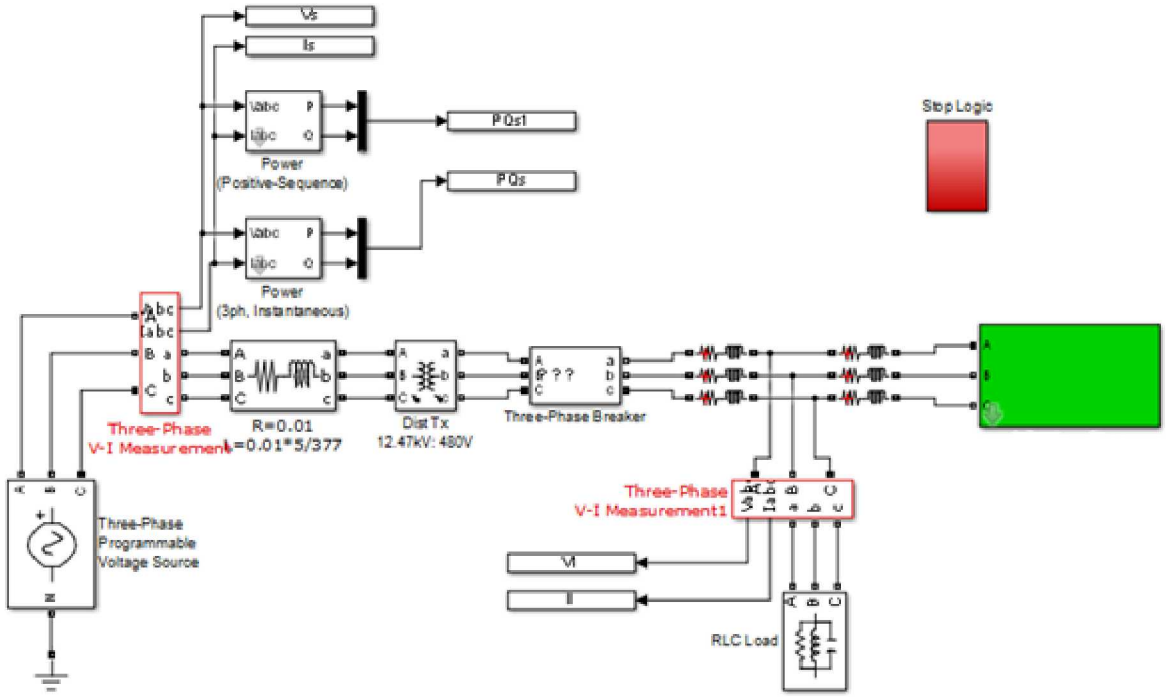

Figure 12. Testbed setup for islanding three units of Inverter A in delta, plus one unit of Inverter B. Line impedances are included on the 12.47 kV and 480 V sides of the YG:yg GSU transformer. The load is connected in delta.

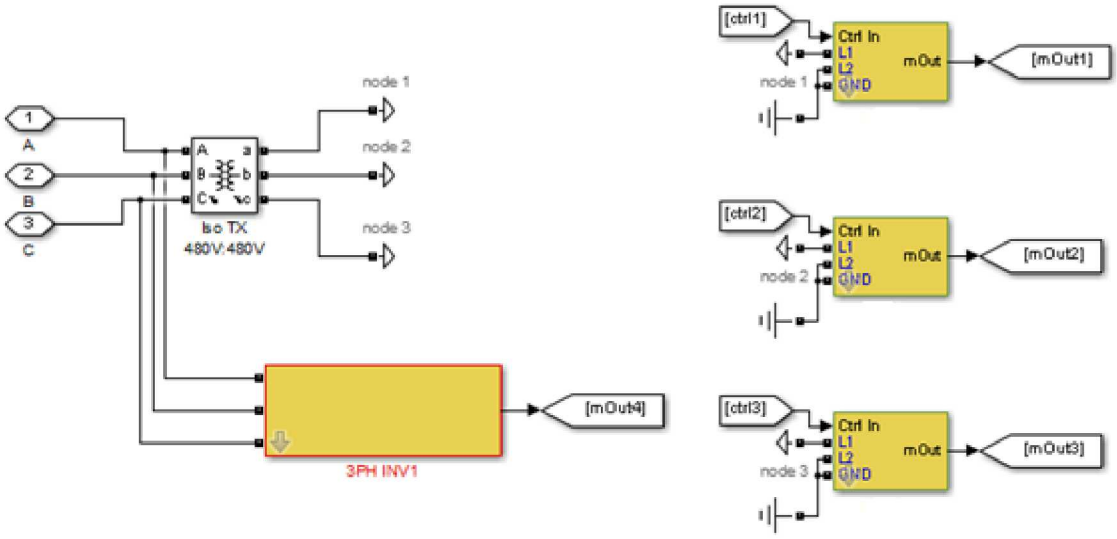

Figure 13. This figure shows the contents of the green inverter block in Figure 12. The three units of Inverter A are isolated by a 480V:480V Yg-Yg tx and connected line to ground (wye). Inverter B is connected directly to the 480V bus.

4.2. Brief summary of results

For convenience, this section briefly summarizes the results obtained from Part II of this work.

1. Without RTs or GSFs, island detection effectiveness is not a strong function of irradiance. The ROT did change somewhat as irradiance varied but the changes were small and there was no clear trend.
2. Widening the relay settings and requiring the inverters to ride through larger voltage and frequency deviations has a clear adverse impact on islanding detection, with ROTs rising by approximately a factor of three over the base case. However, in no case tested in Part II did ROTs exceed 2 sec.
3. Overall, the GSFs had a negligible impact on ROTs. In some cases, the impact of GSFs on ROTs was beneficial; at 100% irradiance there was a clear overall reduction in ROTs when the VV11 and FW21 GSFs were activated. At the 66% and 33% irradiance levels, the distribution of ROTs did shift toward longer values, but the shift was relatively small. The impact of GSFs on ROTs appeared to become more negative as the irradiance level dropped[c].
4. The collaborative controls were effective at restoring most of the effectiveness of the anti-islanding at higher irradiance levels. At lower irradiance levels, in these simulations the improvement in ROTs obtained by adding the collaborative controls was less noticeable.

4.3. Procedure

The GSFs tested here were volt-var and frequency-watt. In Part II, the first step was to run a set of simulations in which the relays were set to IEEE 1547-2003 default values (no ride-throughs [RTs]), the GSFs were disabled, and the collaborative controls were off. This set of simulations was taken to be the base or reference case. Then, simulations were run for each of the following combinations of factors:

Table 2. Cases tested in Part II of this work.

Case	GSF status	RT status	CC status
Base	Off	Off	Off
1	On	Off	Off
2	On	On	Off
3	On	Off	On
4	On	On	On

[c] The VV11 function assumes watt priority, and thus when the inverter is at or near rated output current, the VV11 function's activity is limited. Thus, at full irradiance, the FW21 function will have the greater influence, and the trend seen in ROTs versus irradiance with the GSFs active *might* suggest that FW21 has a modest tendency to decrease ROTs but VV11 may in some cases increase ROTs. Future work should investigate this possibility.

In each set of simulations, the mismatch in real and reactive power between the generation and loads was varied over a wide range, and the ROT for each generation-load combination was recorded. The raw results for each case are plotted as a set of surface plots, and these surface plots are provided in the Appendix.. Then, to help visualize the impact of each factor on the run-on times, the ROTs from each batch of simulations were binned and a histogram was formed. By overlaying the histogram from one simulation batch atop that from another, it is possible to see the overall shift in ROTs caused by changing that factor. The histograms show the frequency of occurrence for each ROT bin, and thus a rightward shift in the distribution indicated by the histogram indicates a trend toward increasing ROTs.

4.4. Results

The above-described histograms are presented in this section. There are two series in all of these histograms, a brown one and a blue one. The region that appears "bluish-brown" in the histograms is the region in which the two series overlap.

4.4.1. Case 1 vs. base case: Impact of GSFs, no RTs, no CC

Figure 14 shows the histogram (distribution) of the ROTs observed from Case 1, when the GSFs (volt-var and frequency-watt) were activated without the RTs or CC, compared against the distribution of ROTs seen in the base case, for 100% irradiance. Figure 15 shows Case 1 results versus the base case for 66% irradiance, and Figure 16 shows the results at 33% irradiance. The number of loading conditions (data points) is different for the two sets of simulations, so the absolute magnitudes of the histograms are different, but the important information is gained from these histograms by comparing the relative distributions. At all three irradiance levels, the activation of the GSFs has had only a minimal impact on islanding detection effectiveness. At 100% irradiance, the distribution of ROTs actually shifts to the left relative to the base case, indicating (as seen in Part I) that the impact of the GSFs on ROTs has been mildly beneficial. In the 66% and 33% irradiance cases, there is a slight rightward shift in the distribution, indicating a net negative impact of GSFs on ROTs, and the negative impact appears to become larger as irradiance drops, but it is relatively small in any case. This indicates that GSFs have had only a small impact on the ROTs, and in some cases the impact was actually beneficial in the sense that ROTs tended to be reduced. The mechanism behind this effect is believed to be the one described in Figure 11 and its accompanying text above, involving cross-coupling of the real power to frequency and the reactive power to voltage in a way that is not typically true with grid-tied inverters controlled to act as current sources.

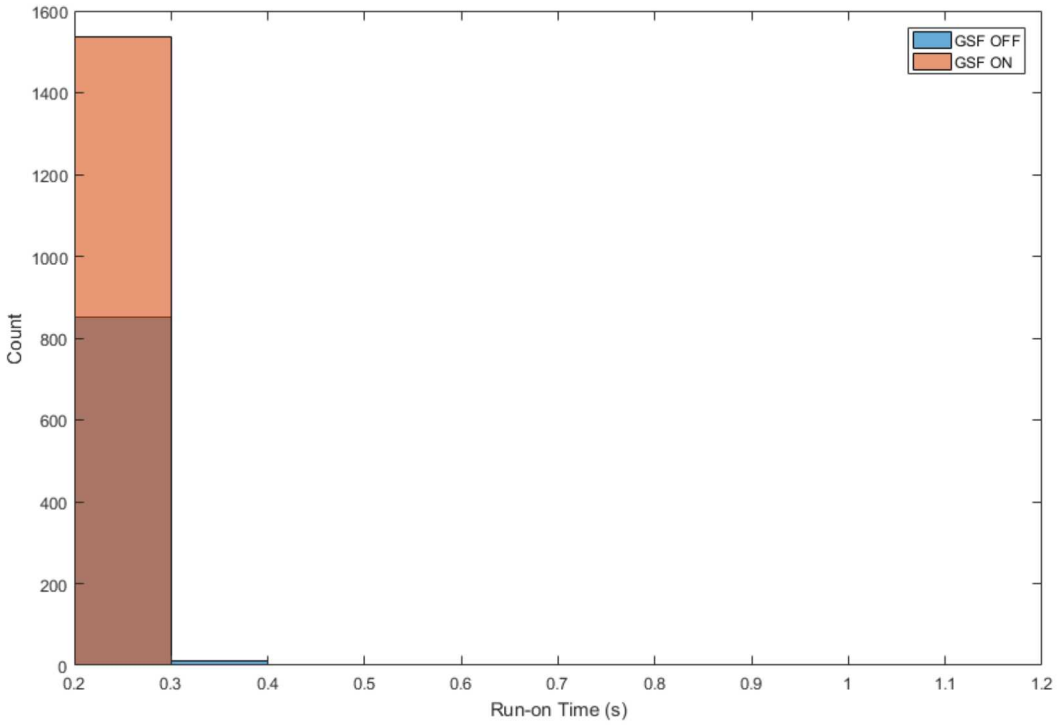

Figure 14. Comparison of histograms (distributions) of ROTs comparing Case 1 and the base case (GSF vs. no GSFs, no RTs, no CC), 100% irradiance.

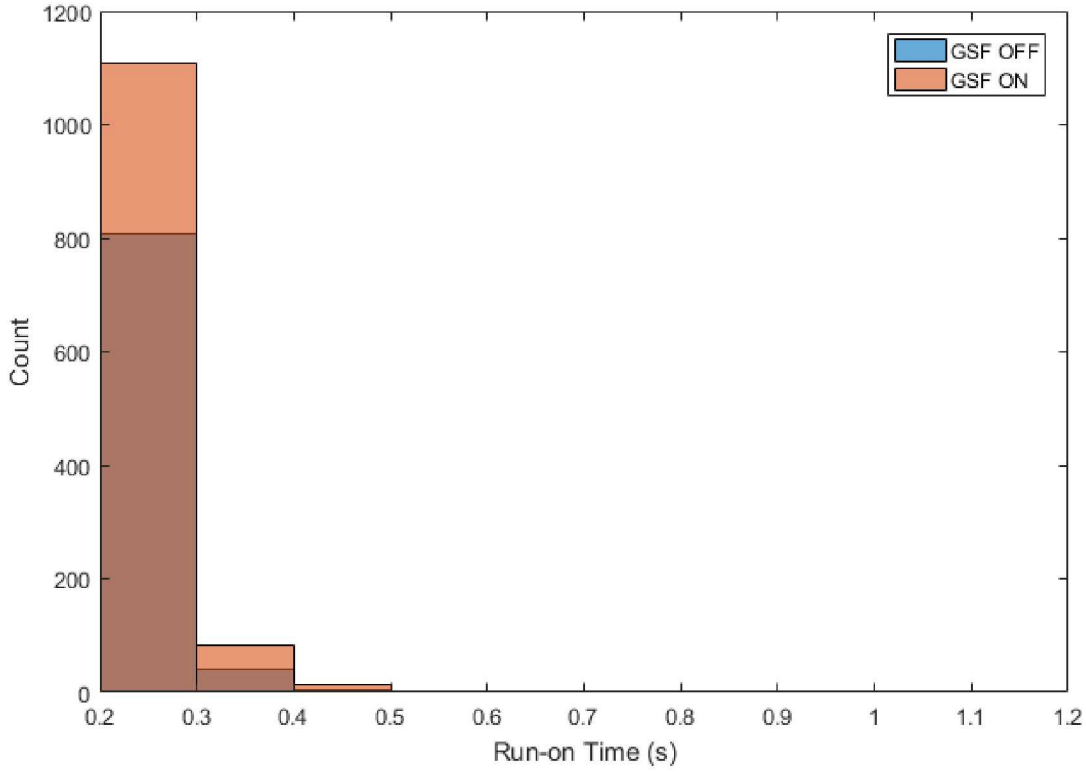

Figure 15. Comparison of histograms (distributions) of ROTs comparing Case 1 and the base case (GSF vs. no GSFs, no RTs, no CC), 66% irradiance.

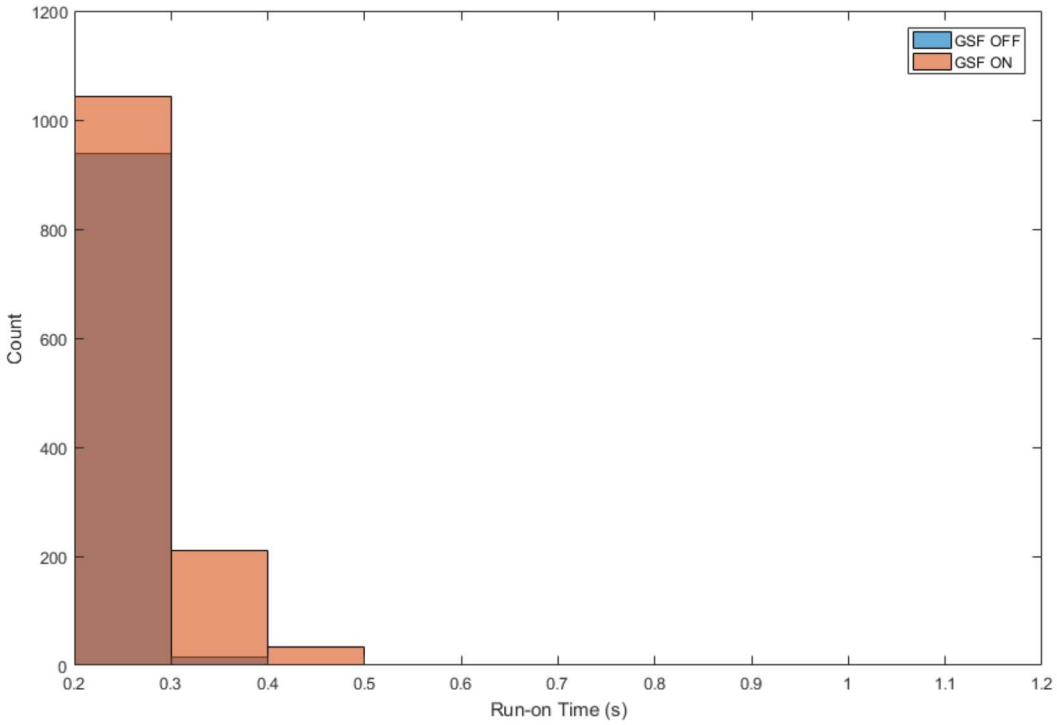

Figure 16. Comparison of histograms (distributions) of ROTs comparing Case 1 and the base case (GSF vs. no GSFs, no RTs, no CC), 33% irradiance.

4.4.2. Case 2: impact of GSFs with RTs, no CC

Figure 17 shows a comparison of the histogram (distribution) of the ROTs obtained in Case 2 (GSFs and ROTs both on, CC off) with the histogram of the base case. Figure 18 shows the Case 2 vs. base case comparison for the 66% irradiance level, and Figure 19 shows the Case 2 vs. base case comparison for the 33% irradiance level. At all three irradiance levels, when both the GSFs and RTs are active, there is a pronounced rightward shift in the distribution, indicating that the trend is toward increasing ROTs. Because in the previous section it was shown that the impact of GSFs on ROTs is either neutral or slightly beneficial, the rightward shifts seen in Case 2 can be attributed to the addition of the RTs.

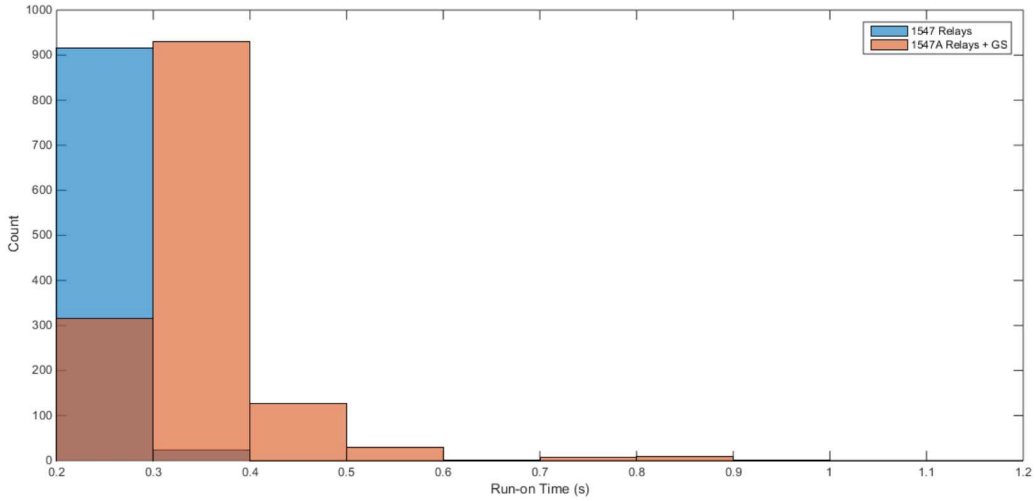

Figure 17. Comparison of the histograms (distributions) of ROTs between Case 2 (GSFs and RTs, no CC) and the base case, 100% irradiance.

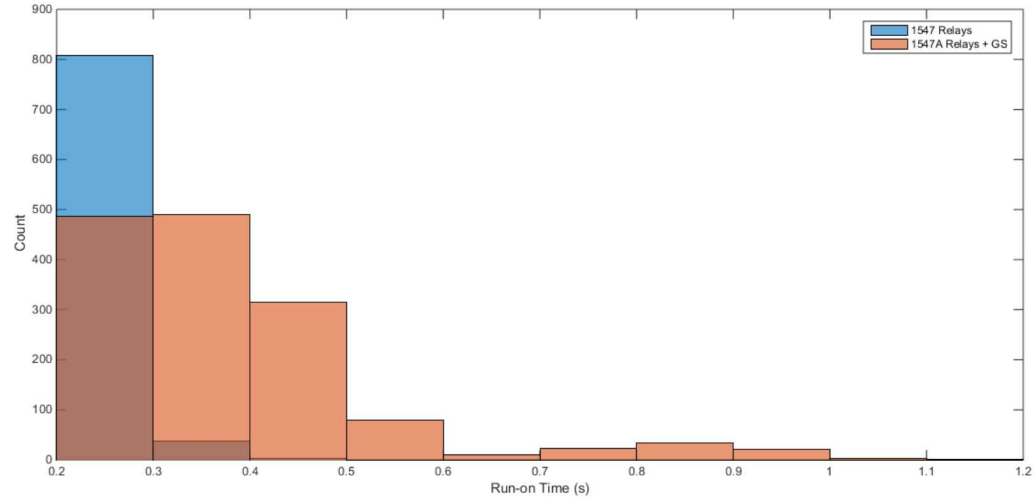

Figure 18. Comparison of the histograms (distributions) of ROTs between Case 2 (GSFs and RTs, no CC) and the base case, 66% irradiance.

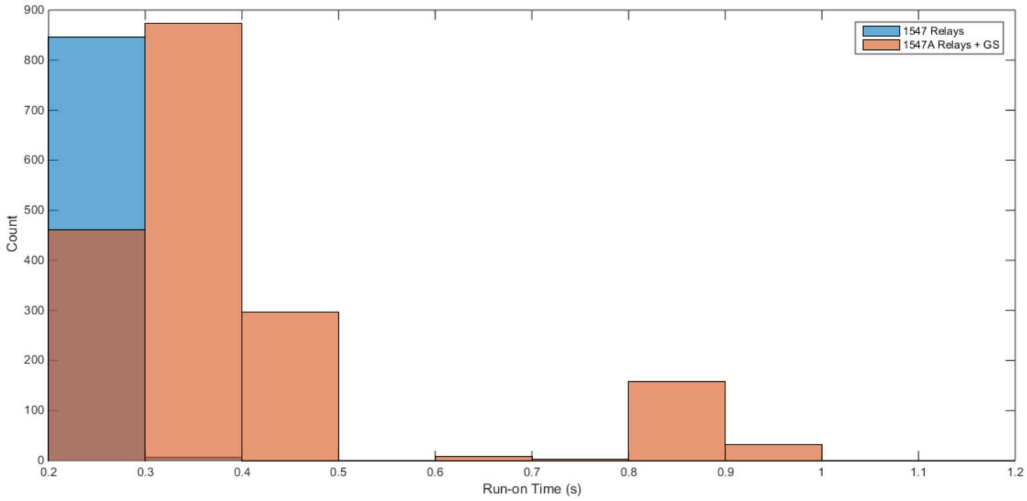

Figure 19. Comparison of the histograms (distributions) of ROTs between Case 2 (GSFs and RTs, no CC) and the base case, 33% irradiance.

4.4.3. Case 3 vs. Case 1: Impact of the CC when GSFs are on but RTs are off

Figure 20 shows a comparison of the histogram (distribution) of the ROTs obtained in Case 3 (GSFs on, RTs off, and CC all on) with the histogram of Case 2 (GSFs on RTs and CC both off), for the 100% irradiance case, and thus provides an indication of the benefit provided by using the CC. In this case the benefit is minimal, but that is at least in part due to the fact that the distributions are both "squashed" against the left side of the plot, so there is not much benefit to be had.

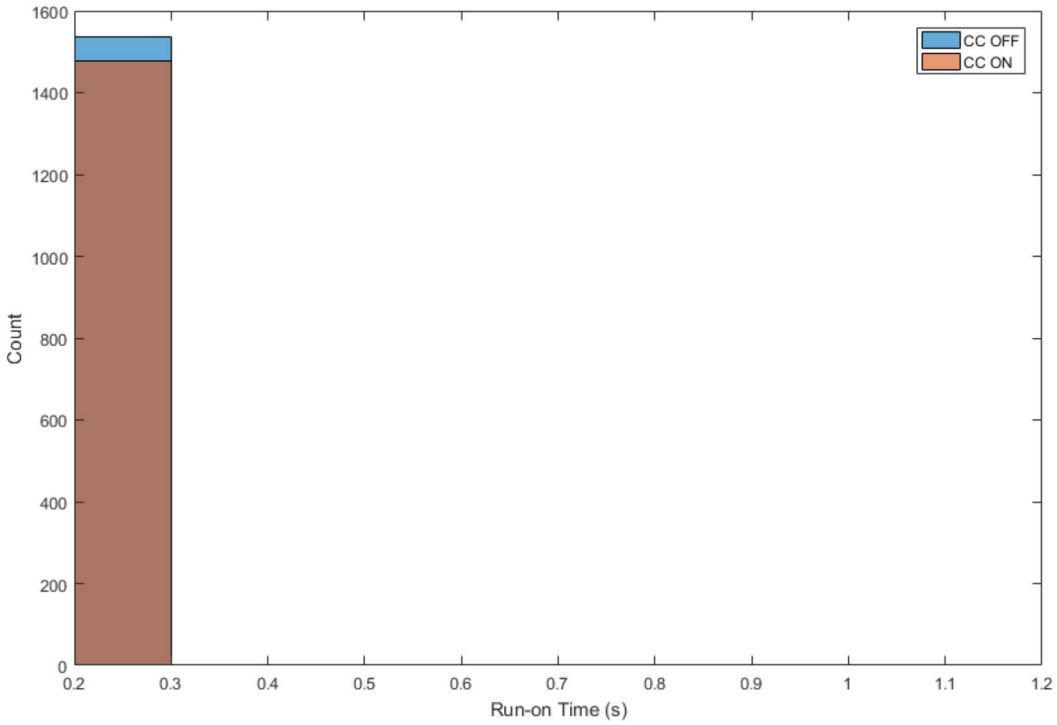

Figure 20. Comparison of the histograms (distributions) of ROTs between Case 3 (GSFs on, but RTs off) and Case 2 (GSFs and RTs without CC), 33% irradiance.

4.4.3. Case 4 vs. Case 2: impact of the CC when both GSFs and RTs are active

Figure 23 shows a comparison of the histogram (distribution) of the ROTs obtained in Case 4 (GSFs, RTs and CC all on) with the histogram of Case 2 (GSFs and RTs both on but CC off), for the 100% irradiance case. This figure gives an indication of the benefit provided by the CC in this case. For the higher irradiance cases, the CC are effective in shifting the distribution back to the left and reducing the maximum ROTs, although not quite all the way to the base-case distribution. At lower irradiance the impact of the CC is reduced.

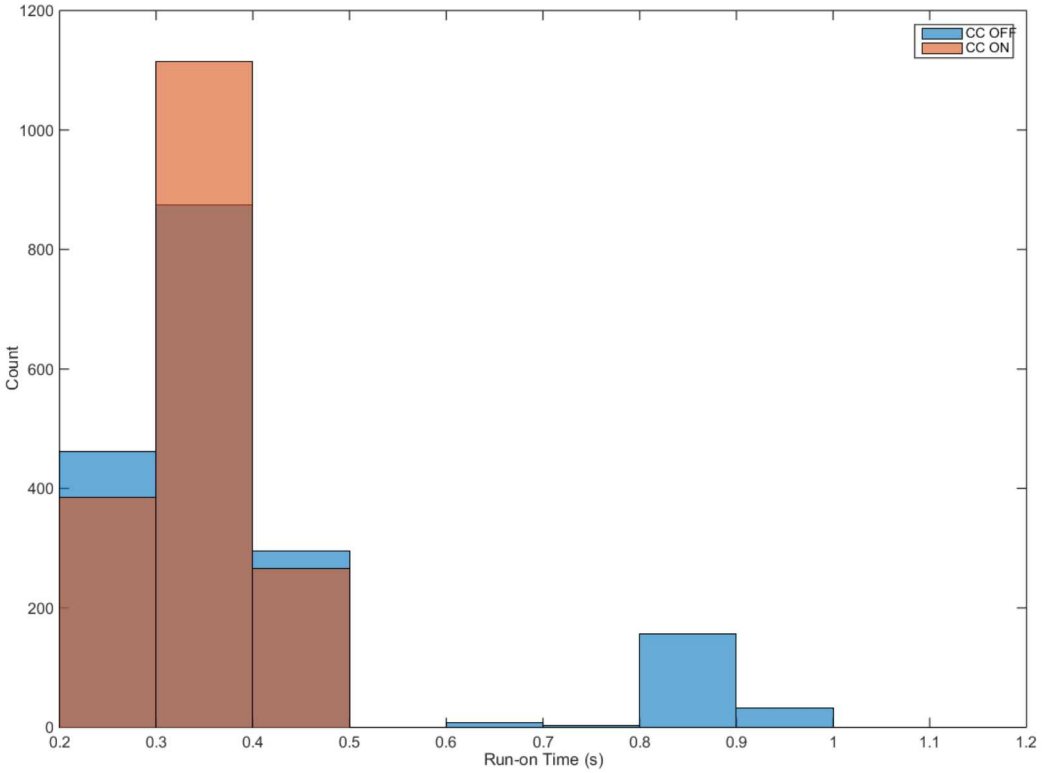

Figure 21. Comparison of the histograms (distributions) of ROTs between Case 4 (GSFs and RTs with CC) and Case 2 (GSFs and RTs without CC), 100% irradiance.

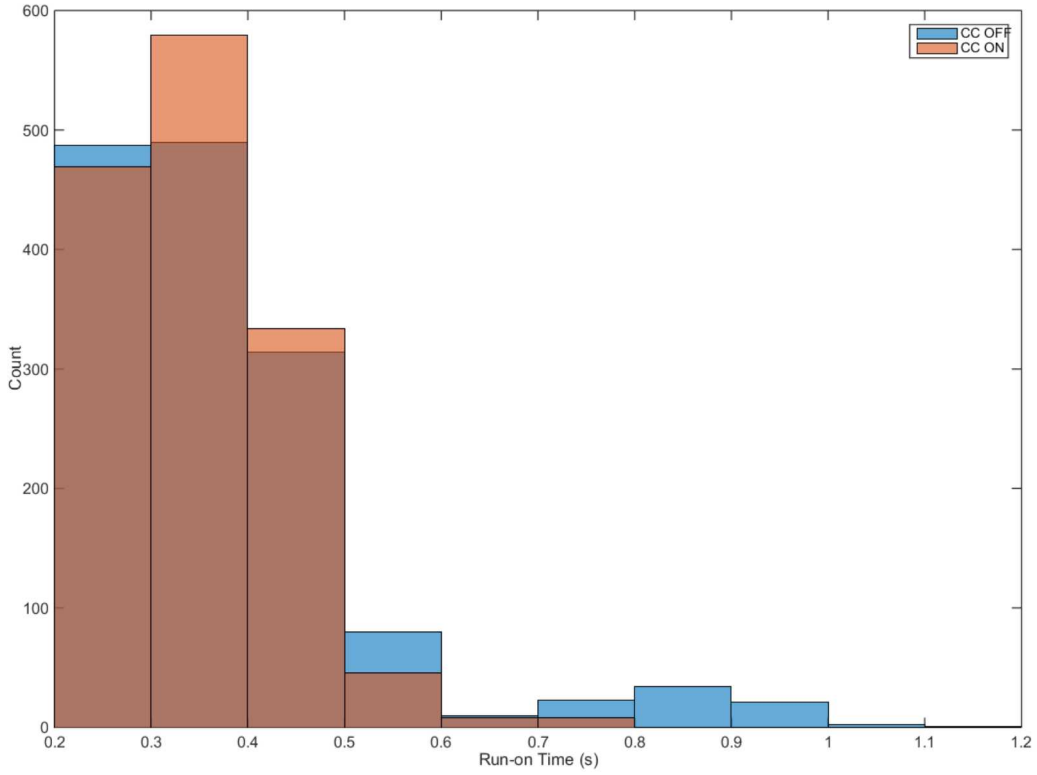

Figure 22. Comparison of the histograms (distributions) of ROTs between Case 4 (GSFs and RTs with CC) and Case 2 (GSFs and RTs without CC), 66% irradiance.

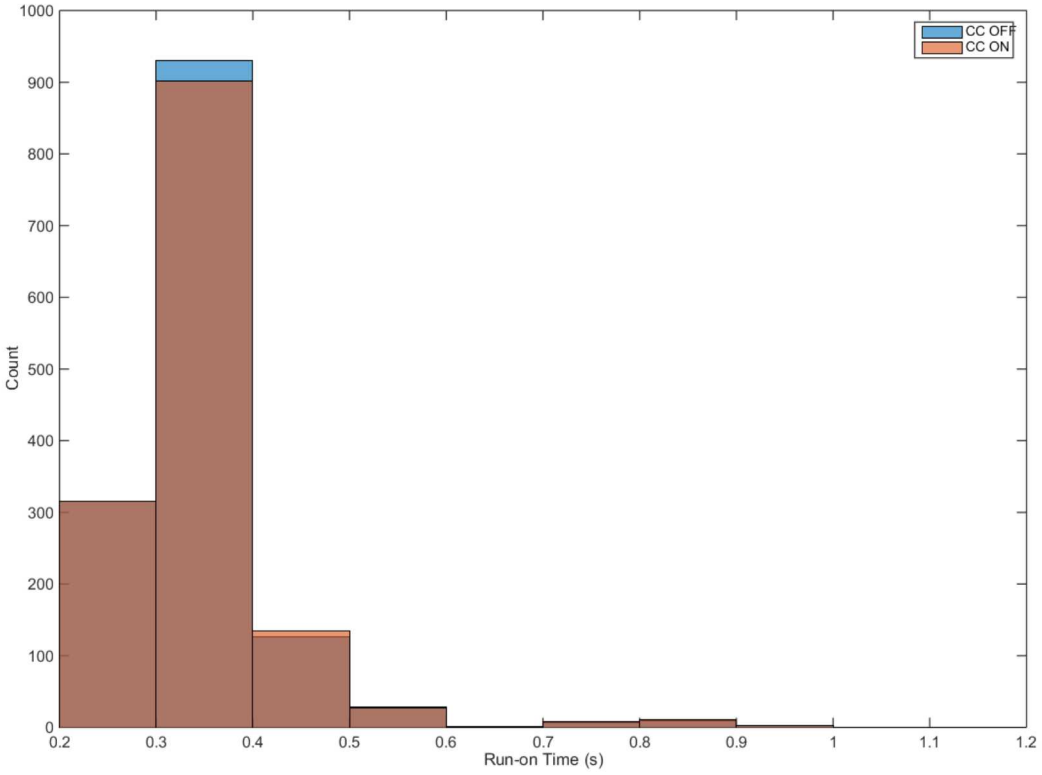

Figure 23. Comparison of the histograms (distributions) of ROTs between Case 4 (GSFs and RTs with CC) and Case 2 (GSFs and RTs without CC), 33% irradiance.

4.4.4. Behavior of voltages during an island event

Inverter A has a property that is atypical among three-phase inverters: because it consists of three single-phase inverters connected in wye, Inverter A can produce significant levels of negative-sequence current, leading to the Group 6 anti-islanding action of these inverters, and Inverter A is also capable of producing zero-sequence current. To illustrate, Figure 24 shows the Inverter A output current from one specific island event in which the GSFs and RTs were active, the CC were off, and the irradiance was 33%. Figure 25 shows the sequence components of the currents in Figure 24. In this case the island is formed at t = 5 sec. Figure 25 shows the impact of the Group 6 islanding detection action that occurs in this inverter: once the island forms the negative sequence, current grows until most of Inverter A's output is negative-sequence, and the island is detected leading to inverter tripping.

As noted above, Inverter A also sources a low level of zero-sequence current during this event, as seen in Figure 25. Because there are no low-impedance paths to ground for the zero-sequence current due to the fact that the load is connected in delta, the zero-sequence currents lead to a significant zero-sequence voltage component. This is evident in Figure 26, which shows the Inverter A phase-ground terminal voltages during this island event; Figure 27, which shows the Inverter B line-ground terminal voltages during the island event; and Figure 28, which shows the sequence components of the voltages shown in Figure 27. The zero-sequence component causes an overvoltage, the peak value of which approaches 2 per unit[d]. Also, the non-positive-sequence voltage causes Inverter B to begin to source unbalanced current, as shown in Figure 29 (current waveforms from Inverter B) and Figure 30 (sequence components of the current waveforms in Figure 29). Inverter B's unbalanced current is entirely negative-sequence because it does not provide zero-sequence continuity.

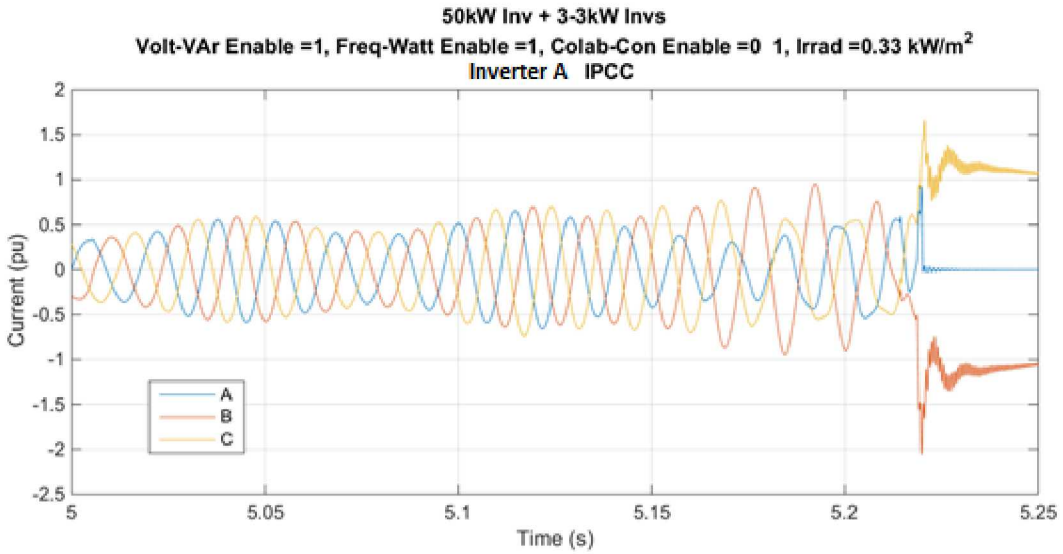

Figure 24. Output current waveforms from Inverter A during the island event.

[d] The reader is reminded that the self-protection overvoltage (SPOV) mechanisms were disabled in these inverter models.

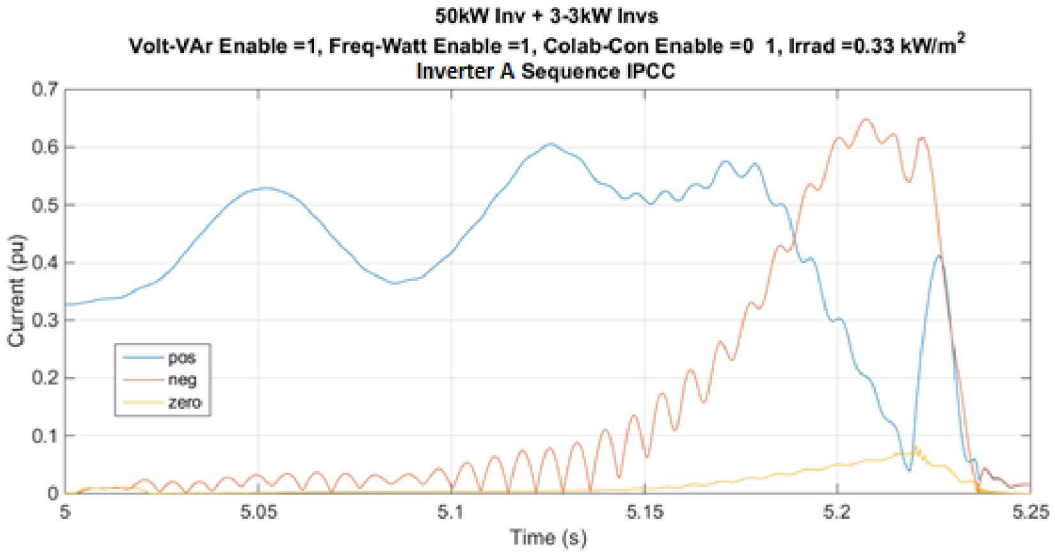

Figure 25. Sequence components of the Inverter A inductor current (prior to the AC filter elements).

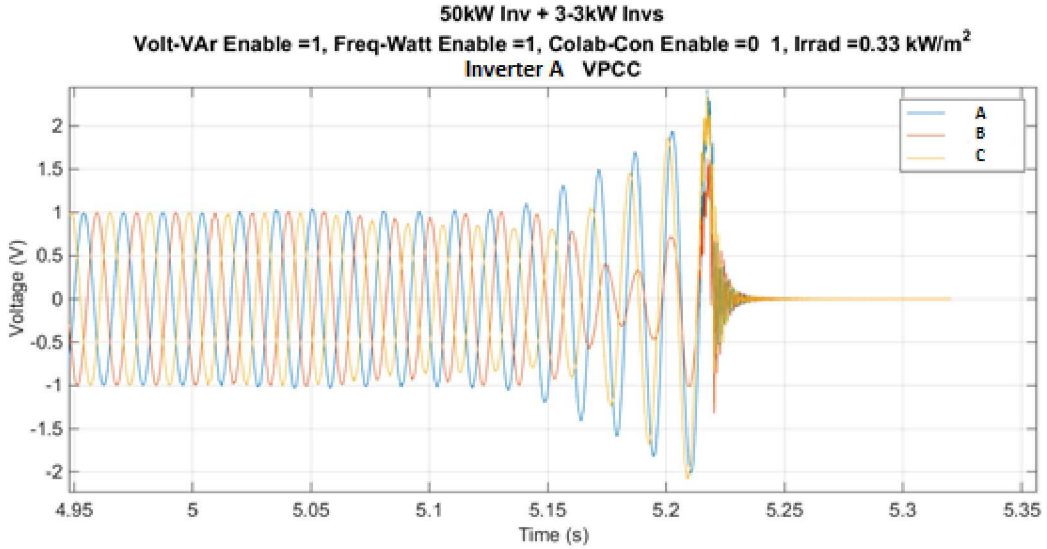

Figure 26. Line-ground voltage waveforms measured at the point of common coupling (PCC) of Inverter A inverter during an island event.

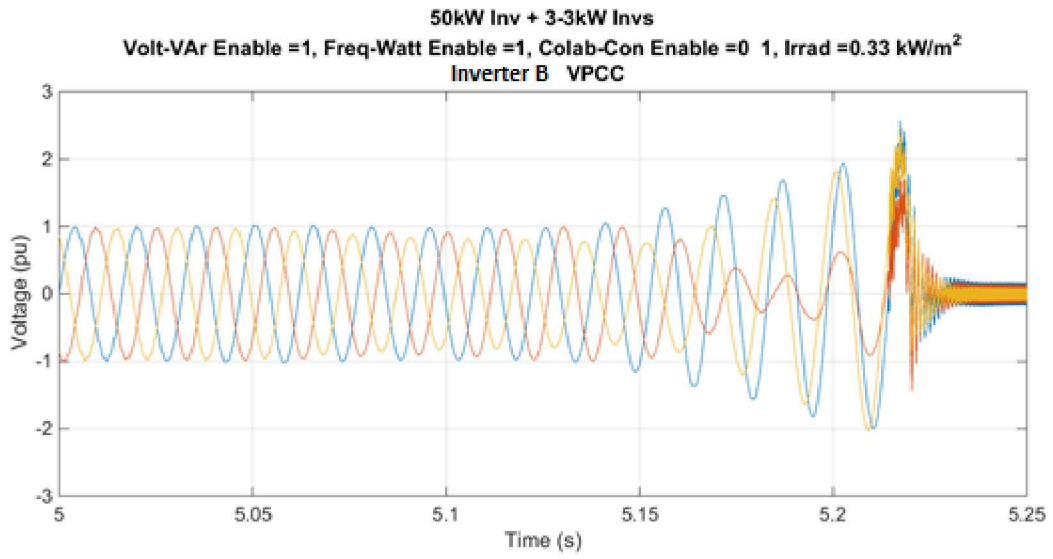

Figure 27. Line-ground voltage waveforms measured at the PCC of Inverter B during an island event.

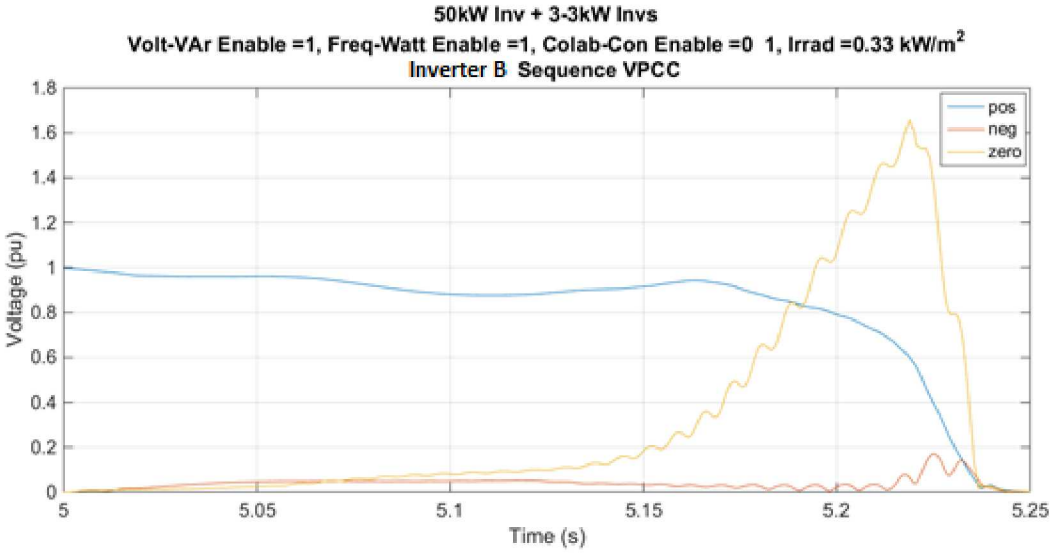

Figure 28. Sequence voltages measured at the PCC of the Inverter B inverter during an island event.

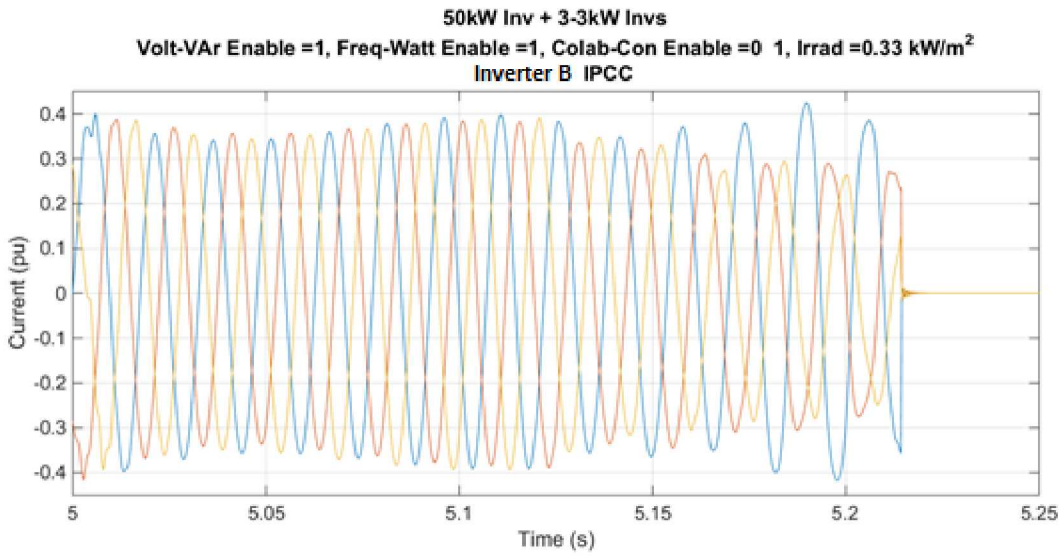

Figure 29. Output current waveforms from Inverter B inverter during the island event.

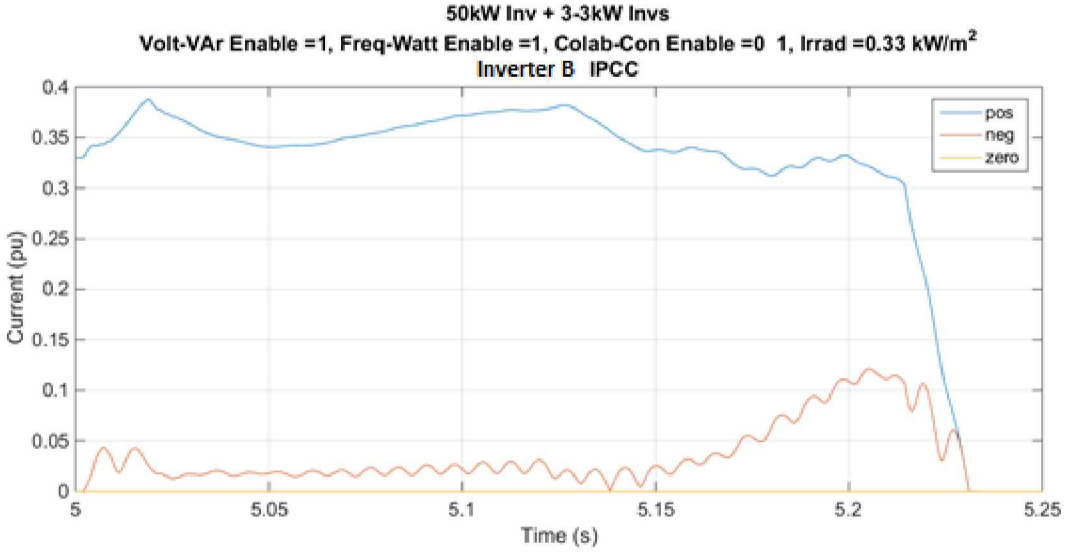

Figure 30. Output sequence currents from Inverter B inverter during the island event.

7. CONCLUSIONS

The work reported here supports the following general conclusions.

1.) When inverters are required to ride through larger voltage and frequency deviations, islanding detection is adversely impacted, with peak ROTs rising by a factor of approximately three in the cases tested here and ROT distributions shifting toward longer values. However, in Part II of this work, all ROTs remained below 2 s, even with RTs active.
2.) It appears that when GSFs and RTs are not active, irradiance has a minimal impact on islanding detection effectiveness. Run-on times did depend weakly on irradiance but there was no clear trend or correlation.
3.) The impact of grid support functions on islanding detection capability appears to be minimal, and in some cases (possibly at higher irradiance levels), appears to be positive in the sense that run-on times become shorter when the GSFs are activated. The mechanism behind this effect is believed to be the cross-coupling of watts to frequency and vars to voltage that does not naturally occur in grid-tied inverters controlled to act as current sources. In Part I, activation of GSFs generally led to reduced ROTs at all irradiance levels. Part II suggested that this effect may not be as dominant at lower irradiance levels; while the ROT distribution did shift leftward at 100% irradiance, it showed a modest rightward shift at 33% irradiance relative both to the base case and to the distribution at 100% irradiance.
4.) The collaborative controls largely mitigated the negative impact of the ride throughs on ROTs and restored the effectiveness of the anti-islanding methods tested here to close to where they were in the base case. The CC were more effective at higher irradiance levels.

LIMITATIONS OF THIS STUDY

The reader should note that this study has the following limitations.

- This work did not separate the impact of volt-var and frequency-watt. It is thus not clear whether one of the two cross-coupling mechanisms may be stronger than the other.
- This work only considered a limited number of islanding detection methods. It would be of value to extend this study to all of the groups.
- It would be highly beneficial to repeat the work studying the impact of GSFs, to get a larger “sample size.”

REFERENCES

[1] Eltawil, Mohamed A., and Zhengming Zhao. "Grid-connected photovoltaic power systems: Technical and potential problems—A review." *Renewable and Sustainable Energy Reviews*, pp. 112-129, 2010.

[2] Enslin, Johan HR. "Network impacts of high penetration of photovoltaic solar power systems." Power and Energy Society General Meeting, 2010 IEEE. IEEE, 2010.

[3] Passey, Robert, Ted Spooner, Iain MacGill, Muriel Watt, and Katerina Syngellakis. "The potential impacts of grid-connected distributed generation and how to address them: A review of technical and non-technical factors." Energy Policy 39, no. 10, pp. 6280-6290, 2011.

[4] IEEE Standard 1547-2018, "IEEE Standard for Interconnection and Interoperability of Distributed Energy Resources with Associated Electric Power Systems Interfaces," February 2018.

[5] IEC 61850-90-7:2013, "Communications networks and systems for power utility automation –Part 90-7: Object models for power converters in distributed energy resources (DER) systems."

[6] M. Ropp, D. Schutz, J. Neely, S. Gonzalez, "Effect of grid support functions and VRT/FRT capability on autonomous anti-islanding schemes in photovoltaic converters," Proceedings of the 43rd IEEE Photovoltaic Specialists Conference, June 2016, p. 1853-1856.

[7] J. Neely et.al., "Accelerating Development of Advanced Inverters: Evaluation of Anti-Islanding Schemes with Grid Support Functions and Preliminary Laboratory Demonstration," Sandia National Laboratories, SAND2013-10231, November 2013.

[8] J. Neely et.al., "Accelerating Development of Advanced Inverters," Sandia National Laboratories technical report, SAND2015-11124R, December 22, 2015.

APPENDIX

This Appendix includes surface plots of the data points used to produce the histograms in the main body of the report. The surface plots begin with the "baseline" results in which the inverters are using the IEEE 1547 default over/undervoltage and over/underfrequency settings. Simulations are run for three different irradiance levels: 1, 0.66, and 0.33 kW/m^2. These baseline cases, given in Figure 31 through Figure 42, corroborate the expected result that the anti-islanding in these inverters is effective when the GSFs and RTs are not active; the longest ROTs approach 450 ms. The various experimental cases are shown after that.

For each test condition, four plots are shown. The first two are a representative example of the surface plot obtained for one of the inverters, in perspective view and then in x-y plane view. The second two figures show the maximum ROT obtained for any inverter for each P-ΔQ pair. The plots differ slightly because the inverters did not all trip at the same time in many of the simulations, but it was not always the same inverter that ran on the longest. Thus, the "maximum ROT" plots give the ROT of the inverter that stayed online the longest in each case, regardless of which inverter it was. (In other words, the "representative example" plots are all from the same inverter, and the "maximum ROT plots" show results from whichever inverter ran on the longest.)

A.1. Base case simulations

A.1.1. Thirty-three Percent Irradiance

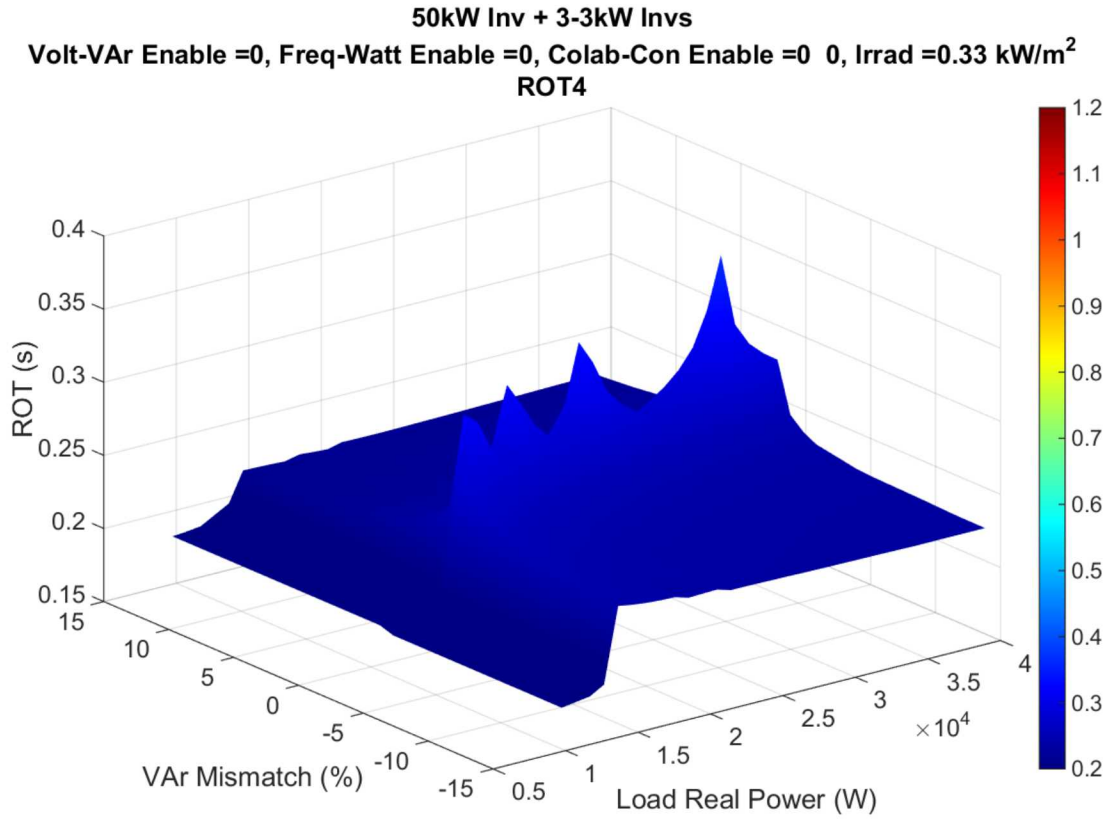

Figure 31. Representative example of ROTs vs. VAr mismatch and load power, 33% irradiance.

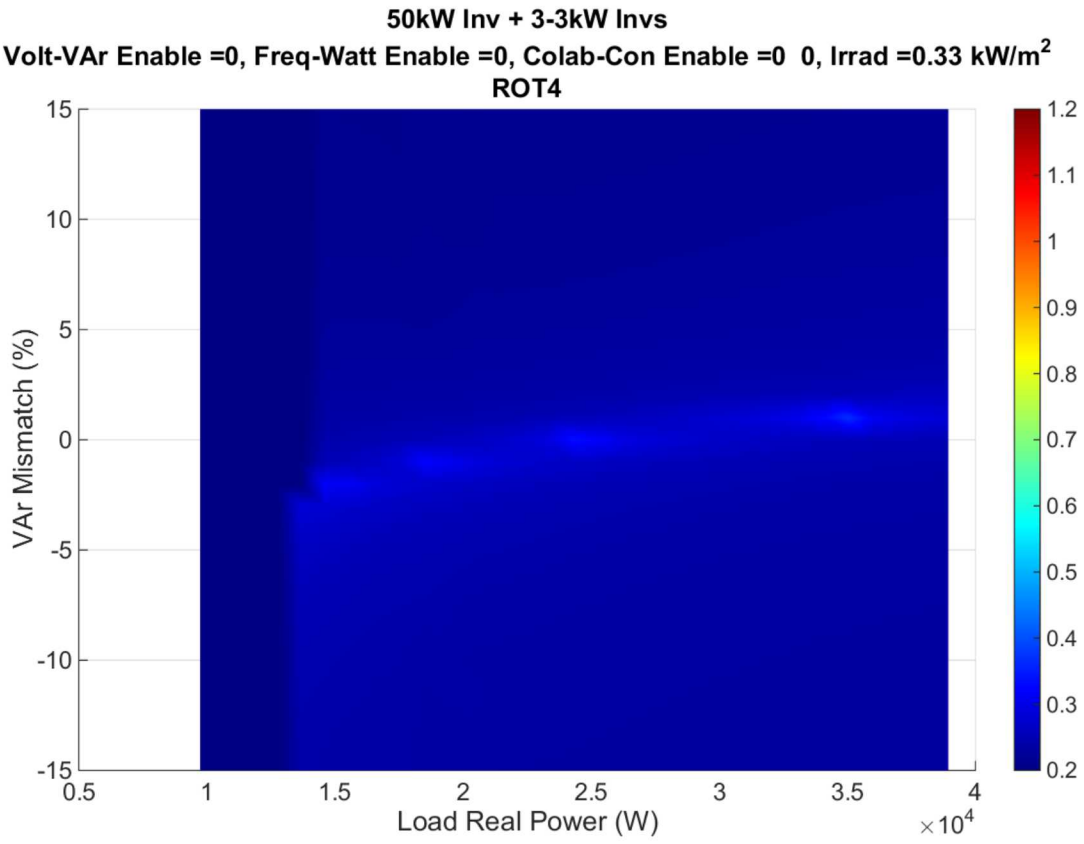

Figure 32. X-y plane view of Figure 31.

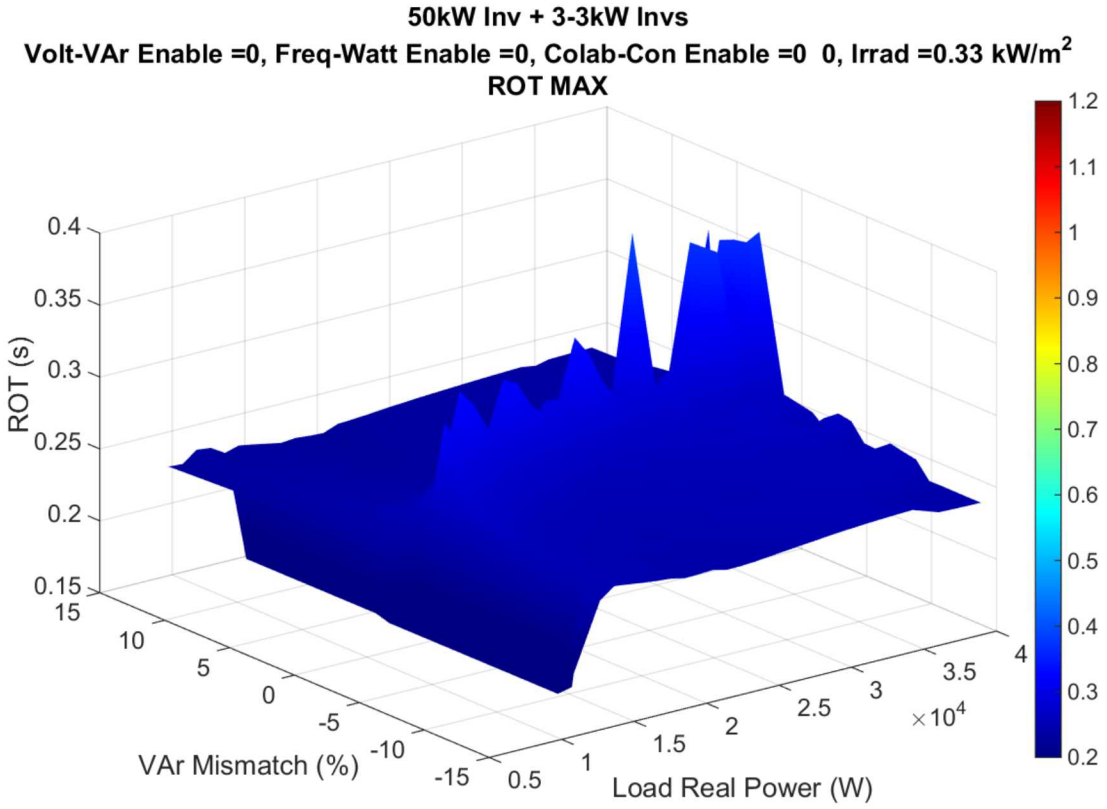

Figure 33. Maximum ROT observed from any inverter for each VAr mismatch-load real power pair, 33% irradiance.

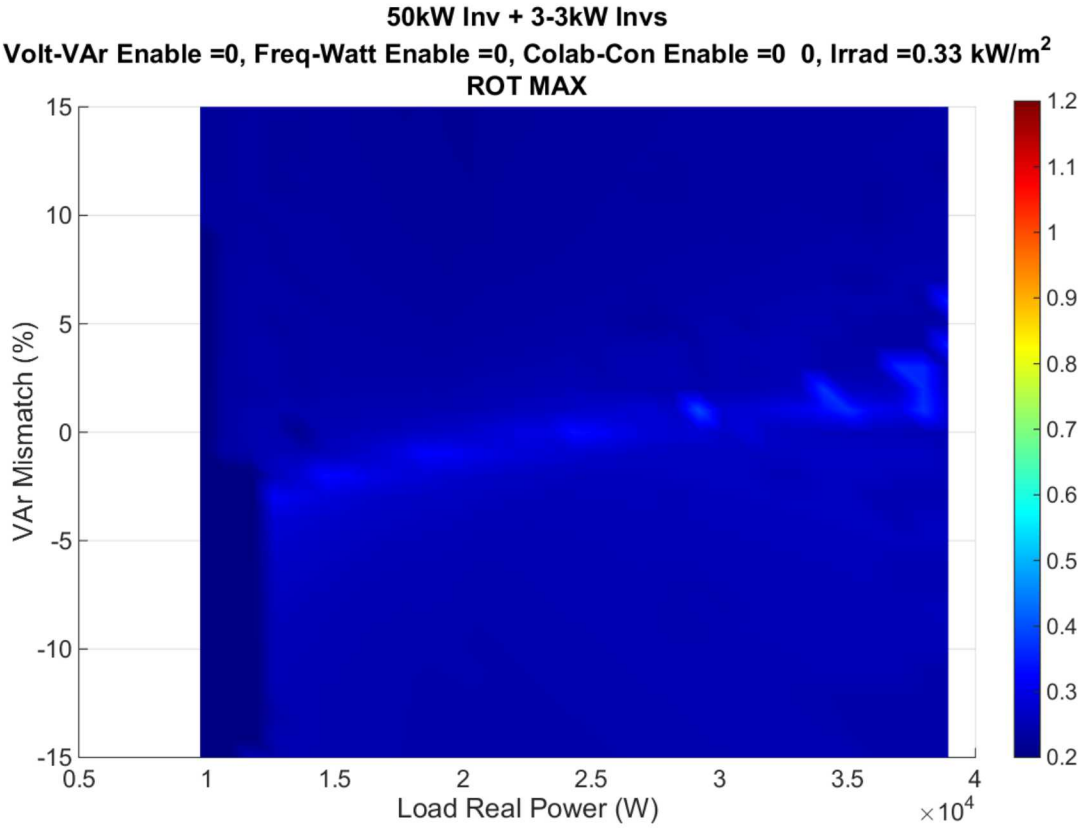

Figure 34. X-y plane view of Figure 33.

A.1.2. Sixty-six Percent Irradiance

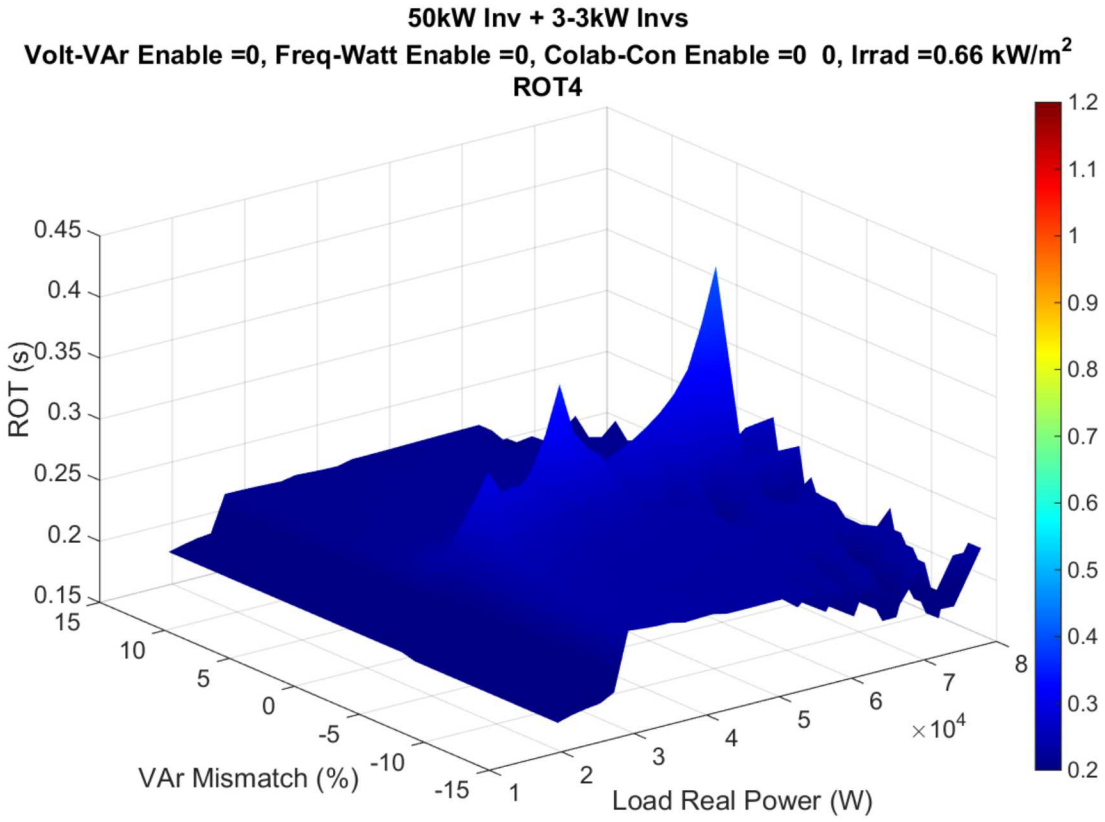

Figure 35. ROTs vs. var mismatch and load real power, 66% irradiance.

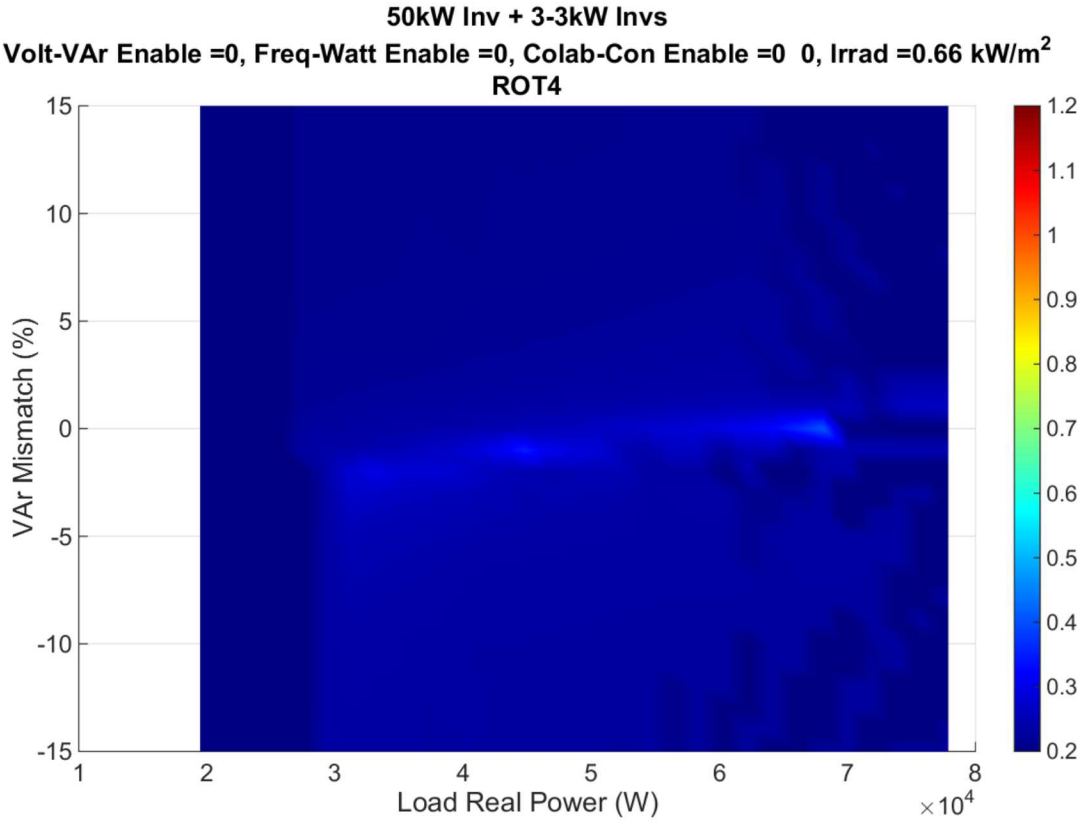

Figure 36. X-y plane view of Figure 35.

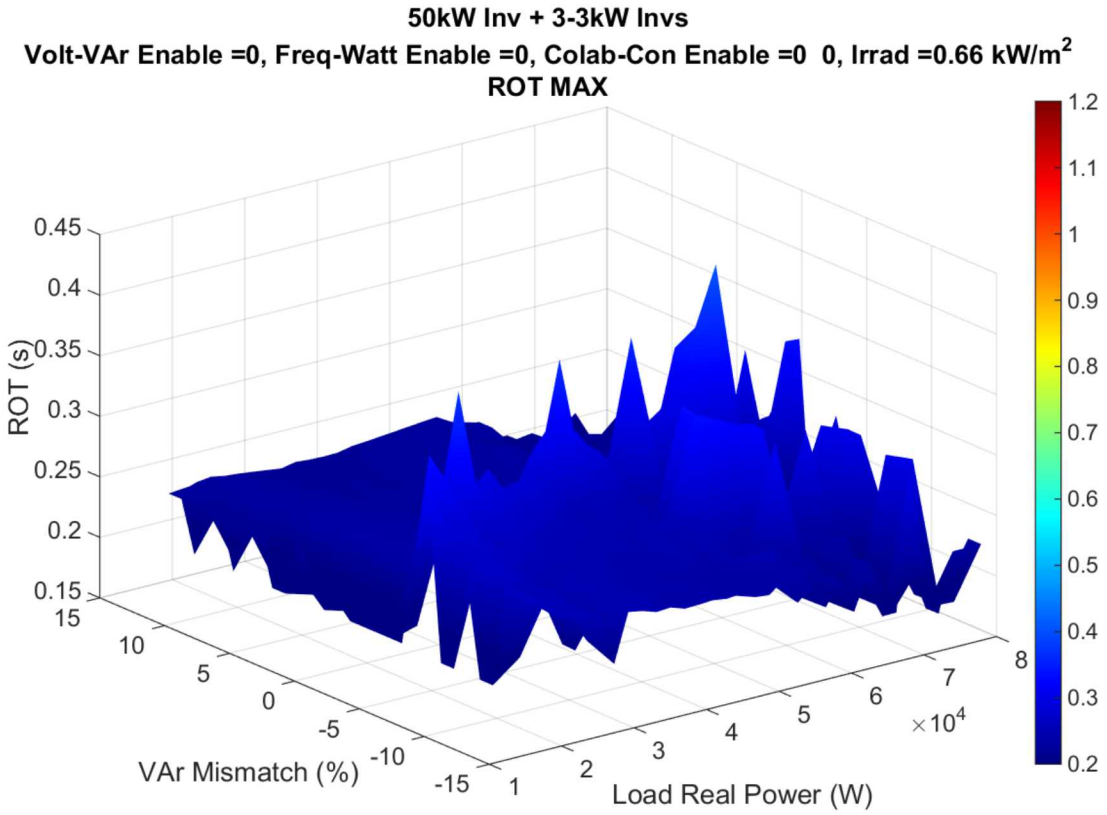

Figure 37. Maximum ROTs observed for any inverter for each var mismatch-load power pair, 66% irradiance.

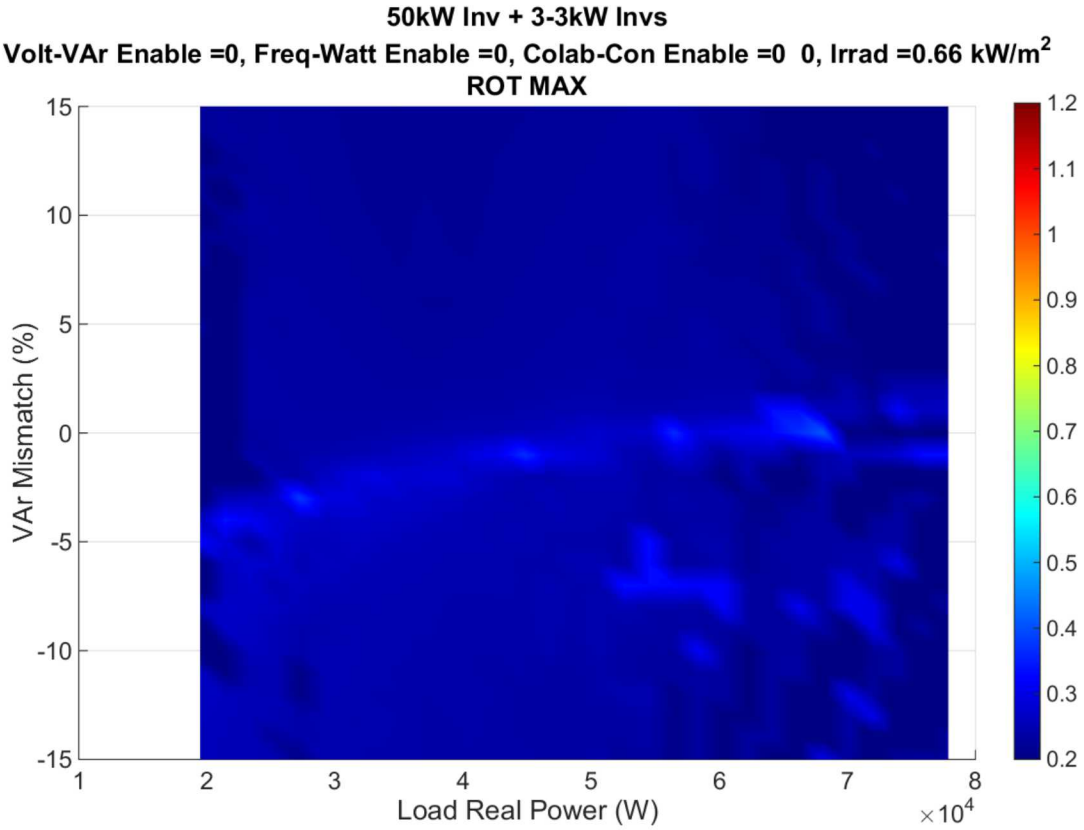

Figure 38. X-y plane view of Figure 37.

A.1.3. One-hundred Percent Irradiance

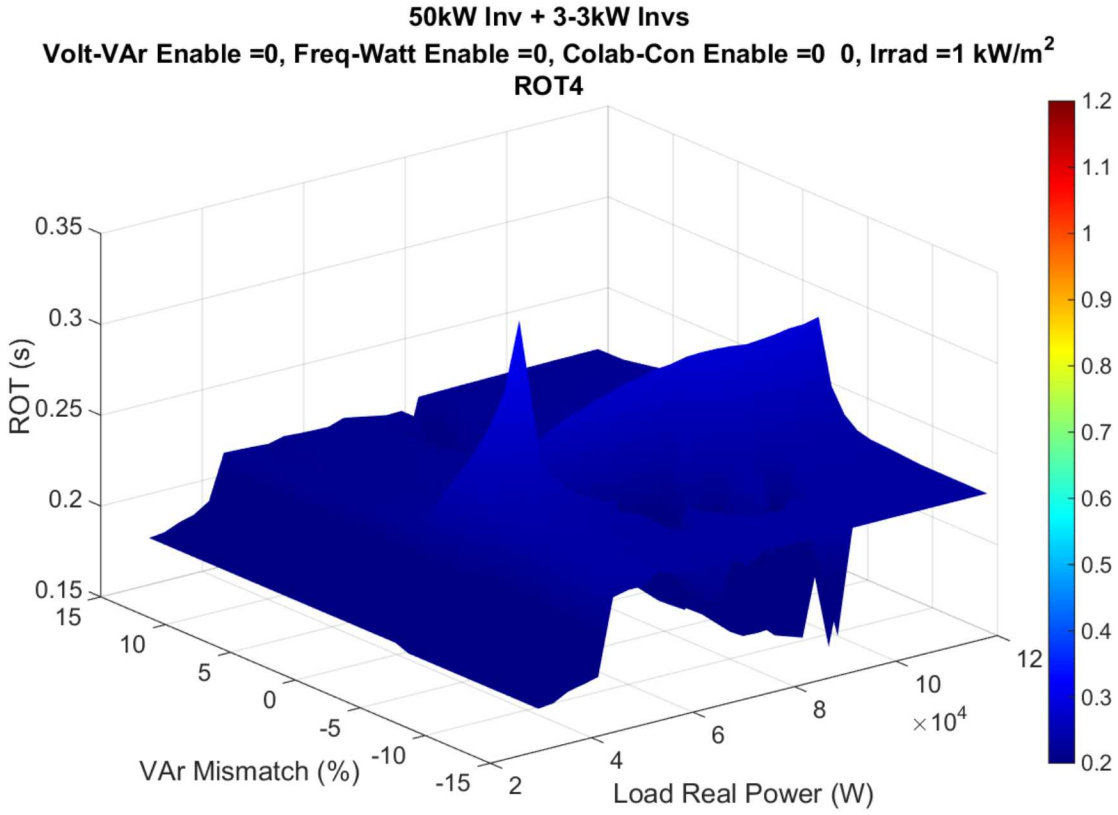

Figure 39. ROTs vs. var mismatch and load real power, 100% irradiance.

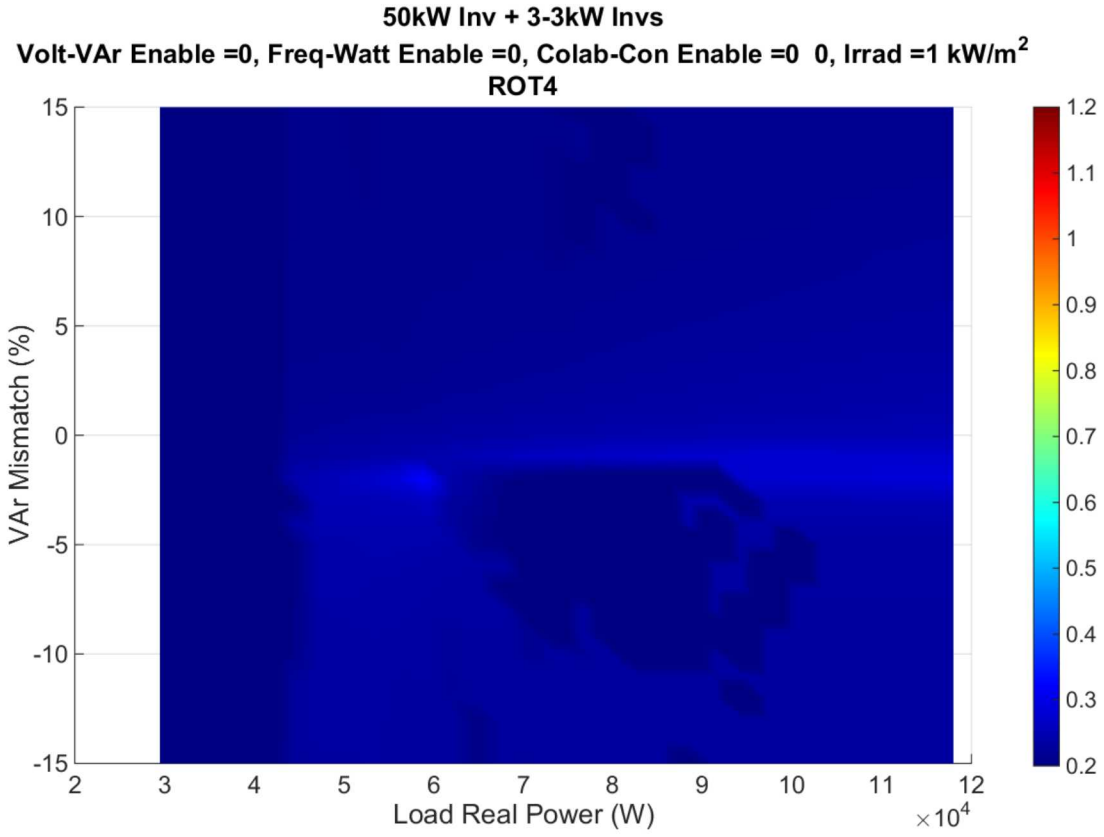

Figure 40. X-y plane view of Figure 39.

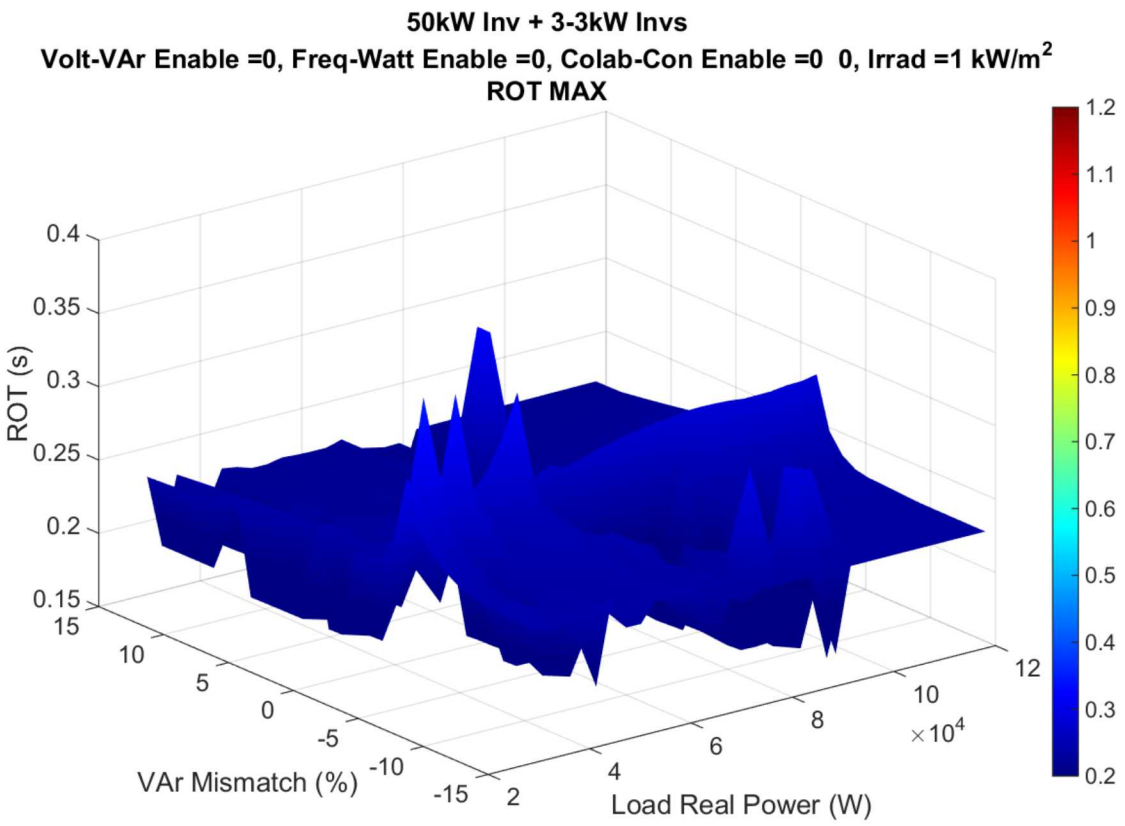

Figure 41. Maximum ROTs observed for each var mismatch-load power pair, 100% irradiance.

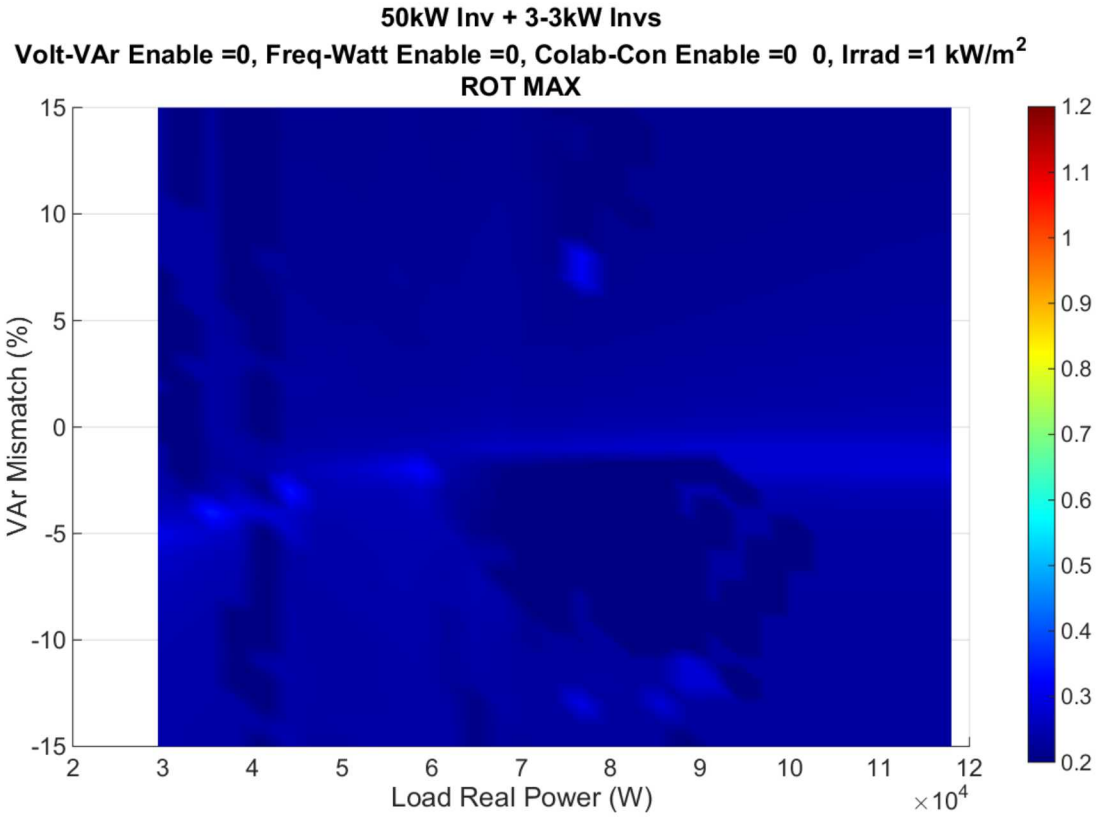

Figure 42. X-y plane view of Figure 41.

A.2. GSFs on, RTs off, CC off

For this next set of simulation results, shown in Figure 43 through Figure 54, the grid support functions (voltage and frequency ride-throughs, volt-var droops, and frequency-Watt droops) are all enabled, but the relays are set to the 1547-2003 values (no ride-throughs). Results are presented for three different irradiance levels: 0.33 kW/m^2, 0.66 kW/m^2, and 1 kW/m^2.

These results indicate that the use of 1547-2003 trips and active GSFs has slightly degraded the ability of the inverters to detect island formation. The maximum ROTs are now approaching 600 ms, which is a roughly 33% increase over the base case. The overall shapes of the surfaces for each irradiance case are essentially the same as in the base case.

A.2.1. Thirty-three Percent Irradiance

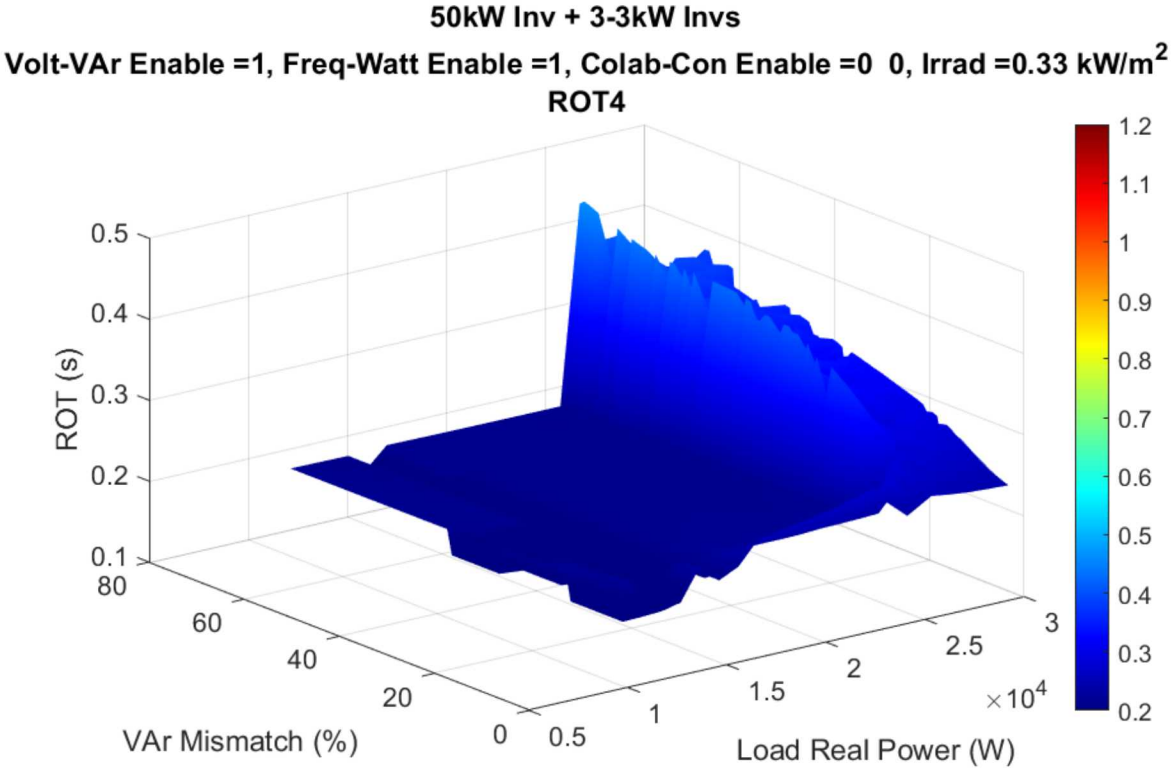

Figure 43. ROTs vs. var mismatch and load real power power, 33% irradiance.

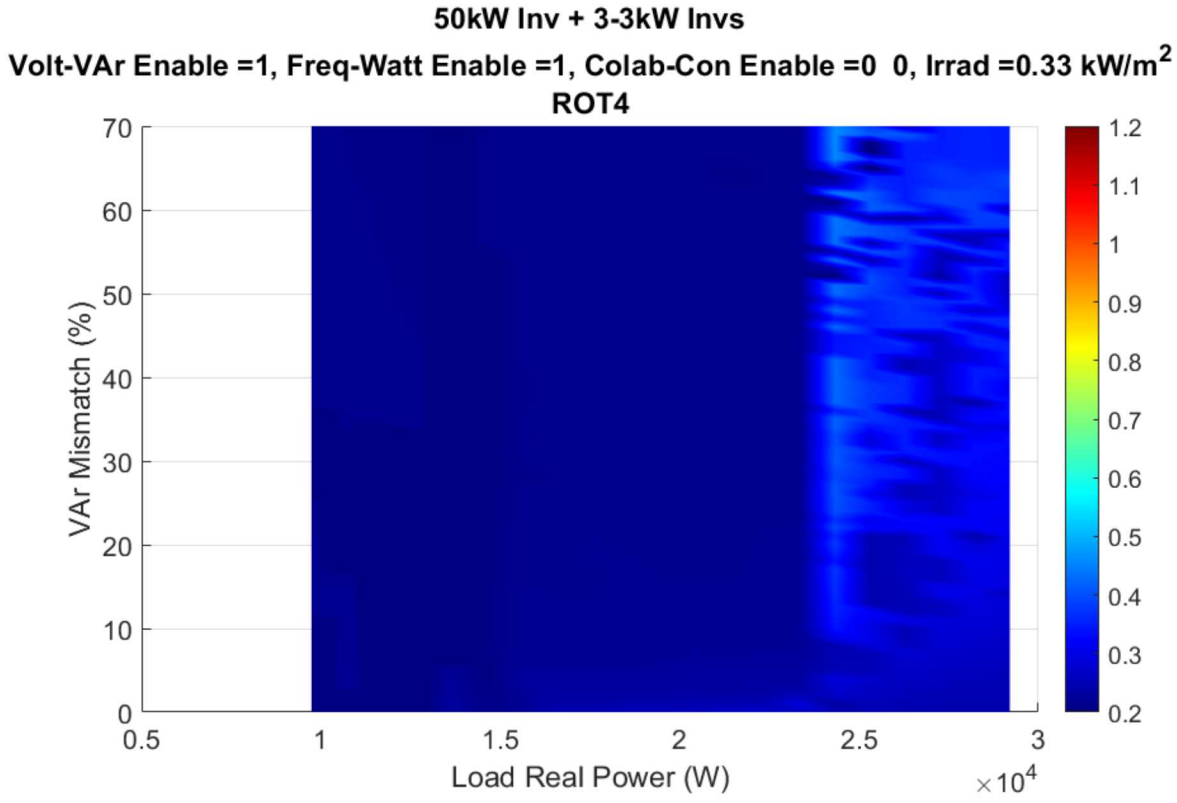

Figure 44. X-y plane view of Figure 43.

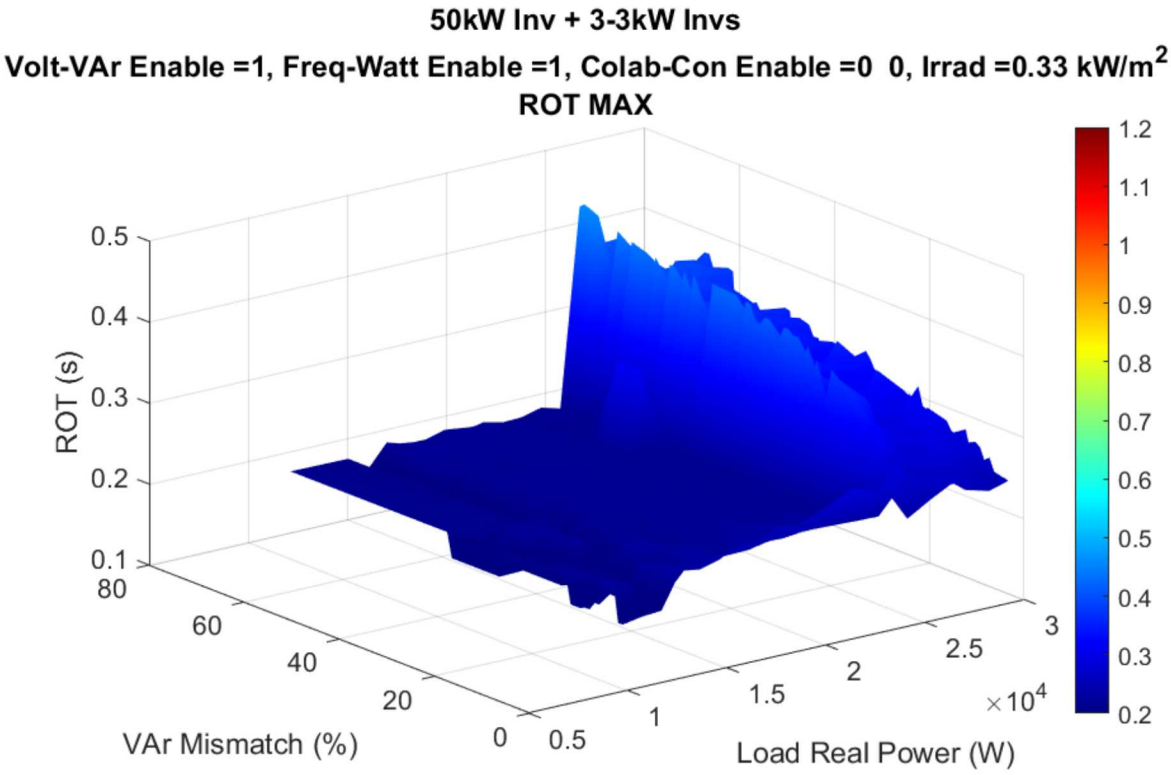

Figure 45. Maximum ROT observed for each var mismatch-load real power pair, 33% irradiance.

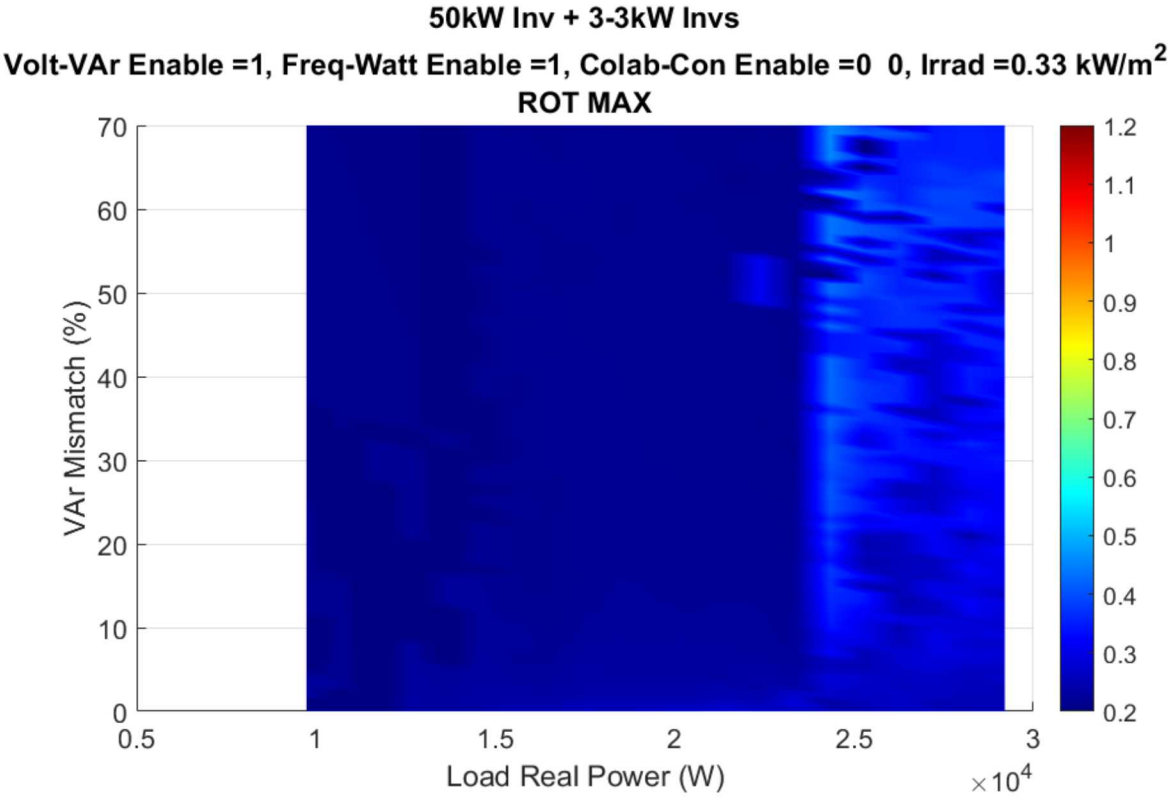

Figure 46. X-y plane view of Figure 45.

A.2.2. Sixty-six Percent Irradiance

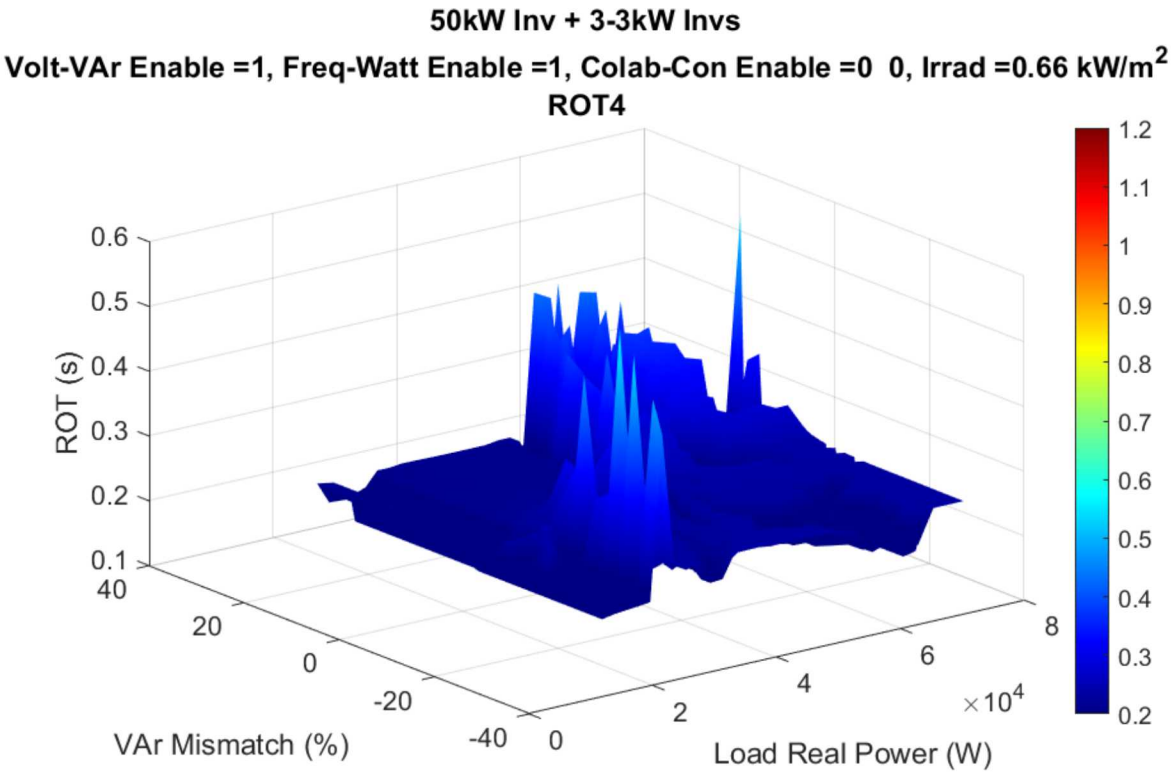

Figure 47. ROTs vs. var mismatch and load real power, 66% irradiance.

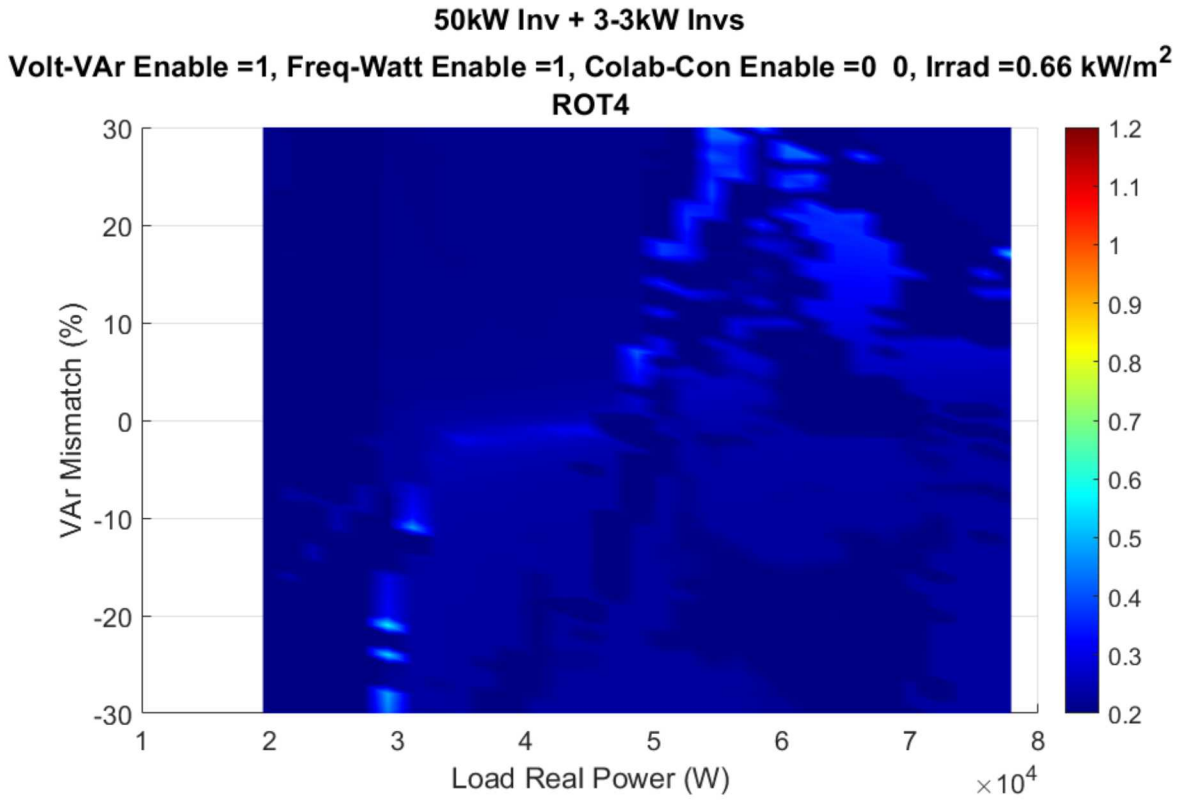

Figure 48. X-y plane view of Figure 47.

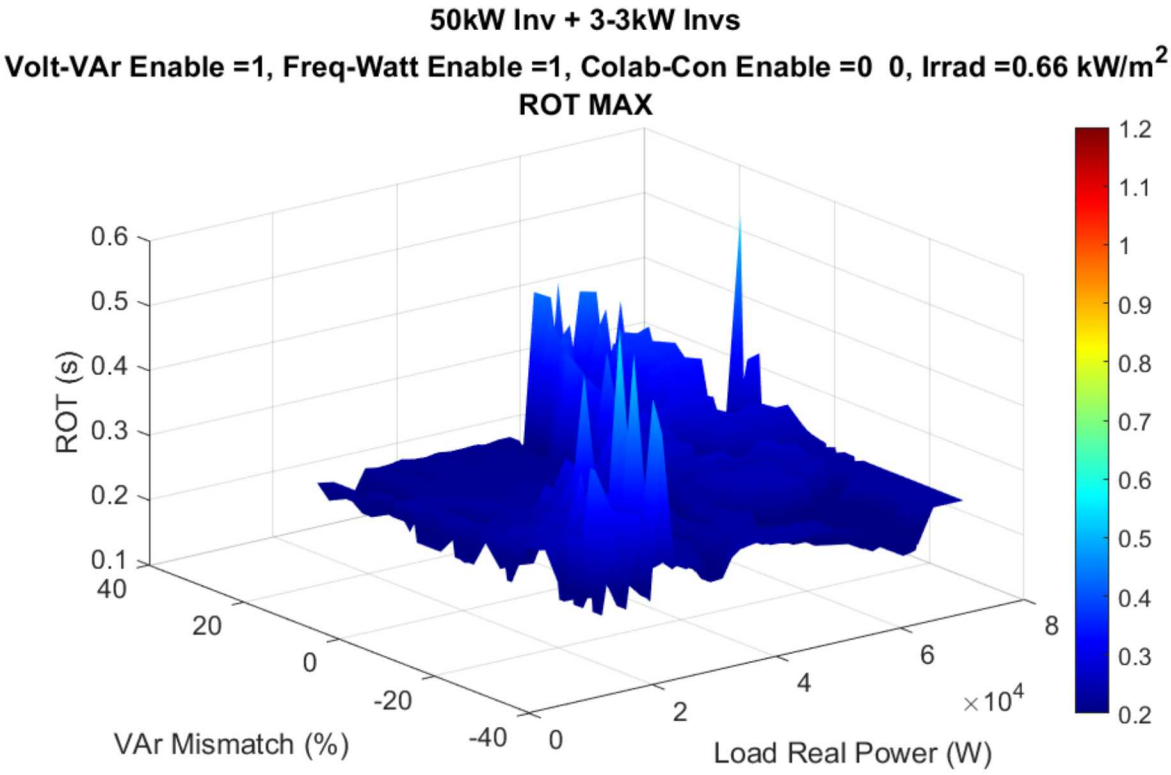

Figure 49. Maximum ROTs observed for each var mismatch-load power pair, 66% irradiance.

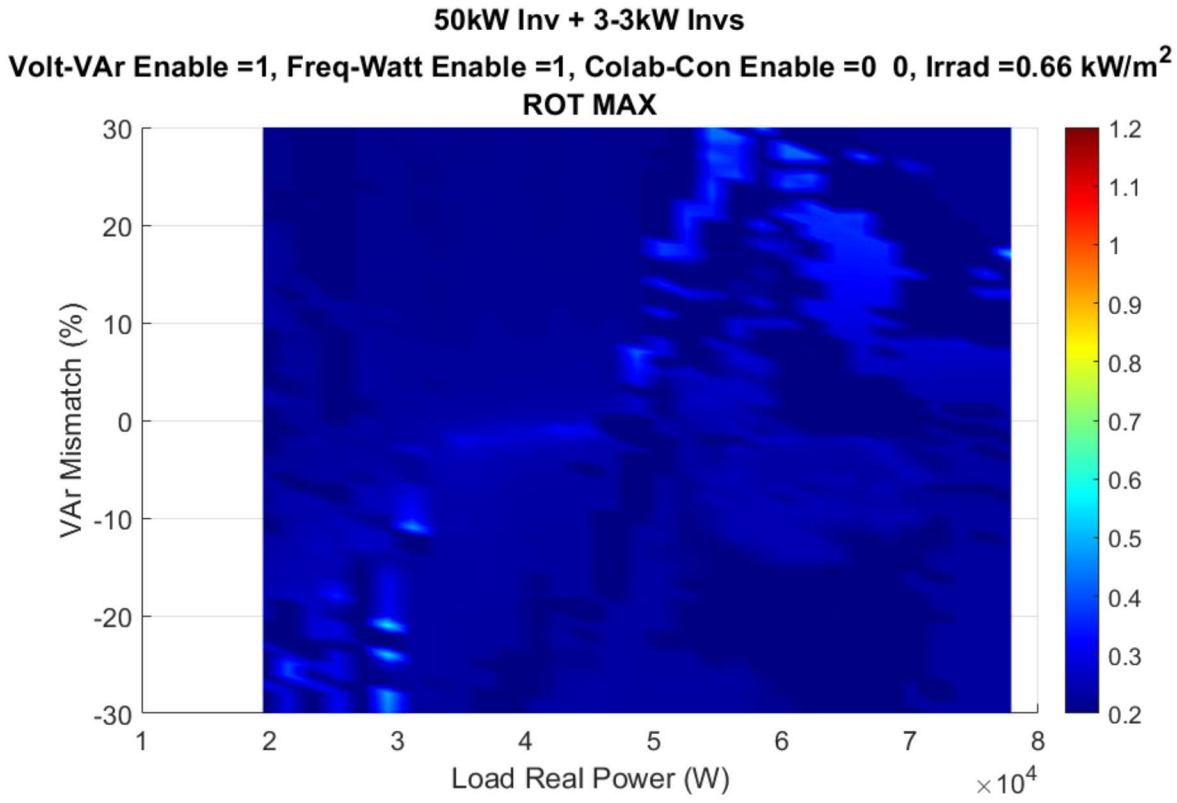

Figure 50. X-y plane view of Figure 49.

A.2.3. One-hundred Percent Irradiance

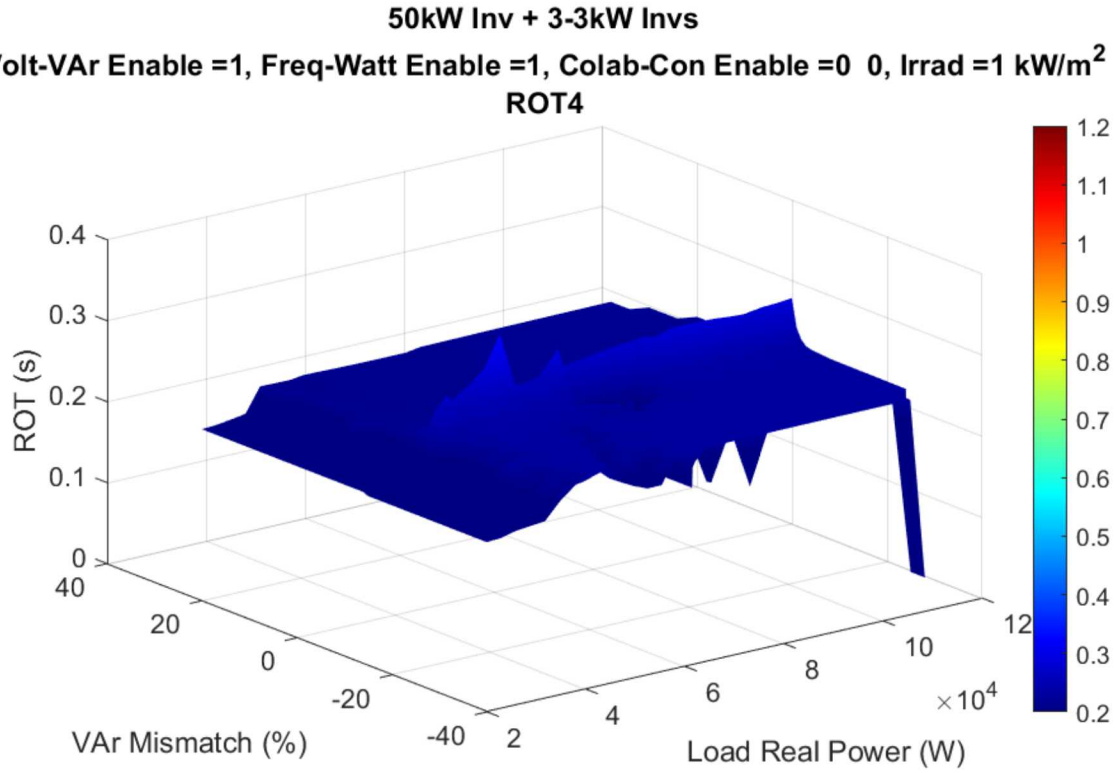

Figure 51. ROTs vs. var mismatch and load real power, 100% irradiance.

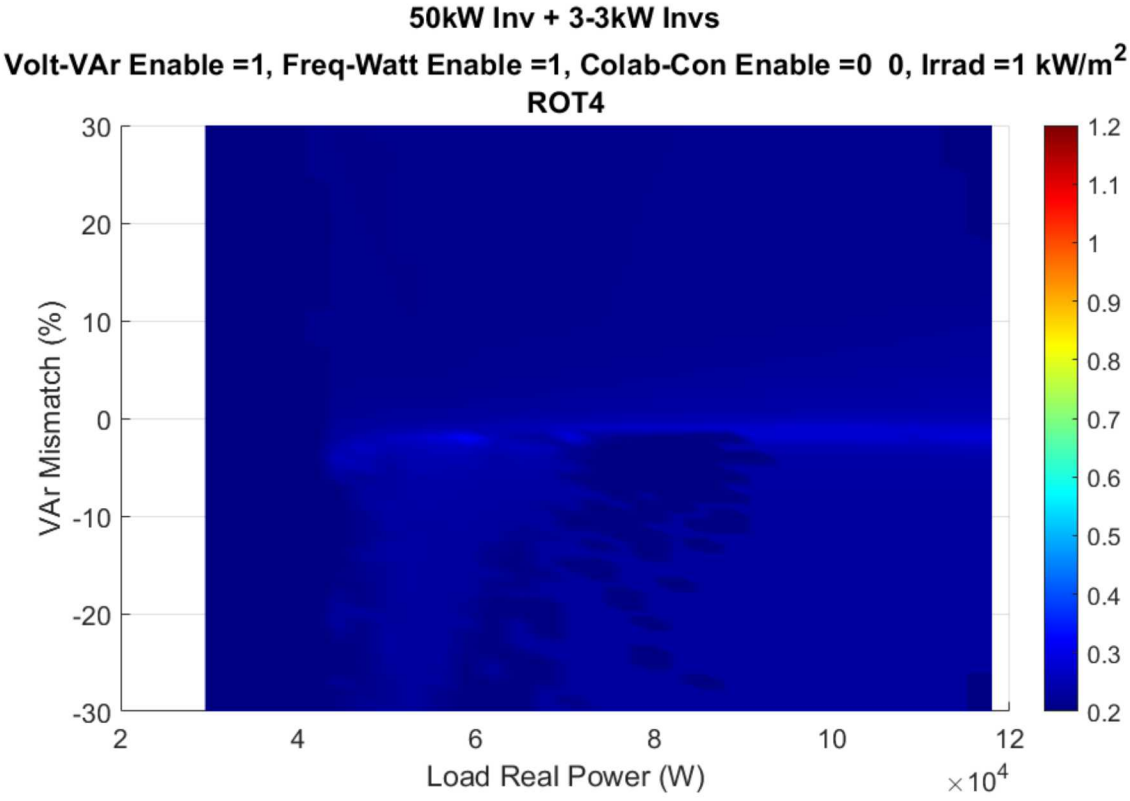

Figure 52. X-y plane view of Figure 51.

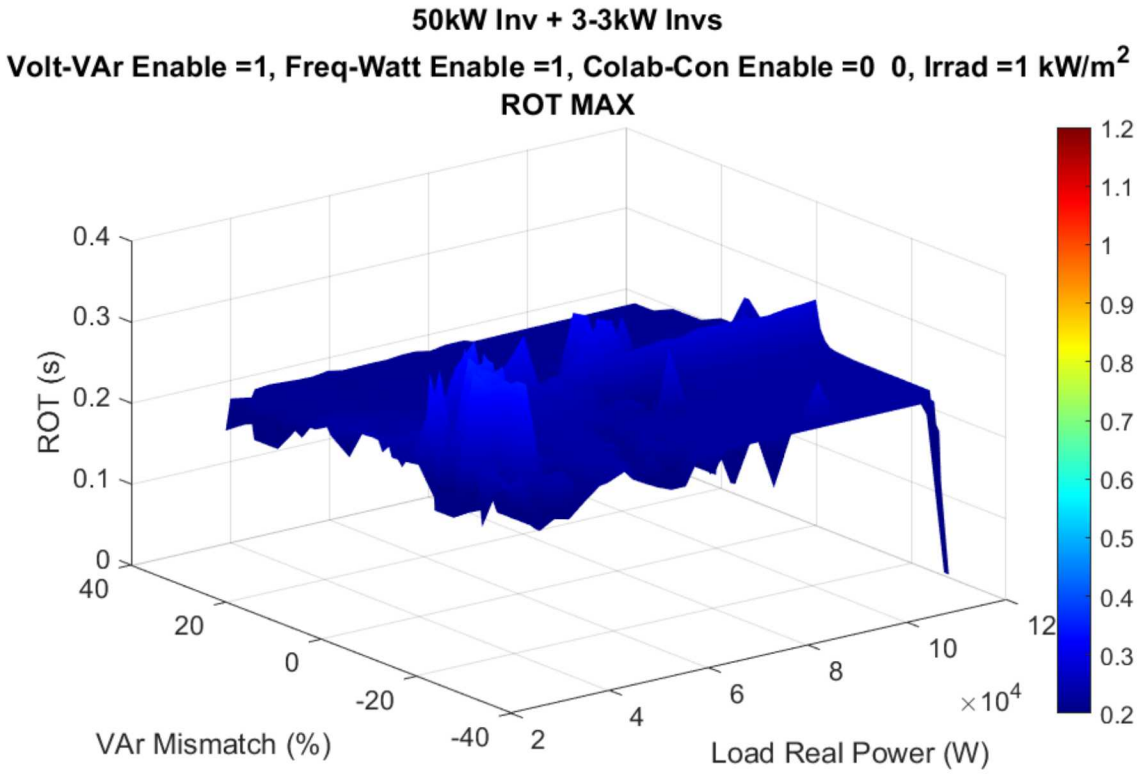

Figure 53. Maximum ROTs observed for each var mismatch-load power pair, 100% irradiance.

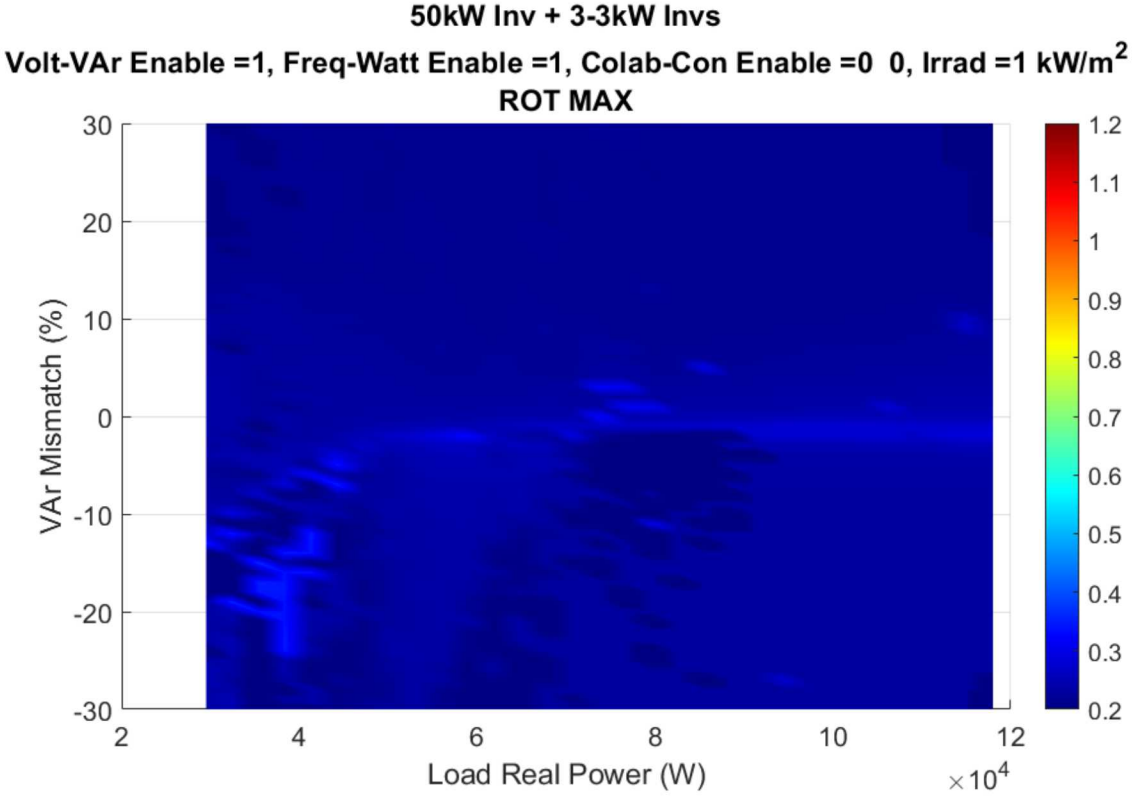

Figure 54. X-y plane view of Figure 53.

A.3. GSFs on, RTs off, CC on

For this next set of simulation results, shown in Figure 55 through Figure 66, the grid support functions (voltage and frequency ride-throughs, volt-var droops, and frequency-Watt droops) are all enabled, the relays are set to the 1547-2003 settings, and the collaborative controls are enabled. Results are presented for three different irradiance levels: 0.33 kW/m^2, 0.66 kW/m^2, and 1 kW/m^2.

These results are quite similar in shape and duration to those of the previous test in which the collaborative controls were off. The maximum ROTs still approach 0.6 sec, and the shapes of the surfaces are essentially the same.

A.3.1. Thirty-three Percent Irradiance

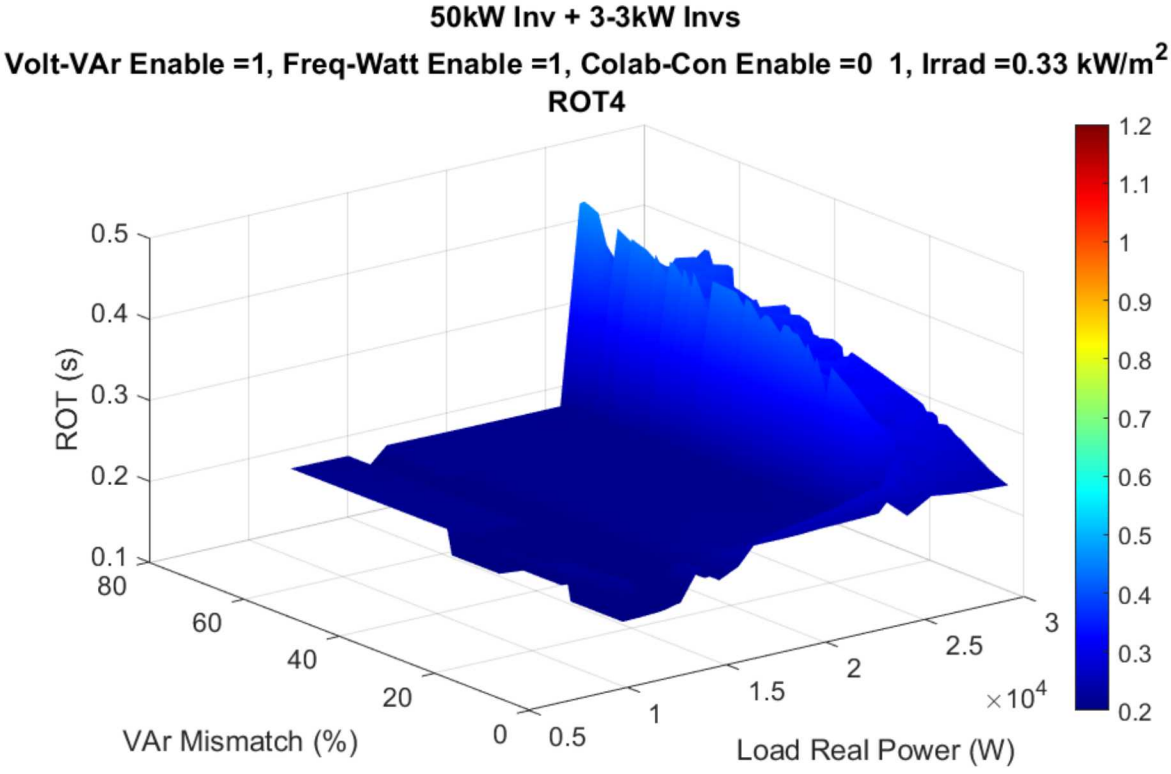

Figure 55. Representative example of ROTs vs. var mismatch and load power, 33% irradiance.

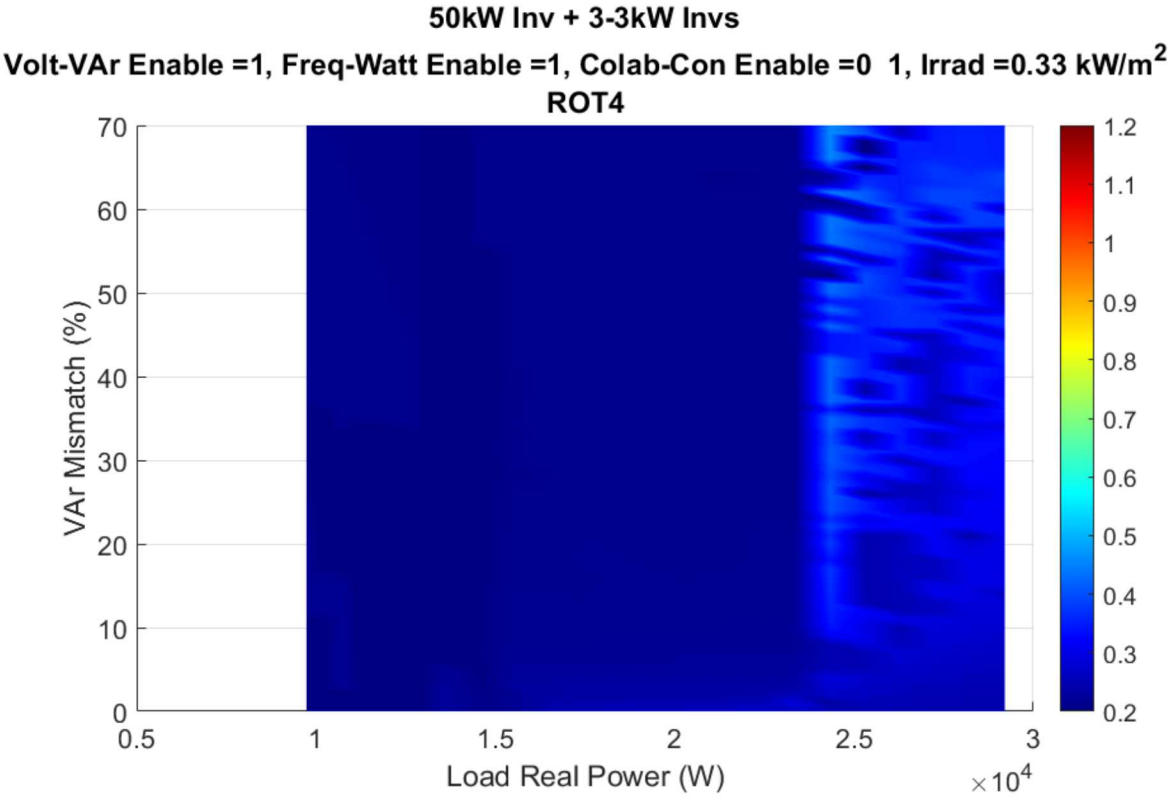

Figure 56. X-y plane view of Figure 55.

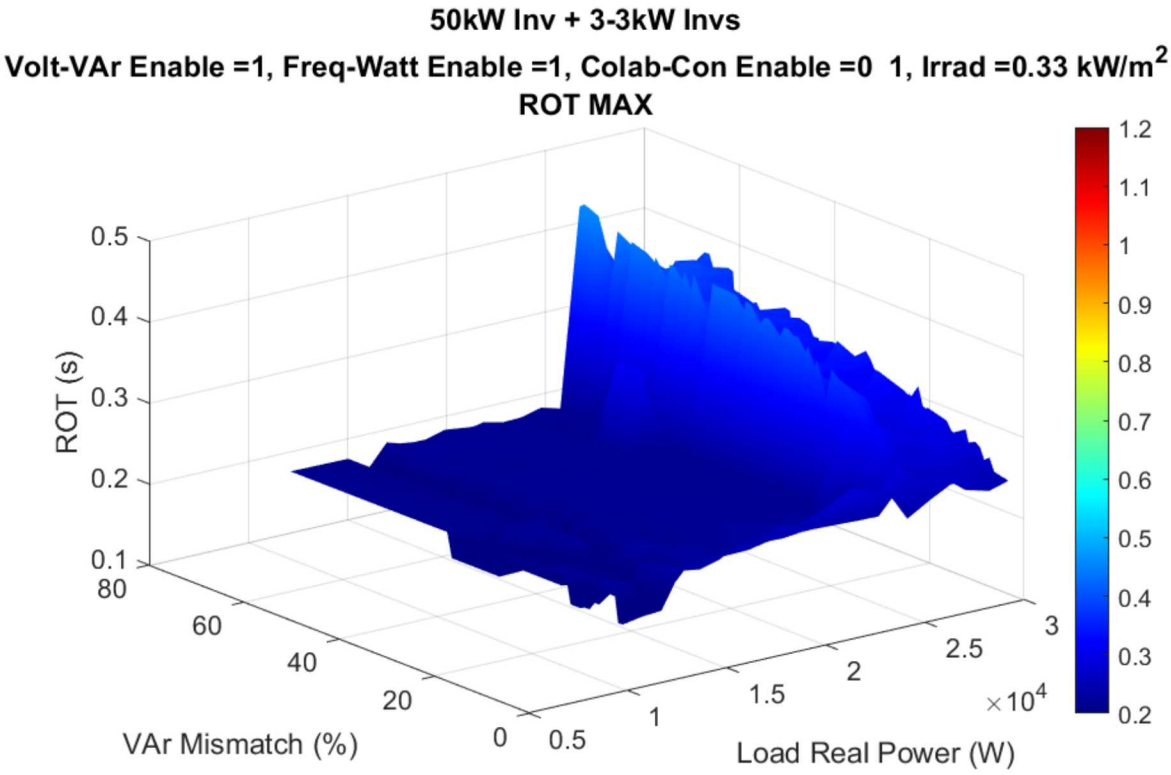

Figure 57. Maximum ROT observed for each var mismatch-load real power pair, 33% irradiance.

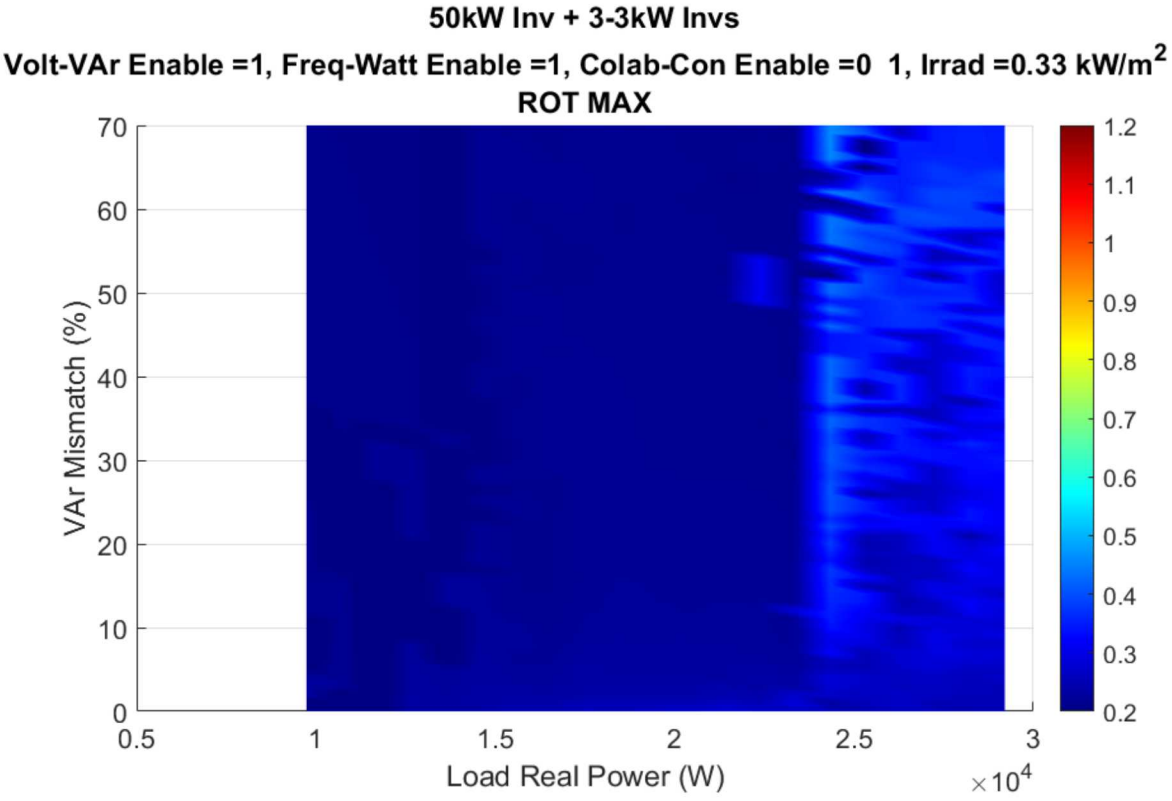

Figure 58. X-y plane view of Figure 57.

A.3.2. Sixty-six Percent Irradiance

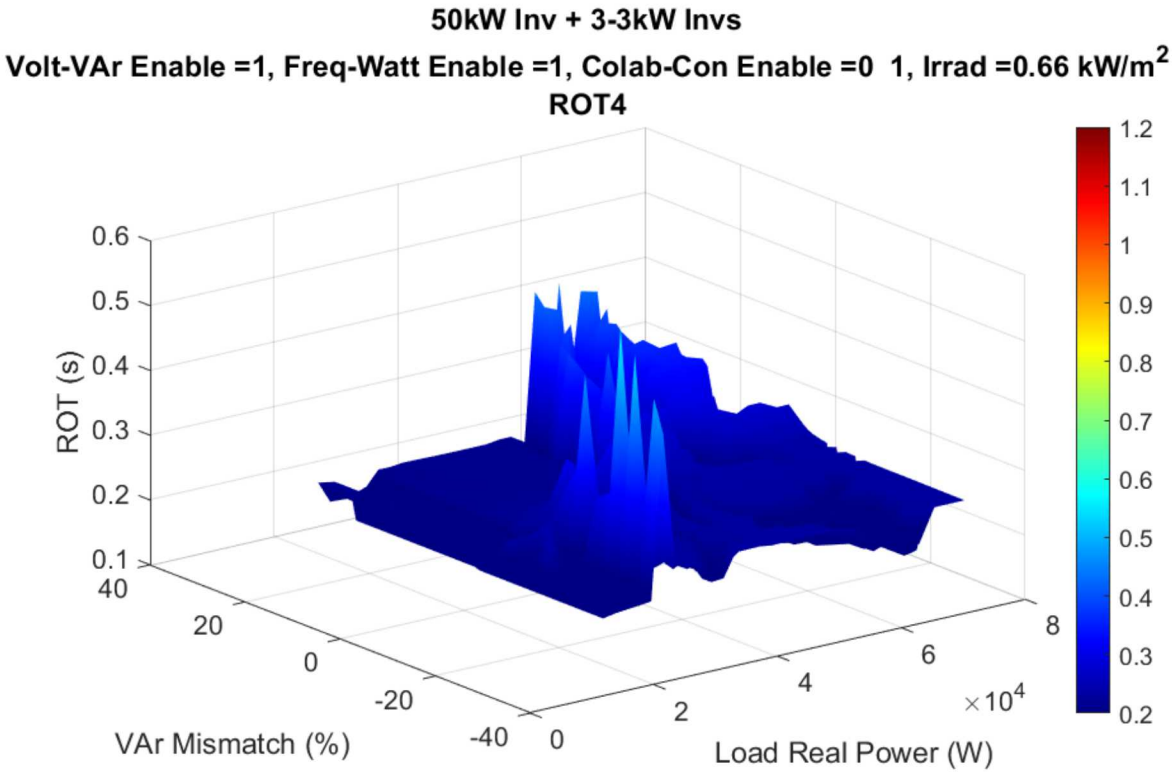

Figure 59. ROTs vs. var mismatch and load real power, 66% irradiance.

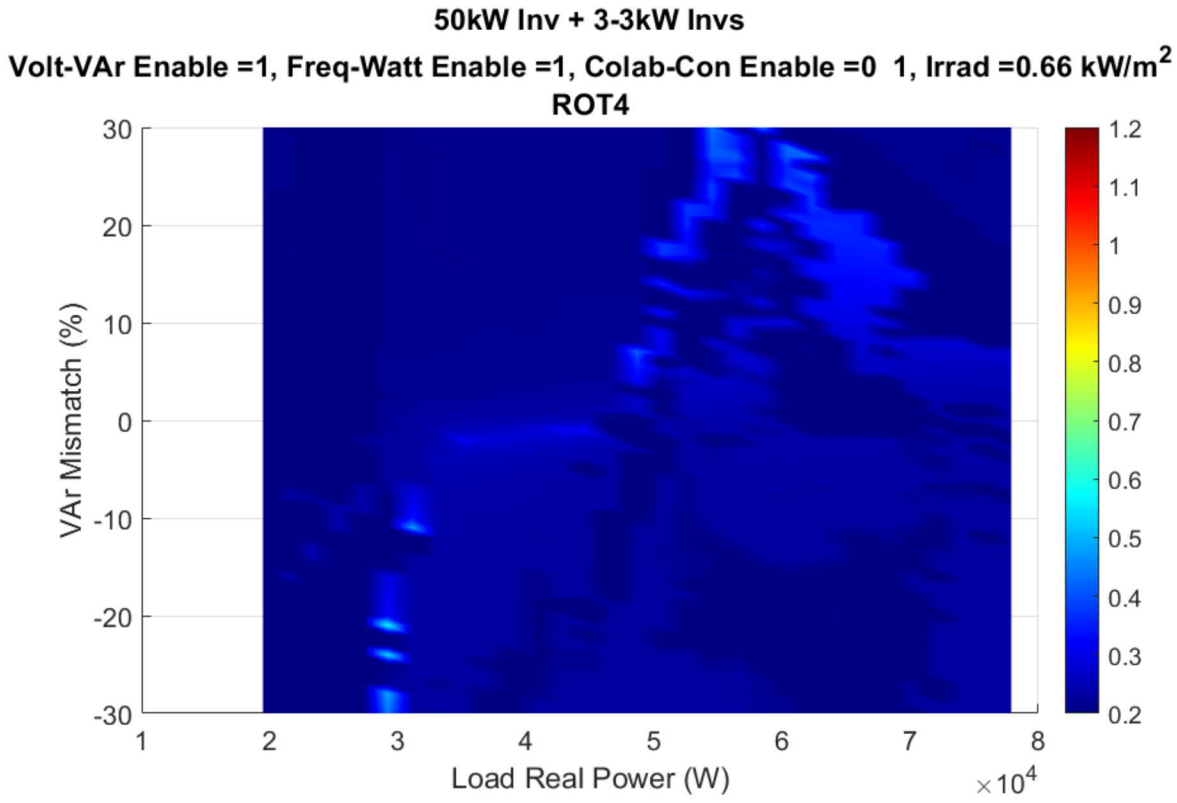

Figure 60. X-y plane view of Figure 59.

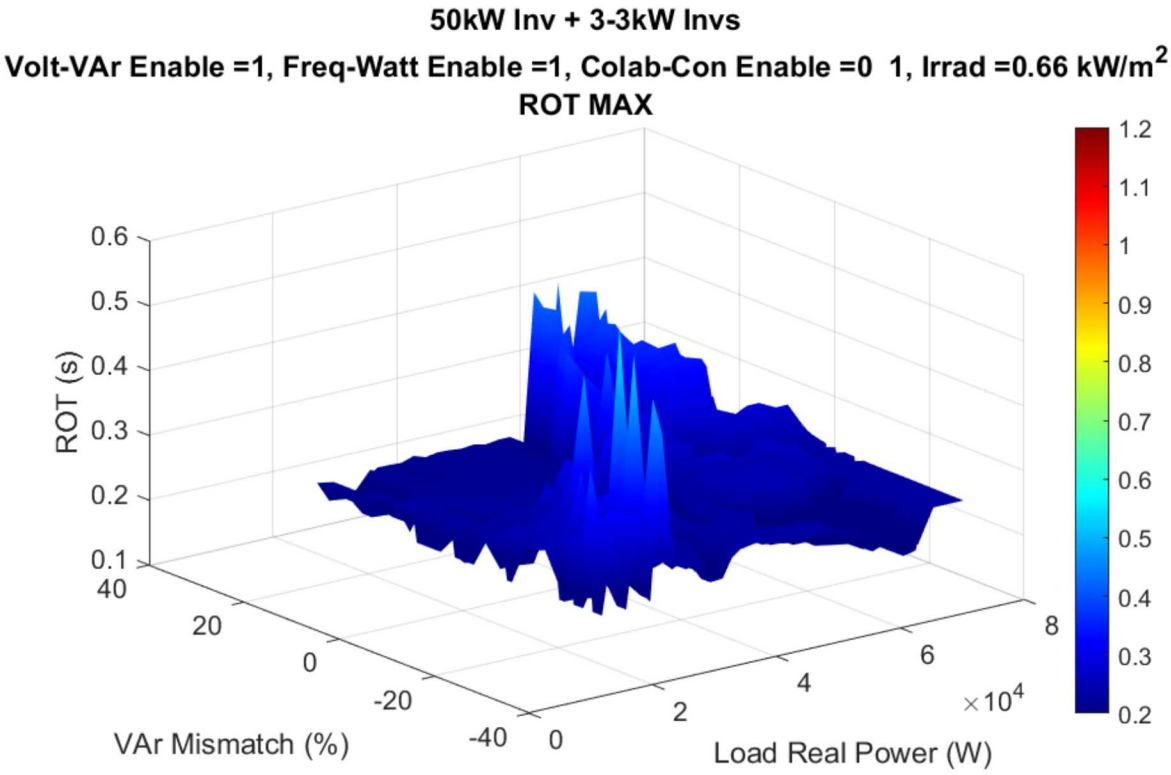

Figure 61. Maximum ROTs observed for each var mismatch-load power pair, 66% irradiance.

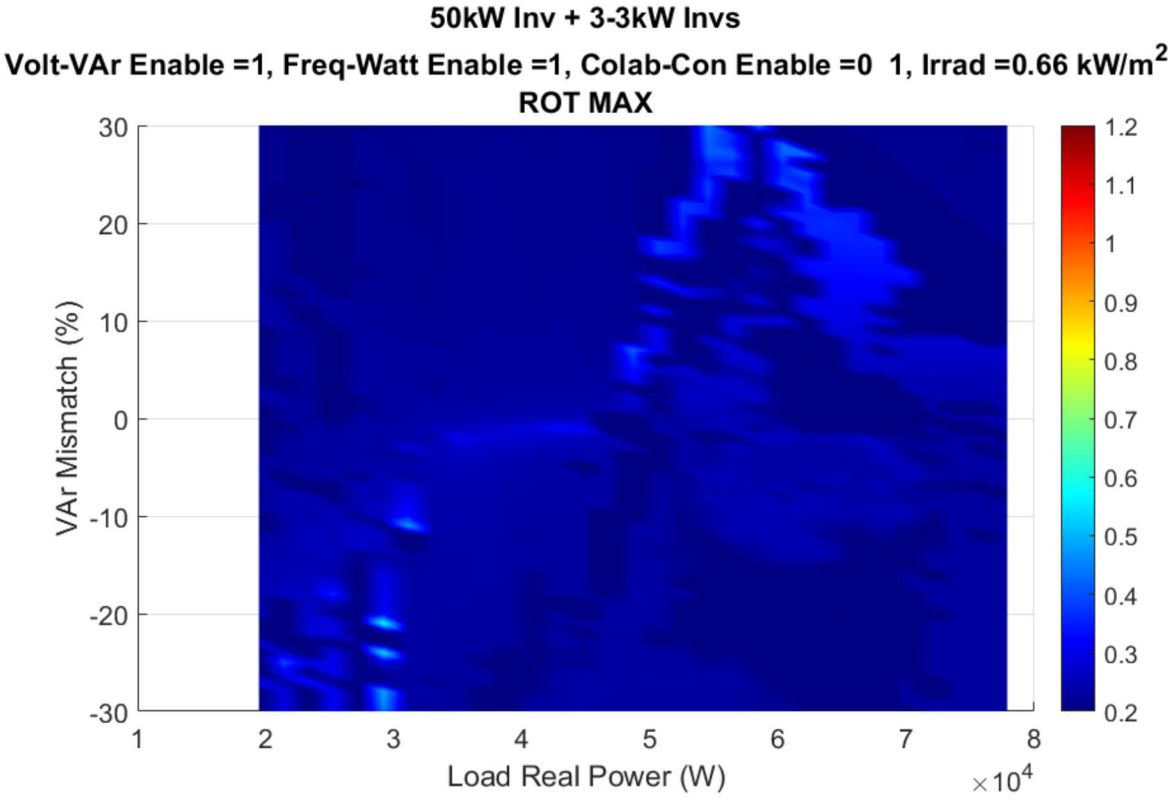

Figure 62. X-y plane view of Figure 61.

A.3.3. One-hundred Percent Irradiance

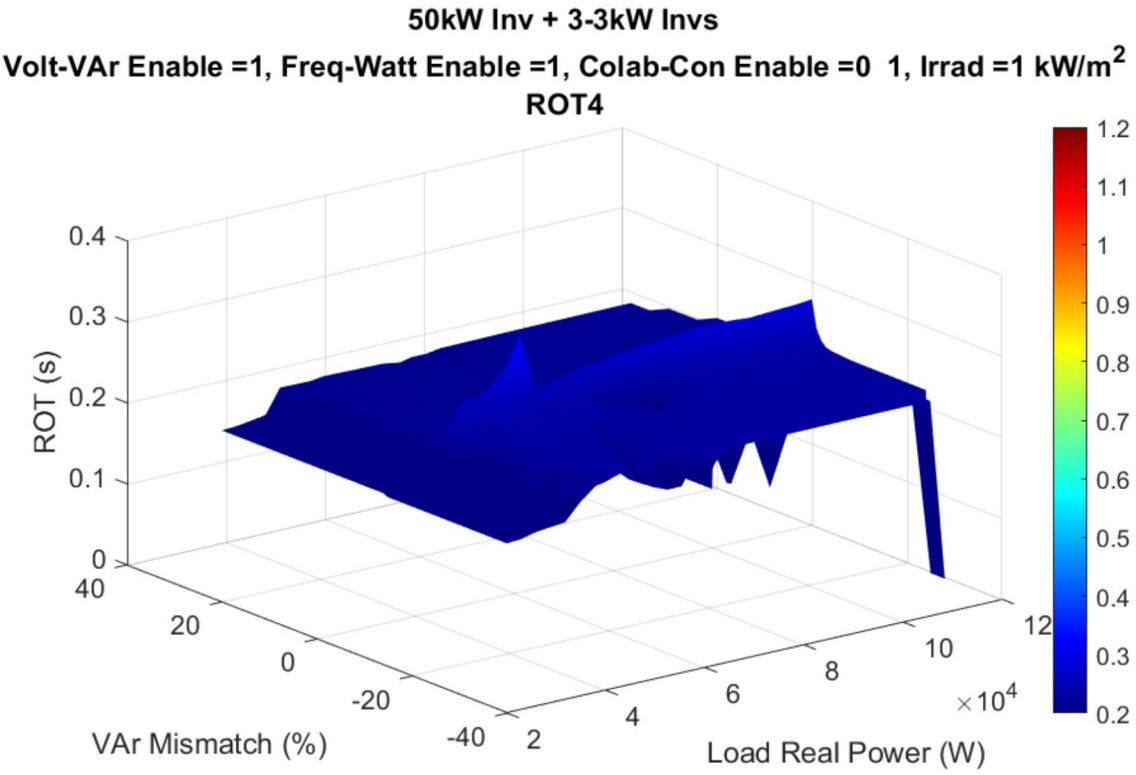

Figure 63. ROTs vs. var mismatch and load real power, 100% irradiance.

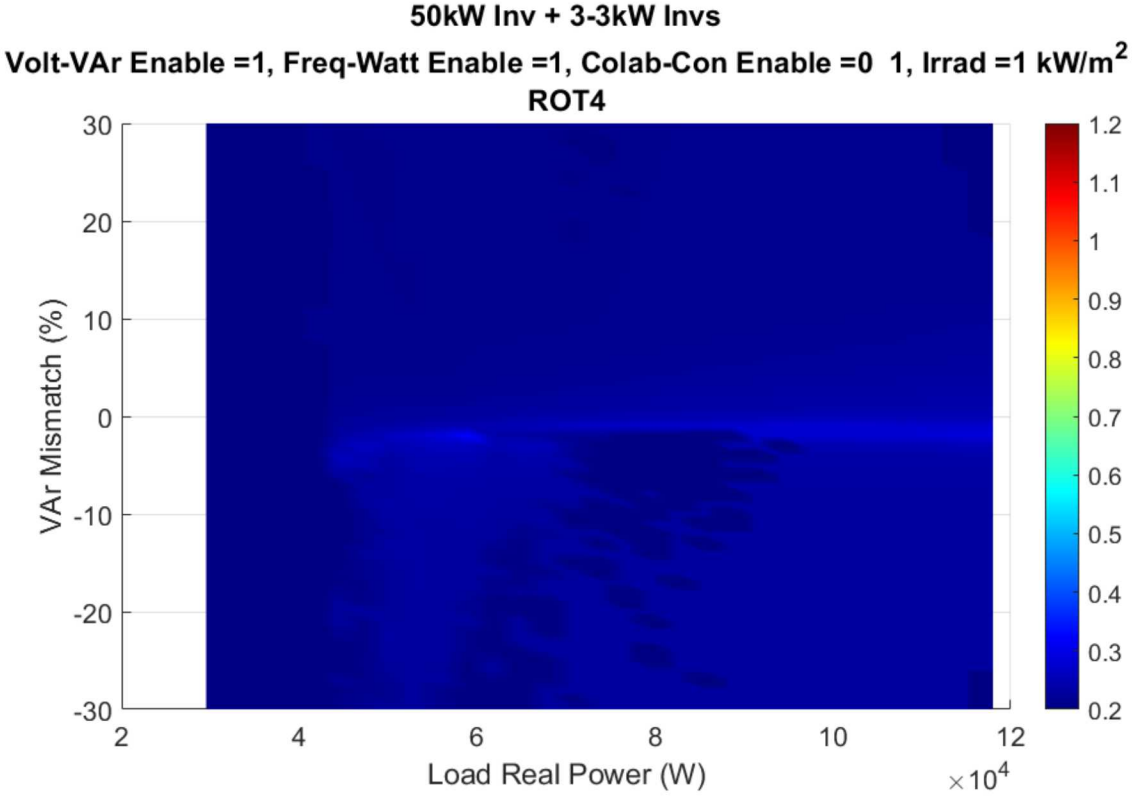

Figure 64. X-y plane view of Figure 63.

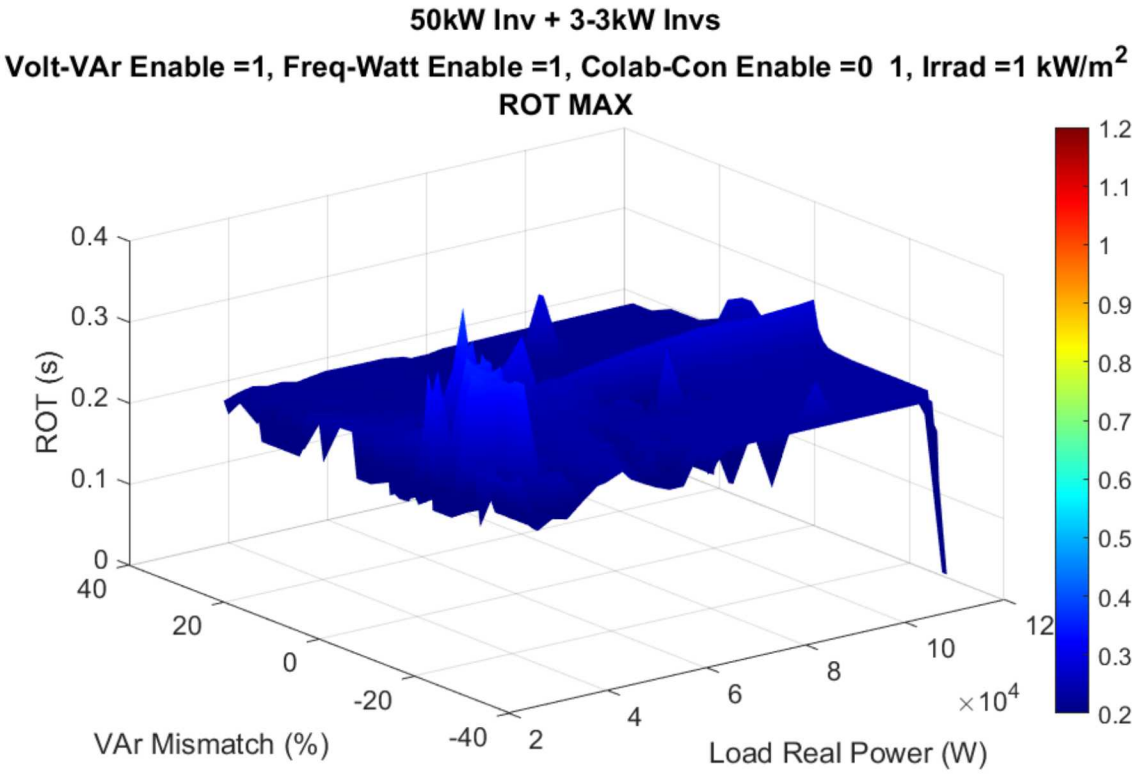

Figure 65. Maximum ROTs observed for each var mismatch-load power pair, 100% irradiance.

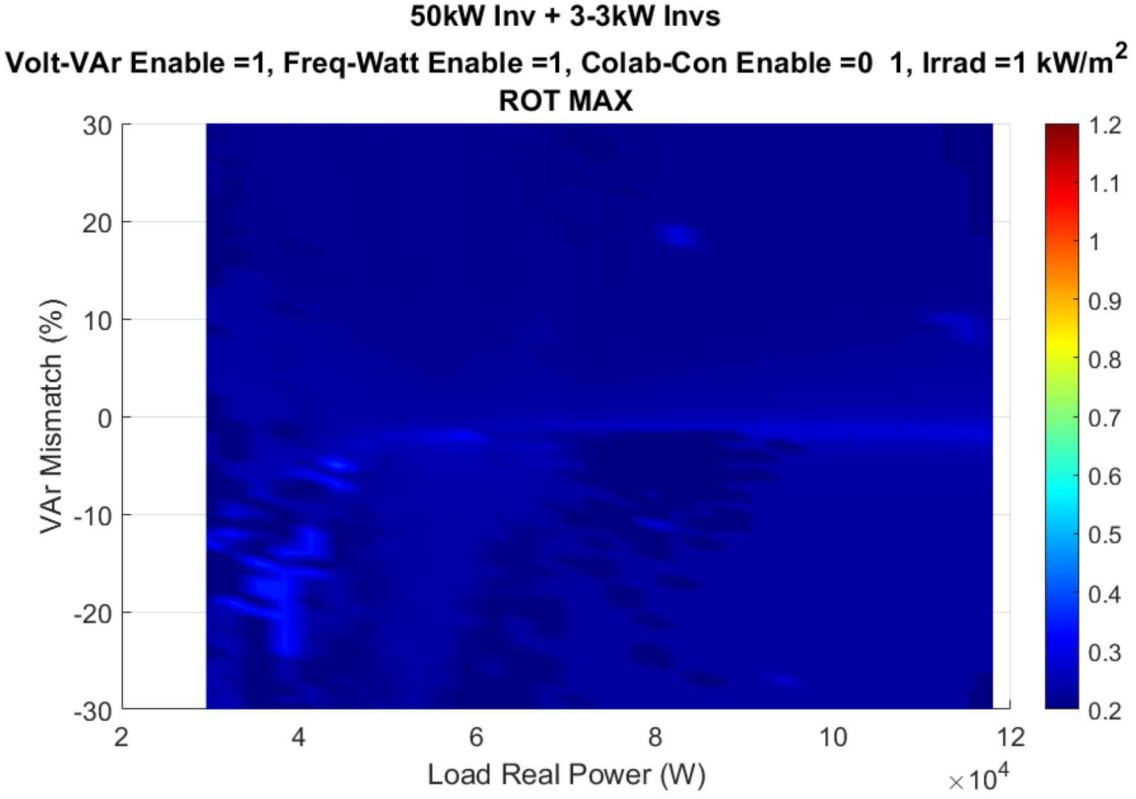

Figure 66. X-y plane view of Figure 65.

A.4. GSFs on, RTs on, CC off

For this next set of simulation results, shown in Figure 67 through Figure 78, the grid support functions (voltage and frequency ride-throughs, volt-var droops, and frequency-Watt droops) are all enabled, and the relay trip settings are widened and times-to-trip lengthened according to the IEEE 1547A recommendations. Results are presented for three different irradiance levels: 0.33 kW/m^2, 0.66 kW/m^2, and 1 kW/m^2.

These results indicate that the use of 1547A trips and active GSFs has definitely degraded the ability of the inverters to detect island formation. No ROT exceeds 2 sec, but the maximum ROTs are now approaching 1.2 sec, or roughly a factor of three increase in maximum ROTs over the base case.

A.4.1. Thirty-three Percent Irradiance

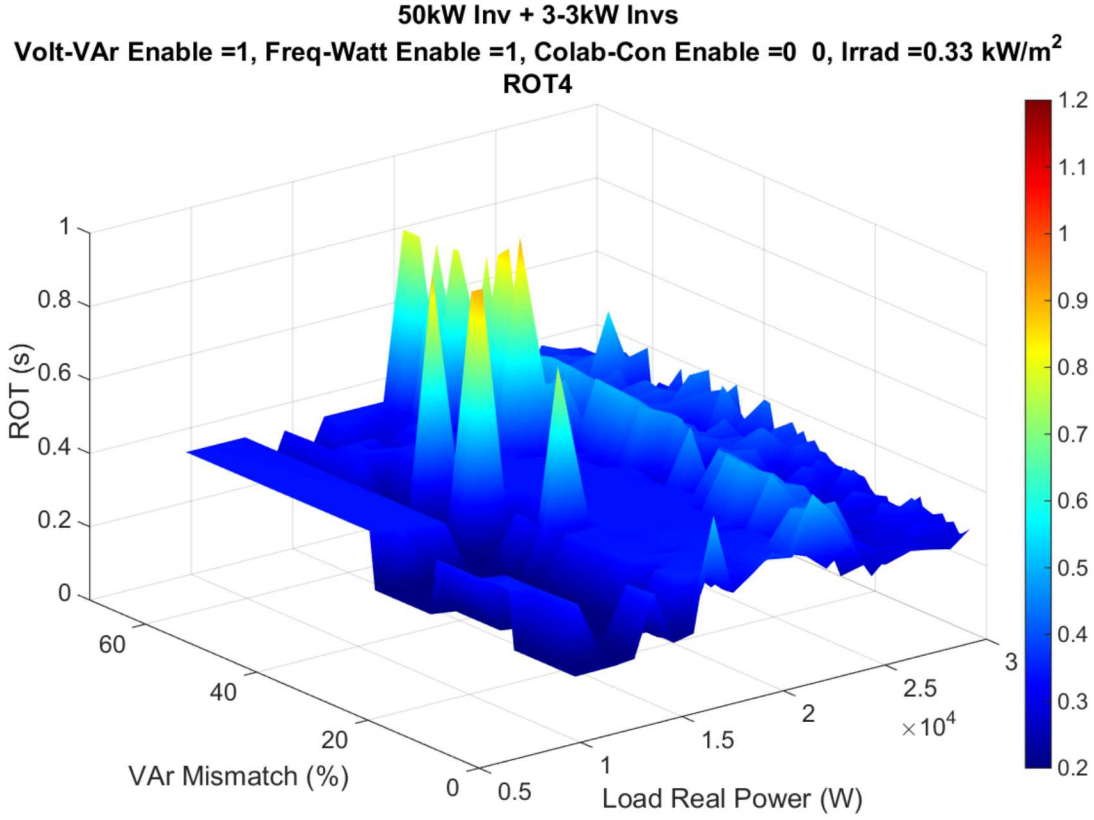

Figure 67. ROTs vs. var mismatch and load real power, 33% irradiance.

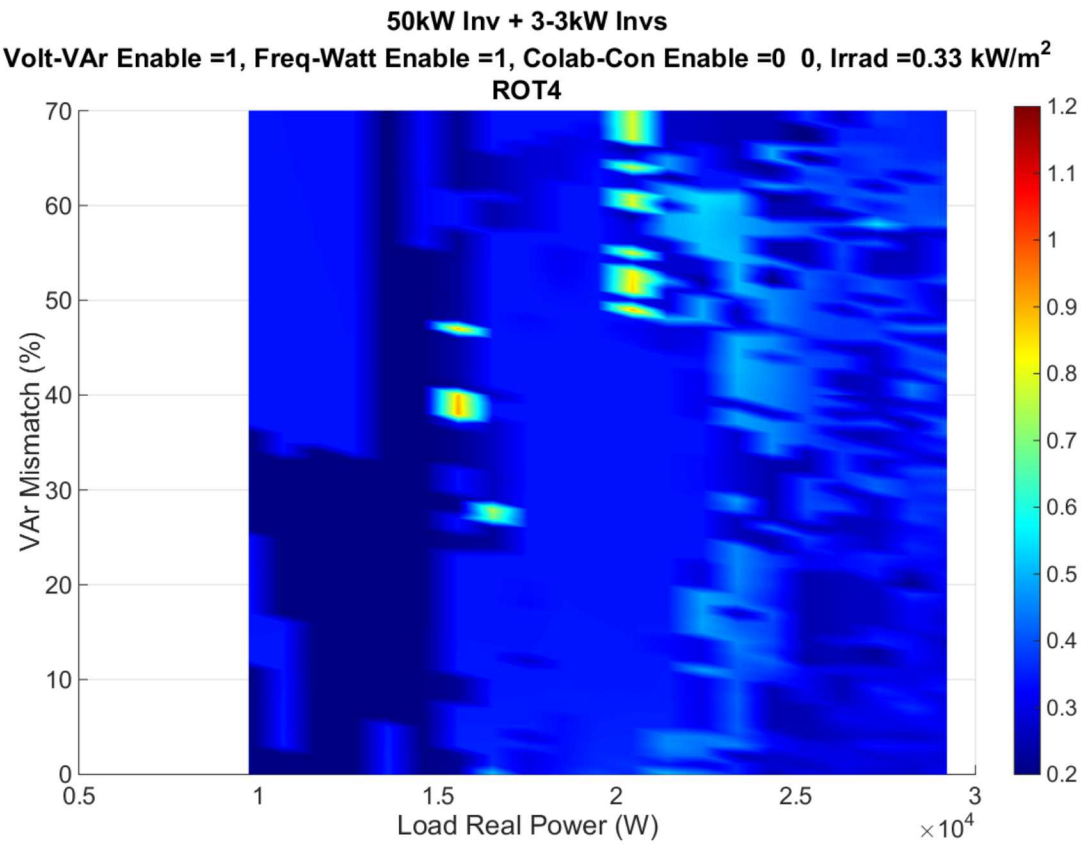

Figure 68. X-y plane view of Figure 67.

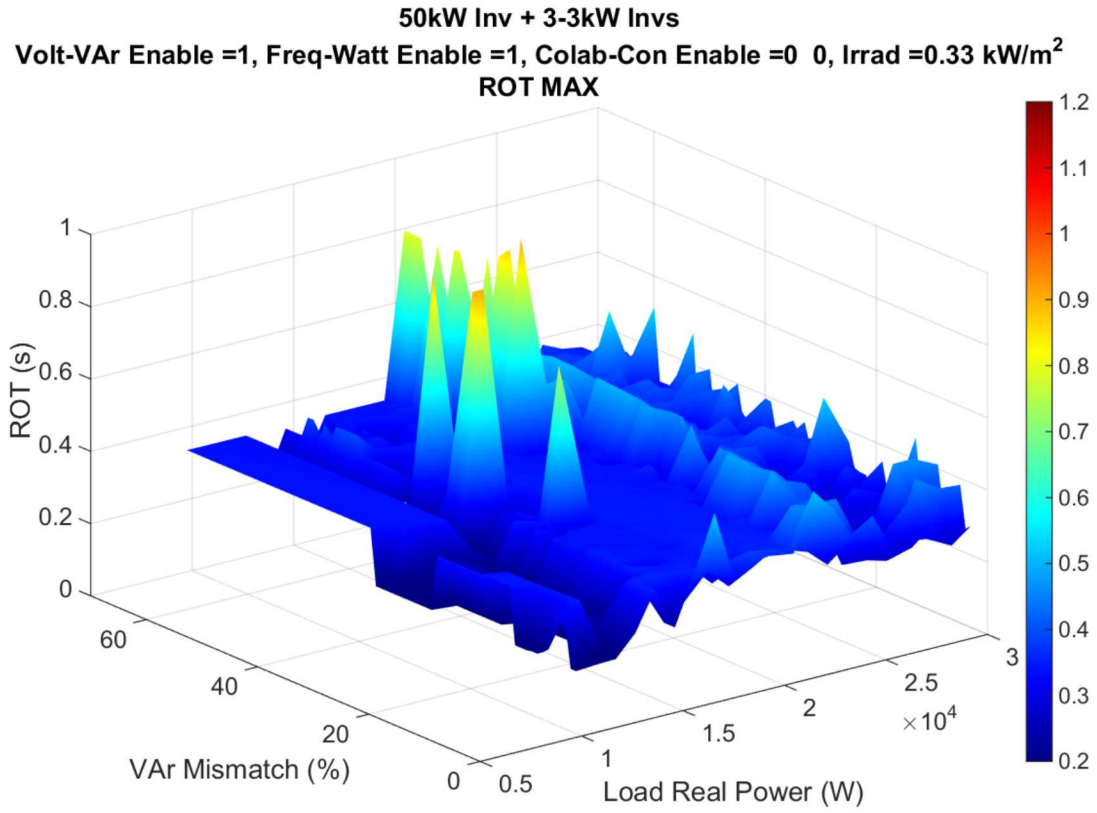

Figure 69. Maximum ROTs observed for each var mismatch-load power pair, 33% irradiance.

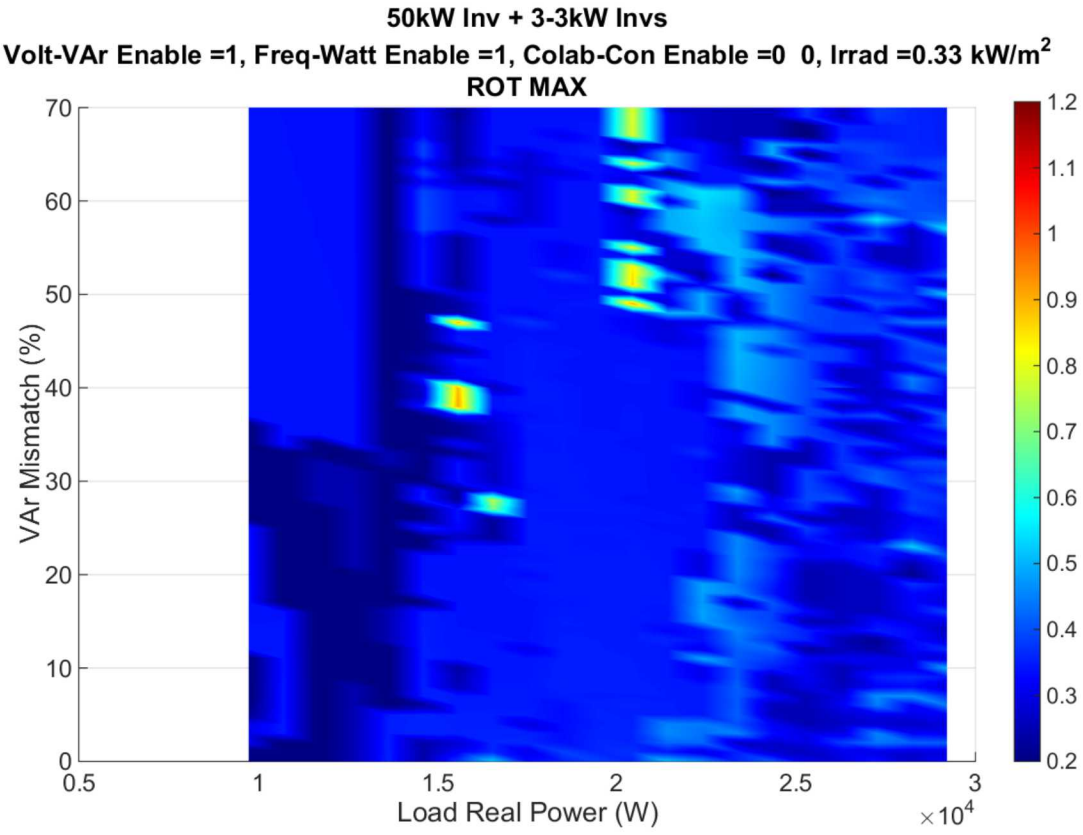

Figure 70. X-y plane view of Figure 69.

A.3.2. Sixty-six Percent Irradiance

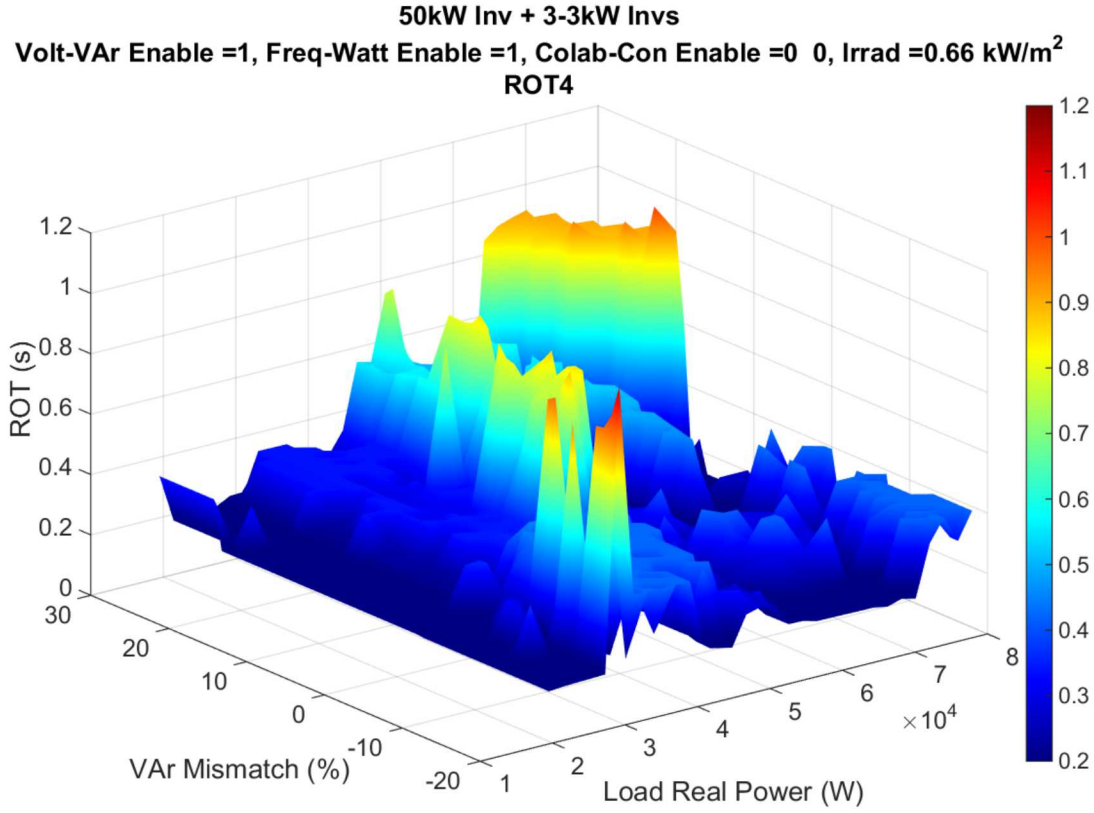

Figure 71. ROTs vs. var mismatch and load real power, 66% irradiance.

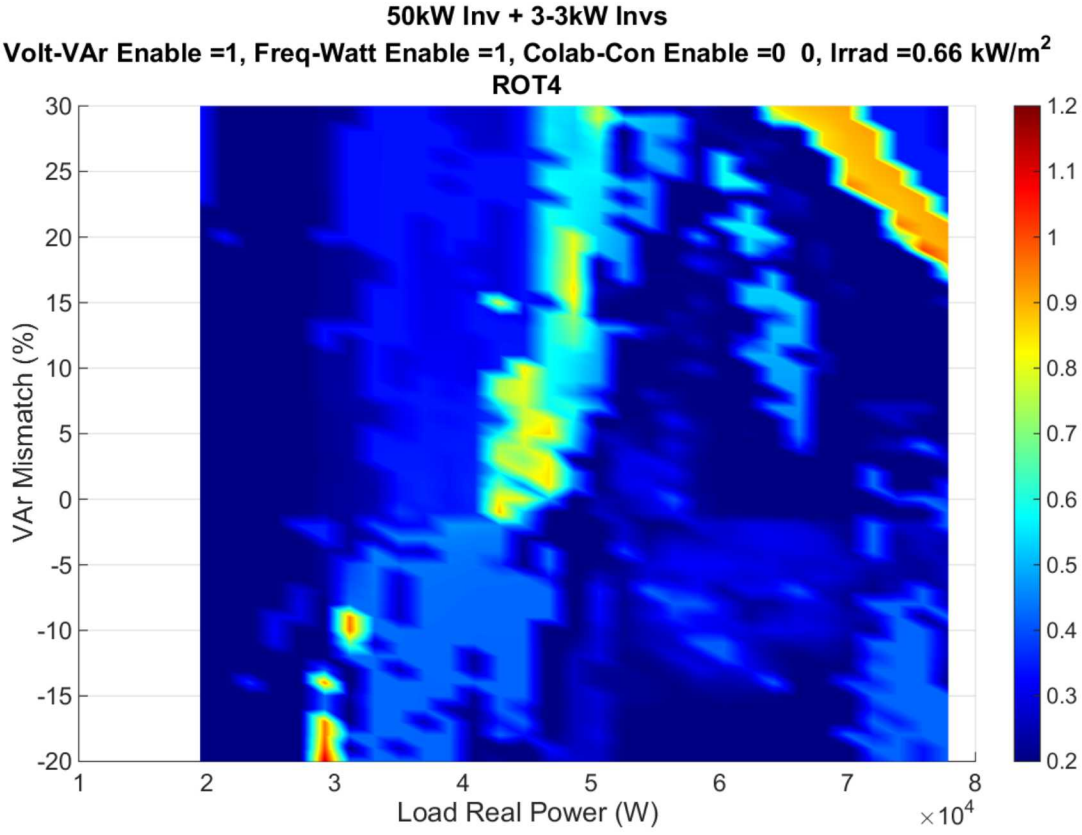

Figure 72. X-y plane view of Figure 71.

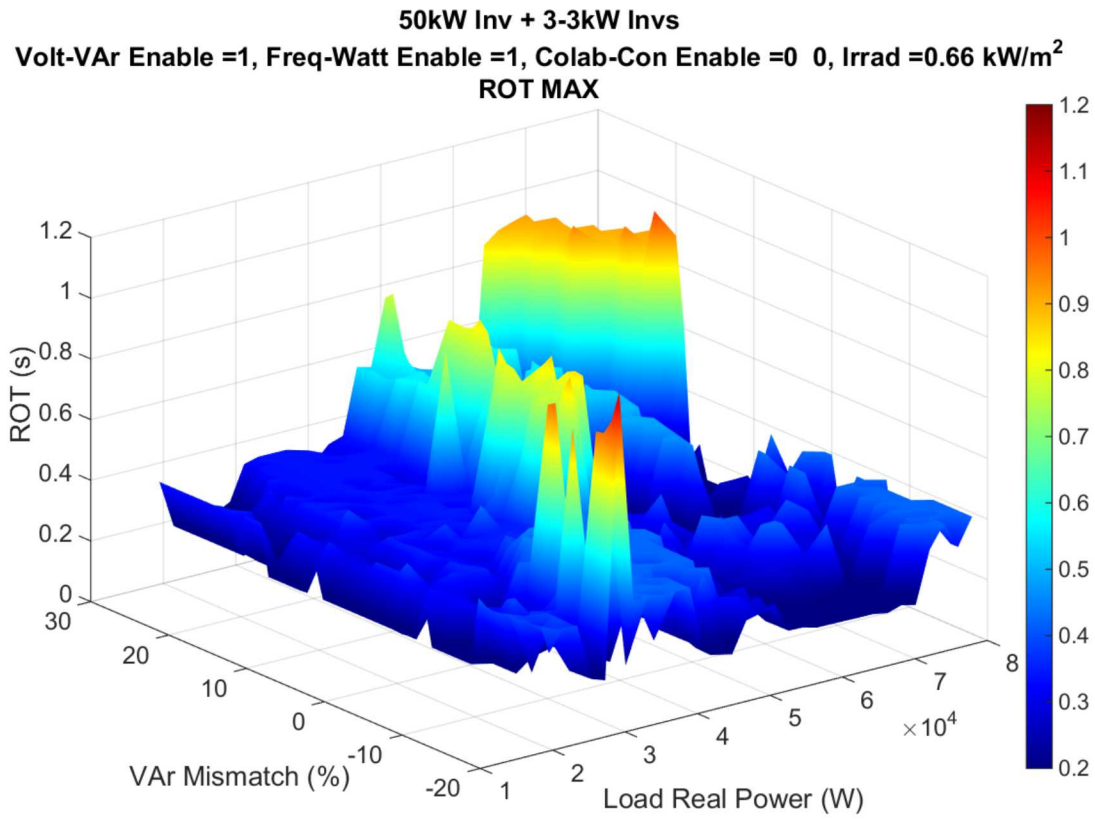

Figure 73. Maximum ROTs observed for each var mismatch-load power pair, 66% irradiance.

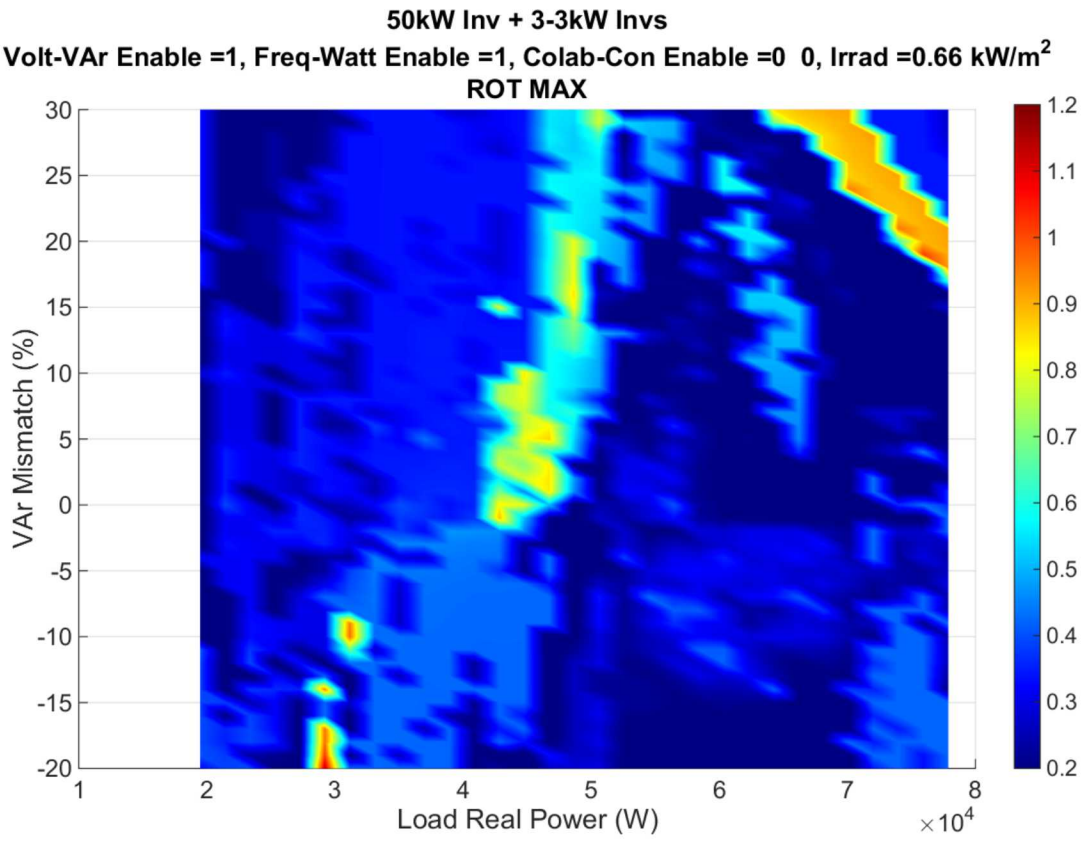

Figure 74. X-y plane view of Figure 73.

A.4.3. One-hundred Percent Irradiance

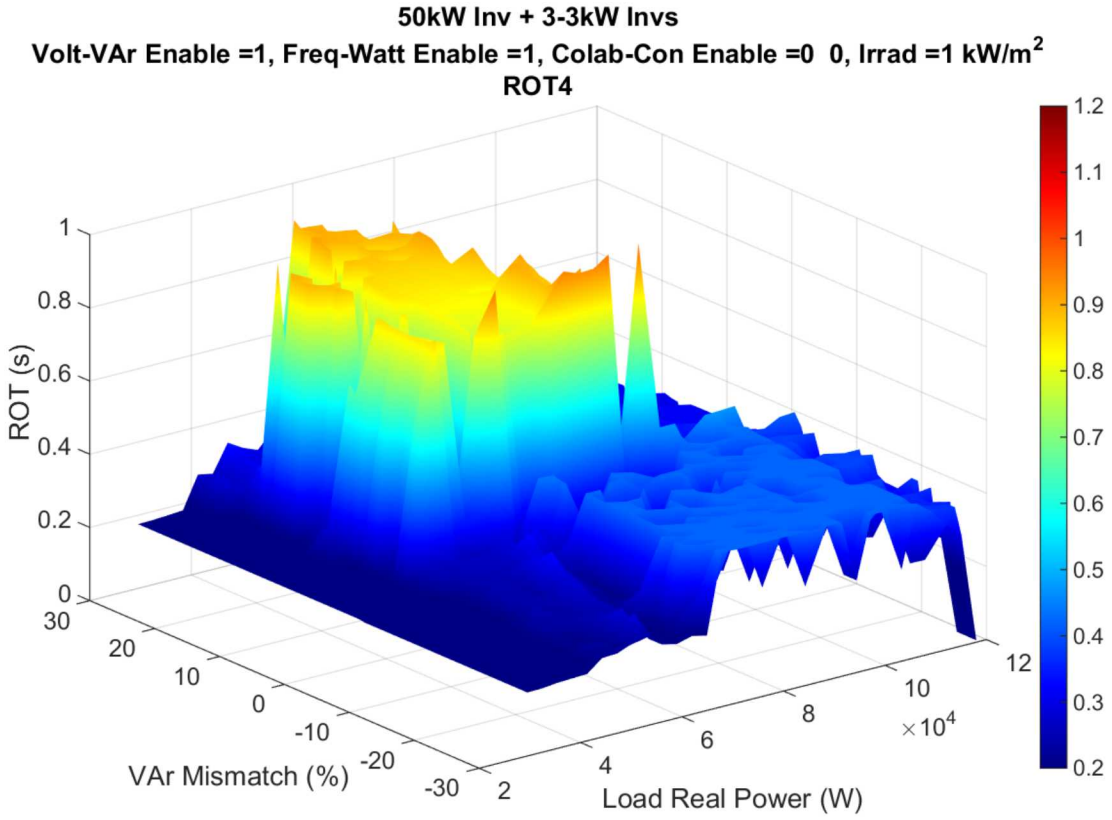

Figure 75. ROTs vs. var mismatch and load real power, 100% irradiance.

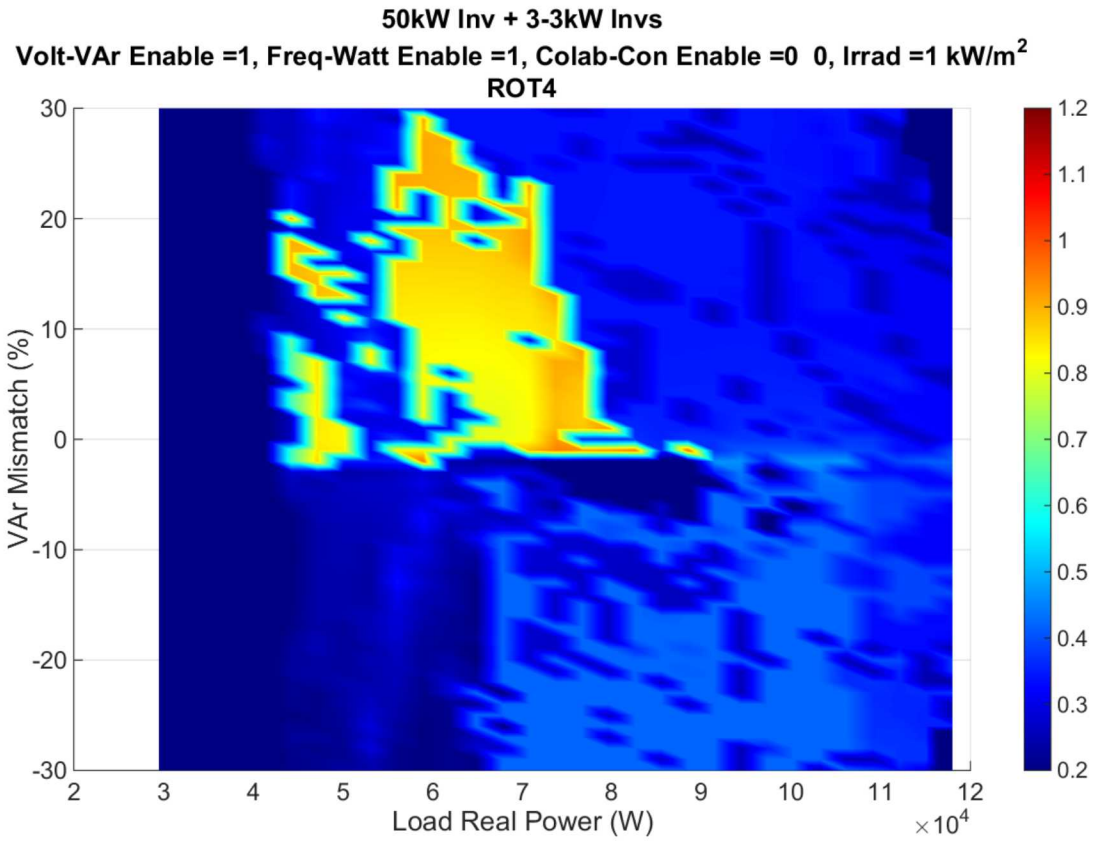

Figure 76. X-y plane view of Figure 75.

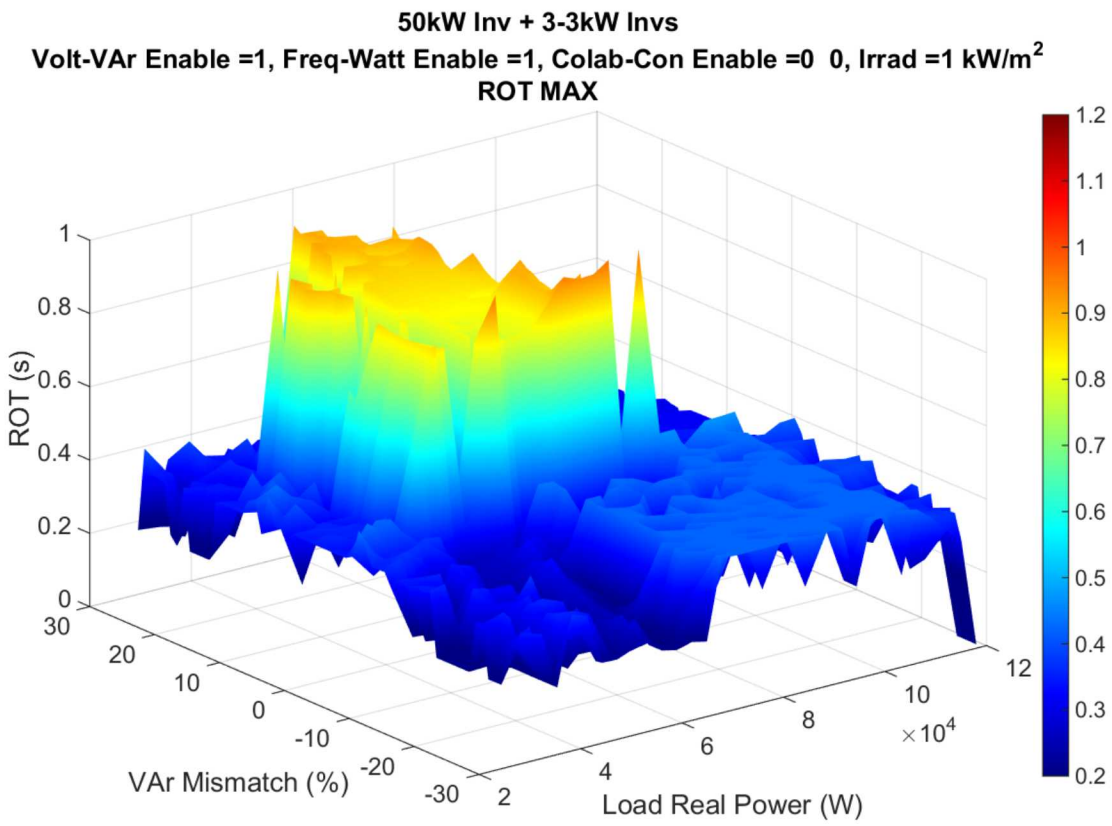

Figure 77. Maximum ROTs observed for each var mismatch-load power pair, 100% irradiance.

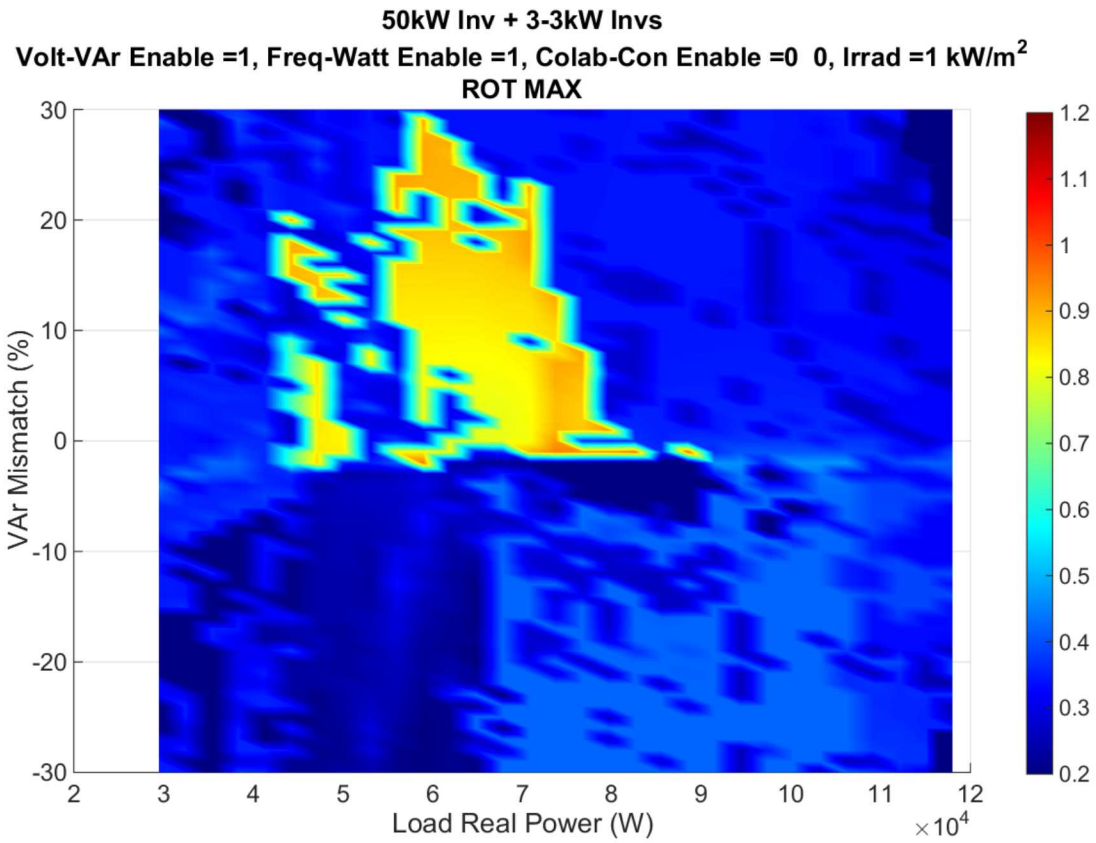

Figure 78. X-y plane view of Figure 77.

A.5. GSFs on, RTs on, CC on

Next, along with the 1547A relays and the GSFs, the collaborative controls were activated, and the results are shown in Figure 79 through Figure 90. On the basis of the maximum ROTs, the effectiveness of the collaborative controls appears to be a function of irradiance: at higher irradiance the collaborative controls reduce the maximum ROTs to values that are close to the base case values, but at lower irradiance there is almost no effect on maximum ROTs.

A.5.1. Thirty-three Percent Irradiance

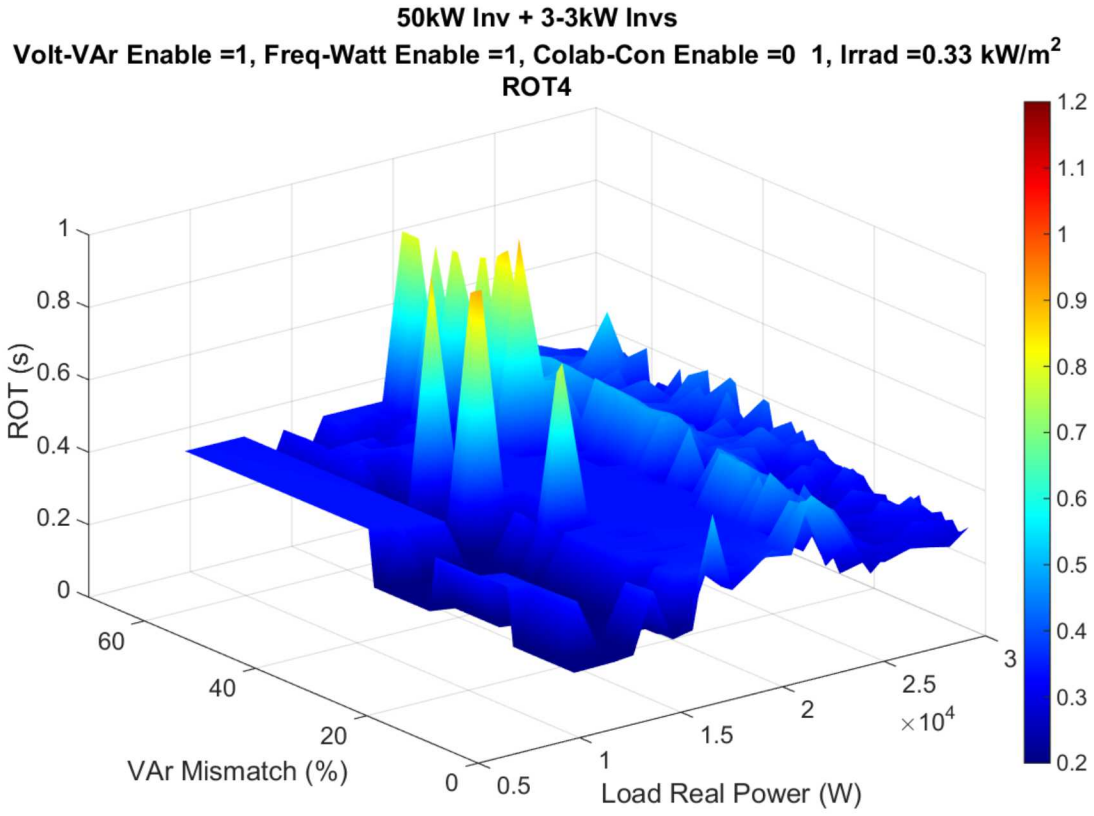

Figure 79. ROTs vs. var mismatch and load real power, 33% irradiance.

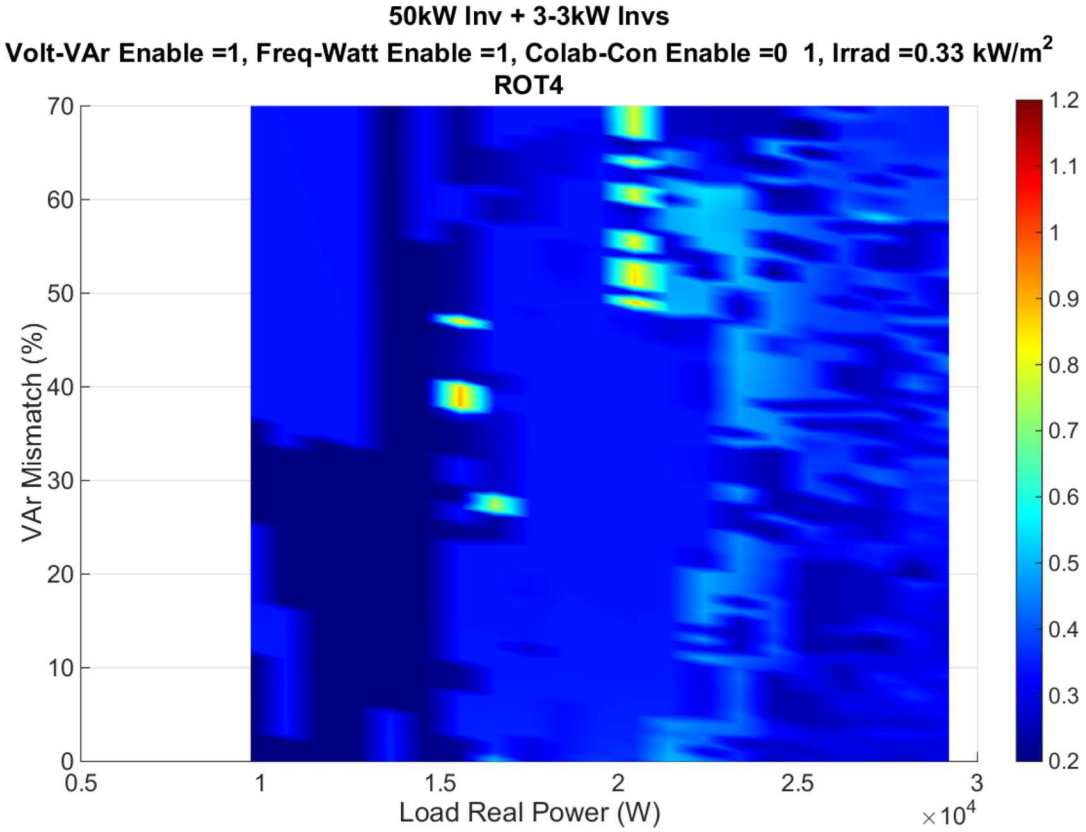

Figure 80. X-y plane view of Figure 79.

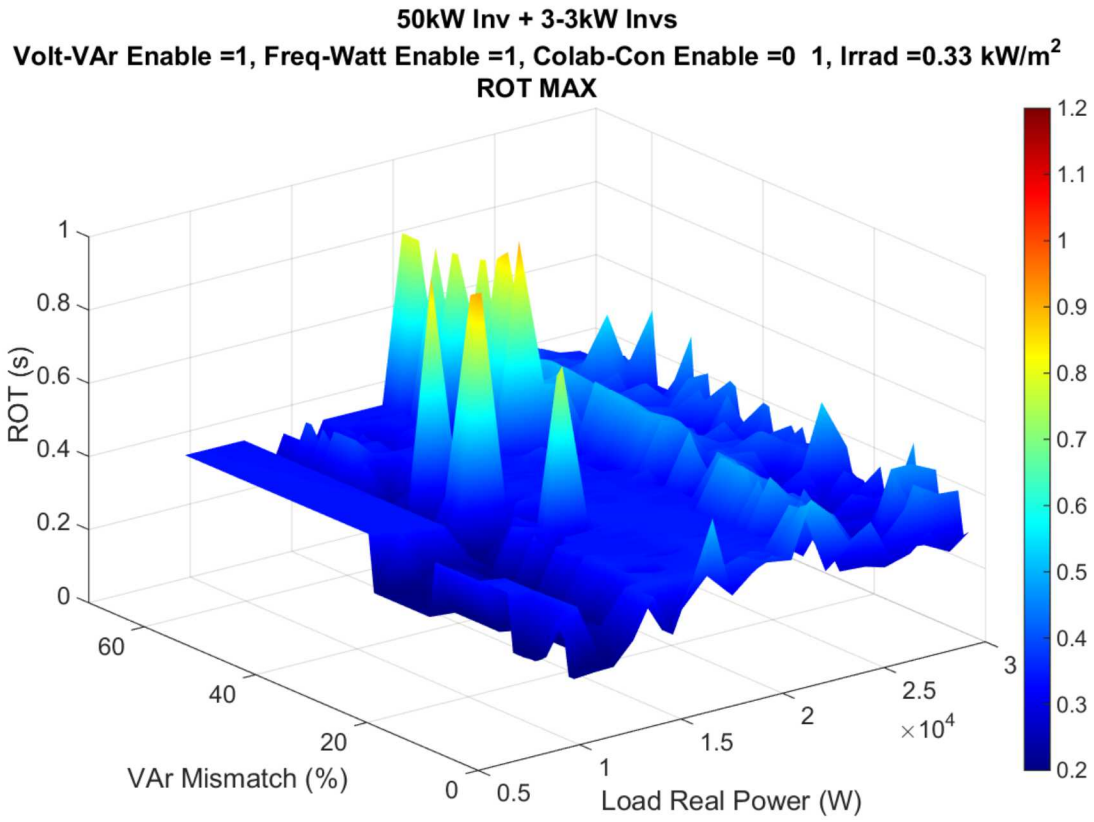

Figure 81. Maximum ROTs observed for each var mismatch-load power pair, 33% irradiance.

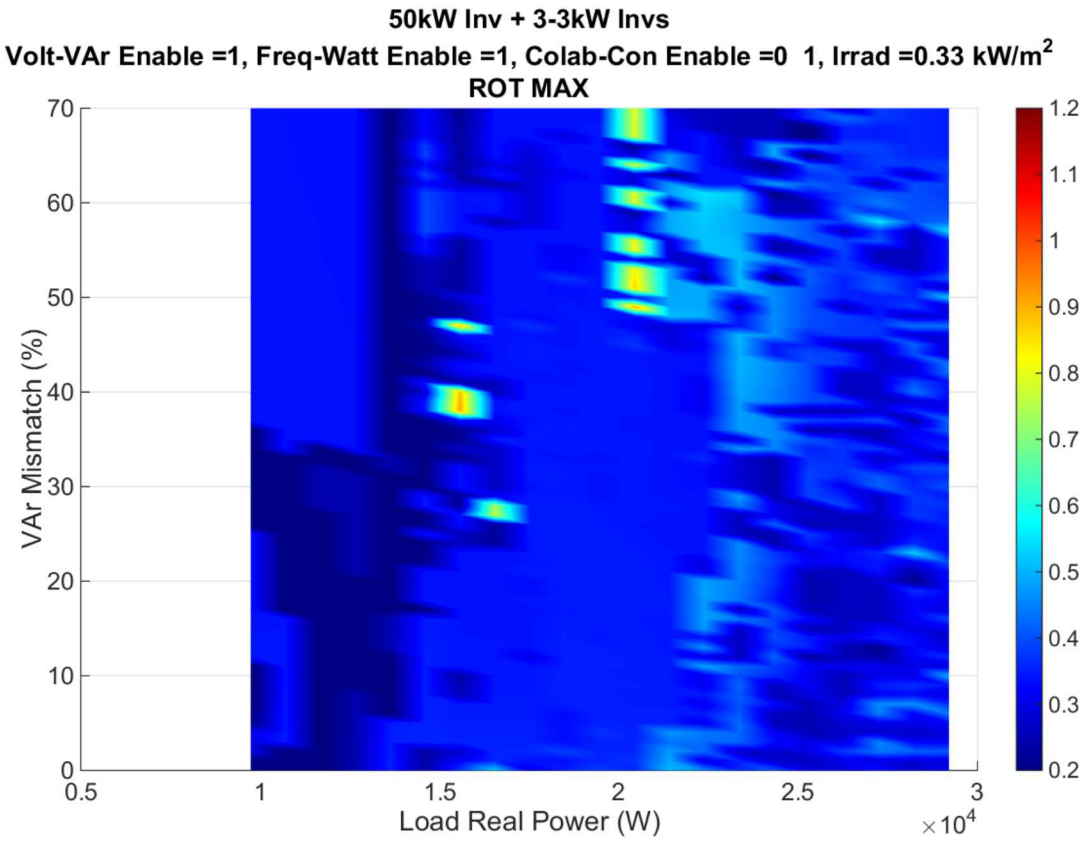

Figure 82. X-y plane view of Figure 81.

A.5.2. Sixty-six Percent Irradiance

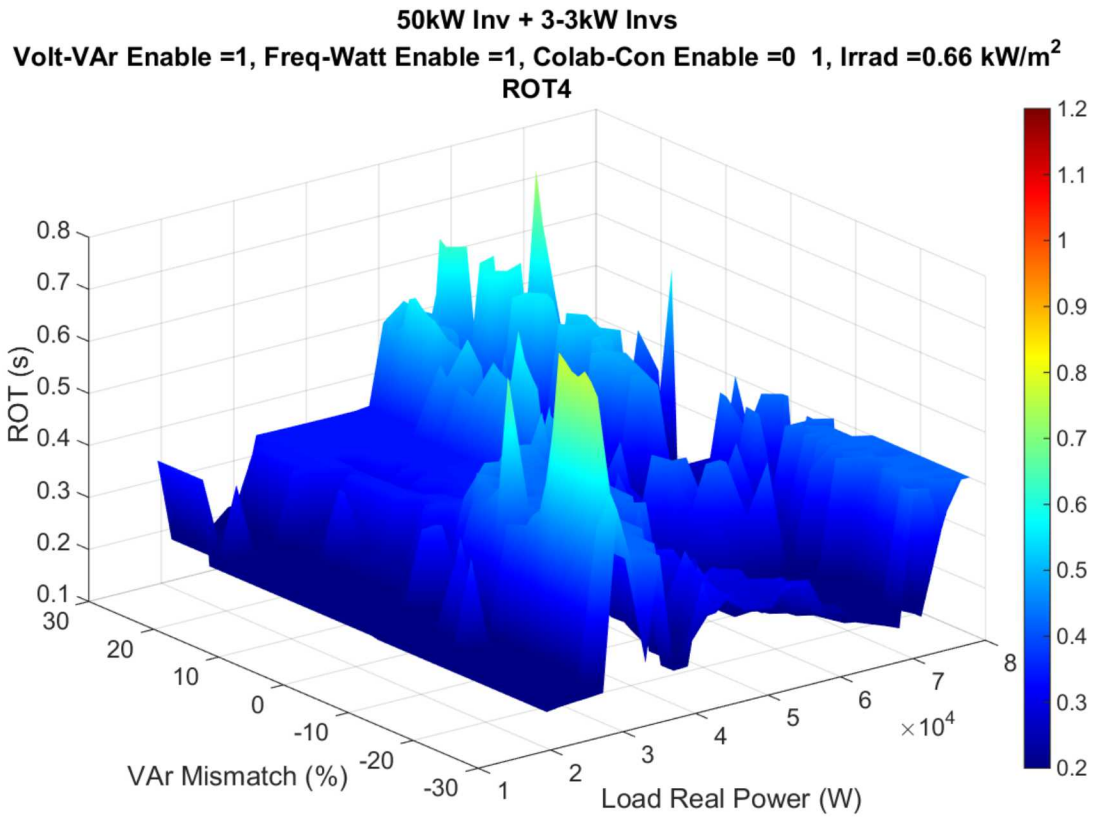

Figure 83. ROTs vs. var mismatch and load real power, 66% irradiance.

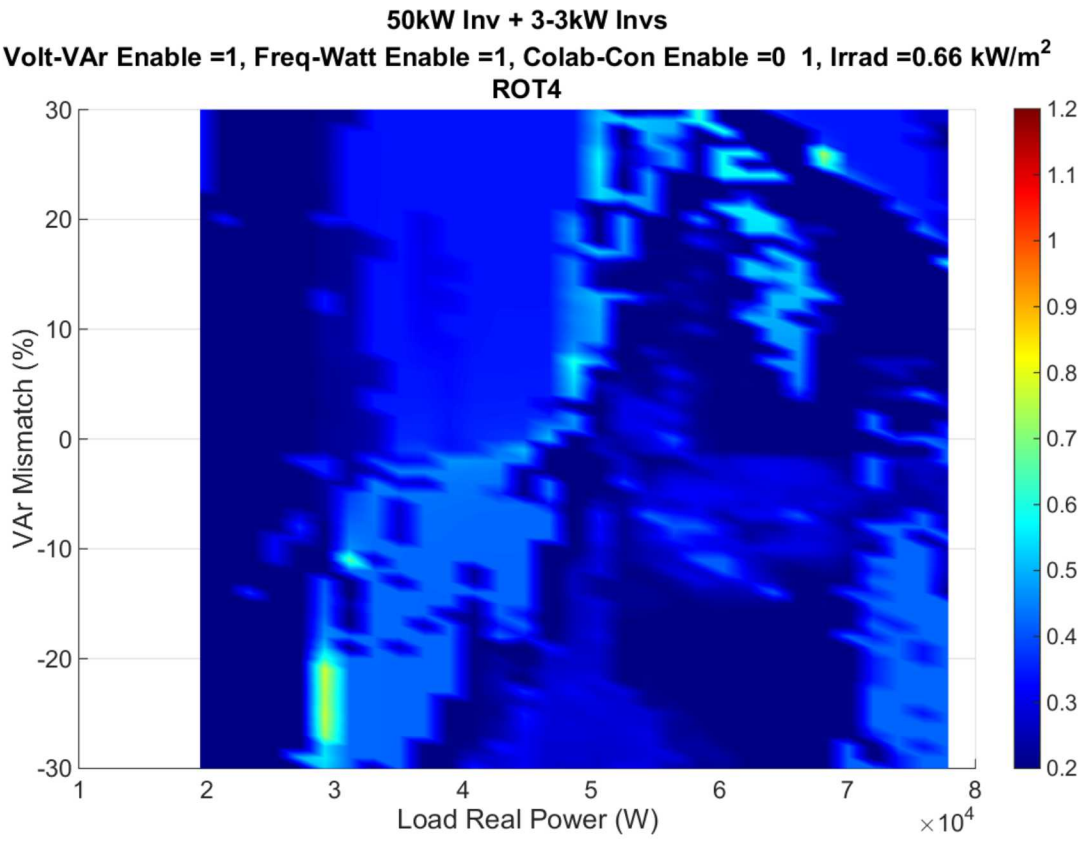

Figure 84. X-y plane view of Figure 83.

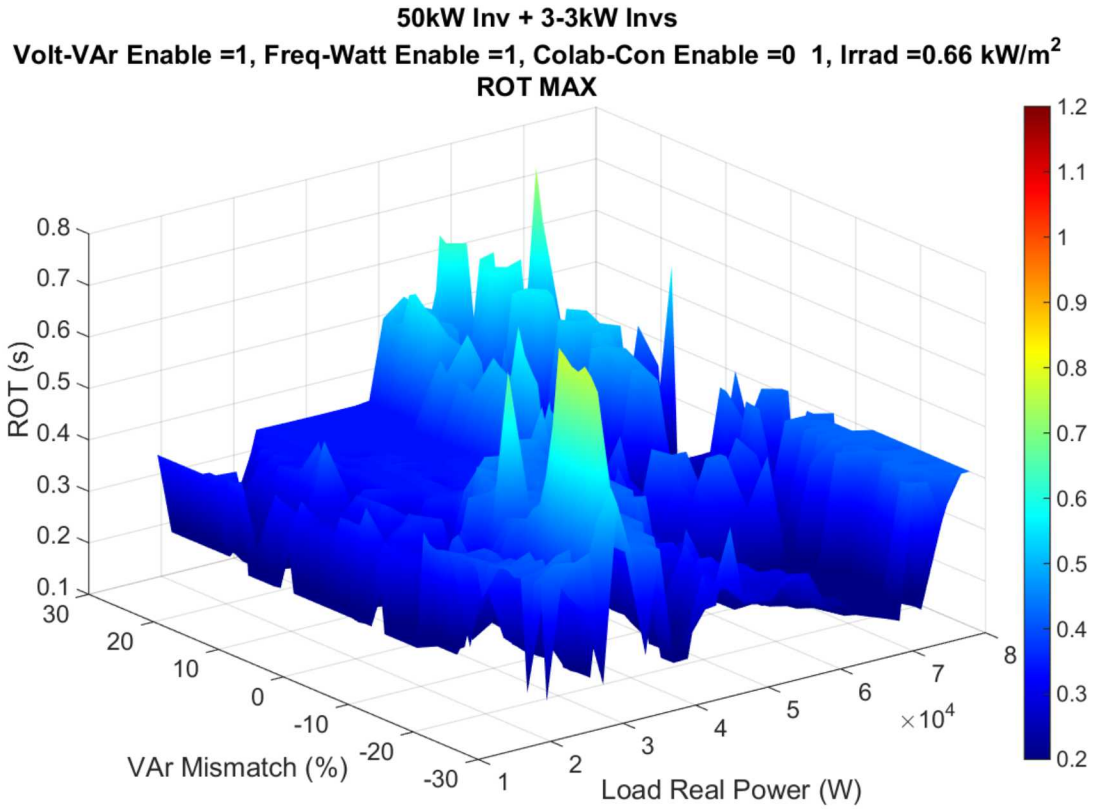

Figure 85. Maximum ROTs observed for each var mismatch-load power pair, 66% irradiance.

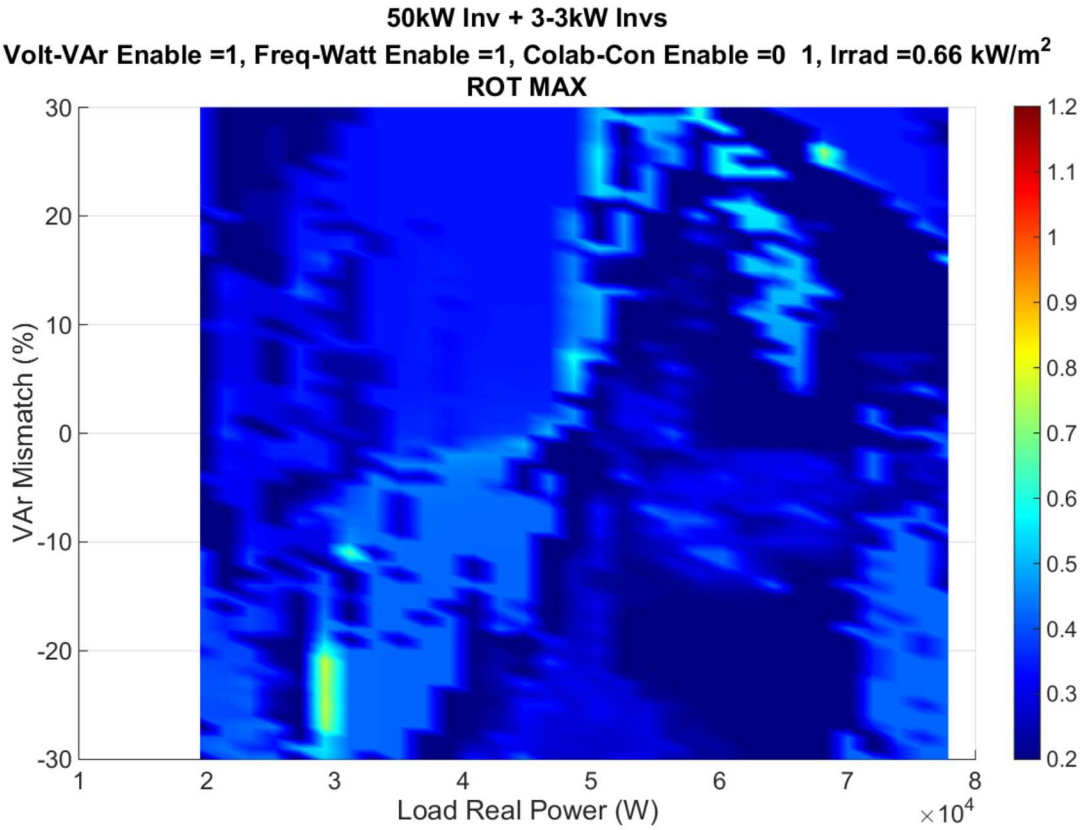

Figure 86. X-y plane view of Figure 85.

A.5.3. One-hundred Percent Irradiance

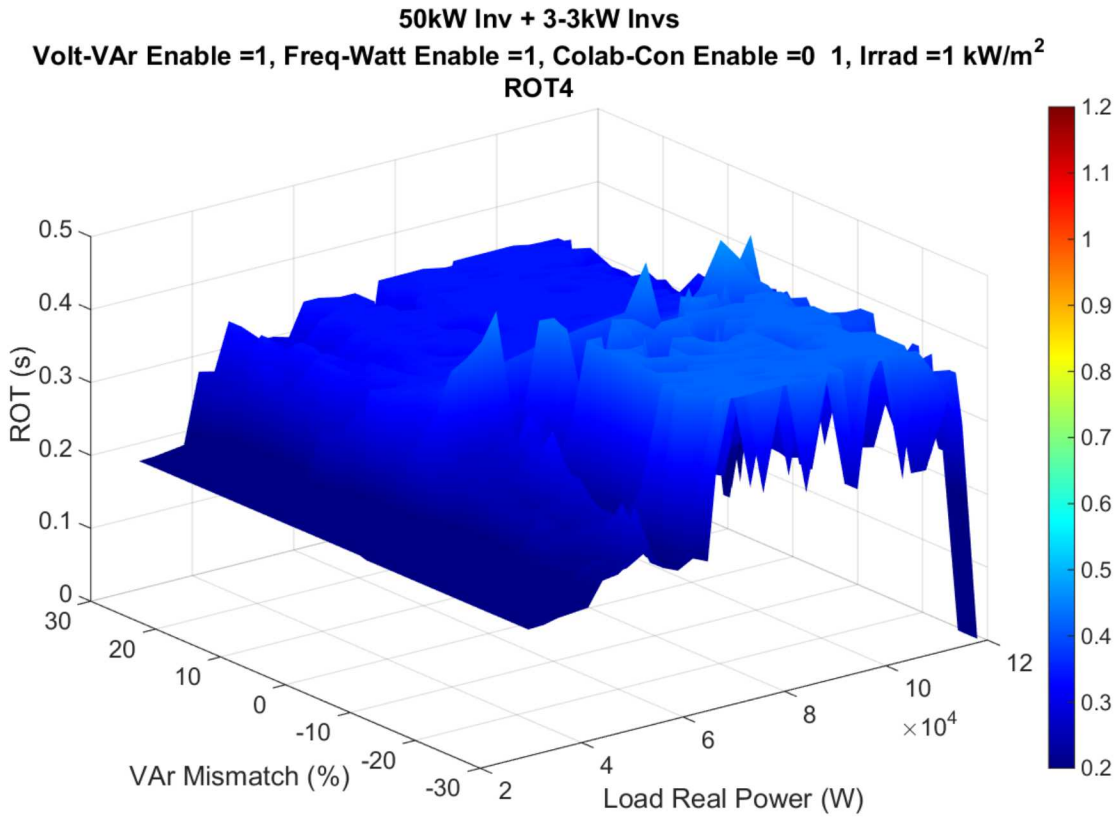

Figure 87. ROTs vs. var mismatch and load real power, 100% irradiance.

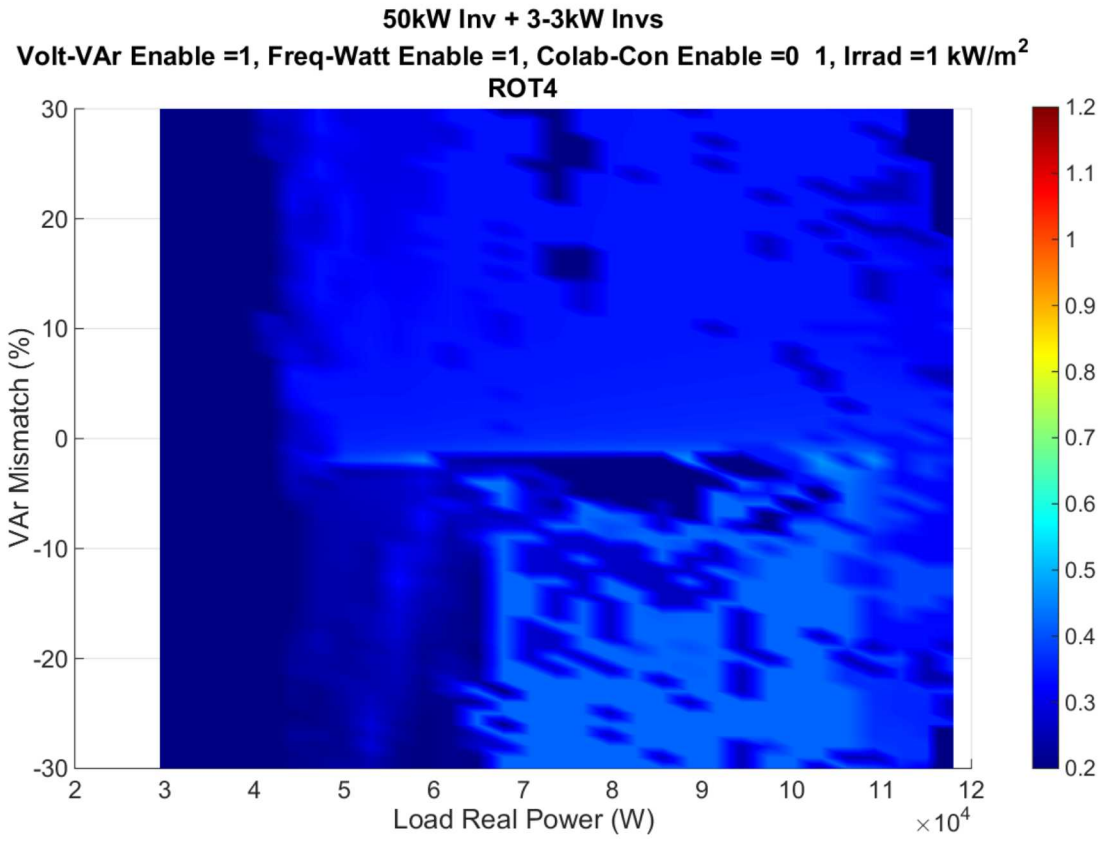

Figure 88. X-y plane view of Figure 87.

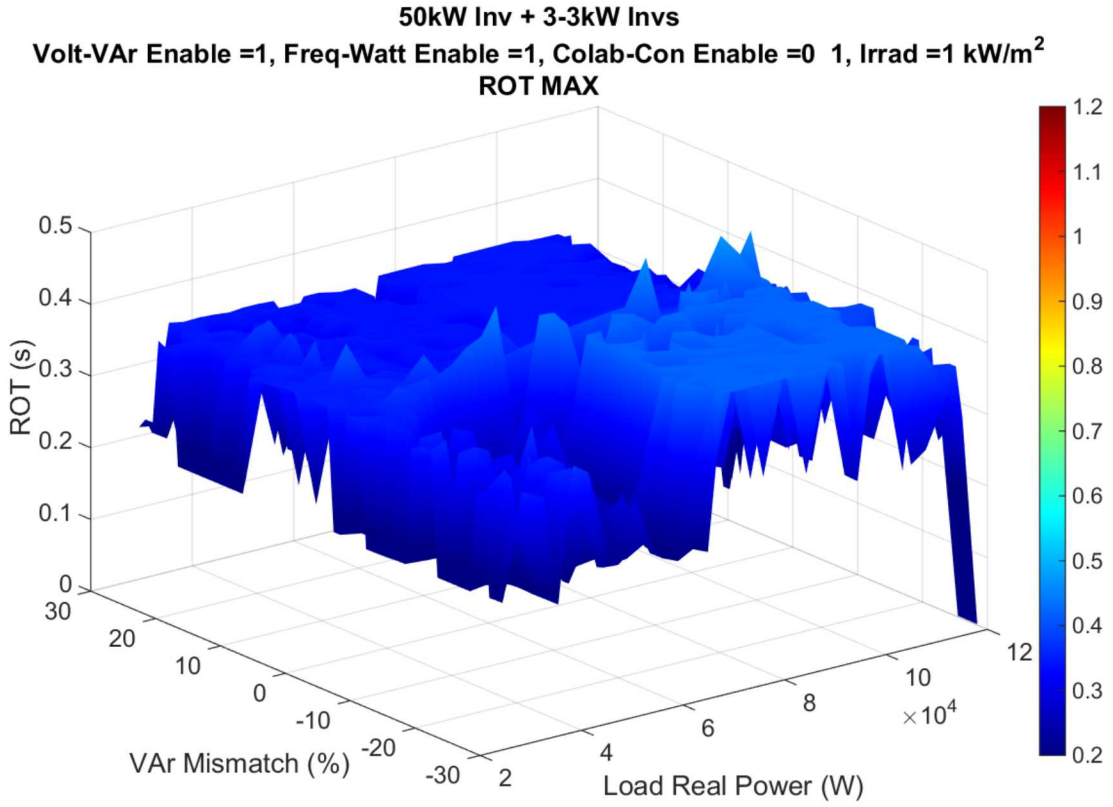

Figure 89. Maximum ROTs observed for each var mismatch-load power pair, 100% irradiance.

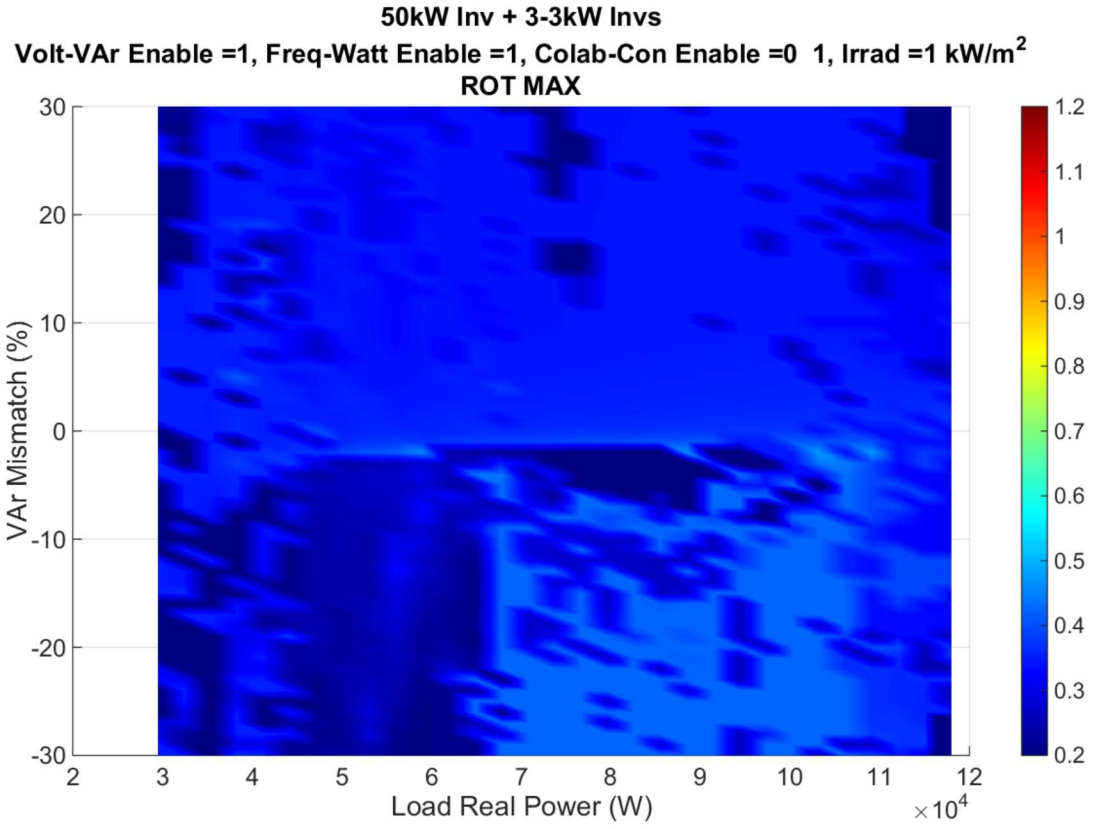

Figure 90. X-y plane view of Figure 89.

DISTRIBUTION

1 Michael Ropp

Northern Plains Power Technologies
807 32nd Avenue
Brookings, SD 57006-4716

http://www.northernplainspower.com/contact.htm

1 Dustin Schutz

Northern Plains Power Technologies
807 32nd Avenue
Brookings, SD 57006-4716

http://www.northernplainspower.com/contact.htm

1 Benjamin Loop

PC Krause and Associates

3000 Kent Ave, Suite C1-100

West Lafayette, IN 47906

http://pcka.com/

1	MS1033	Charles Hanley	Org. 6112
1	MS1033	Abraham Ellis	Org. 6112
1	MS1033	Robert Broderick	Org. 6112
1	MS1033	Sigifredo Gonzalez	Org. 6112
1	MS1152	Jason Neely	Org. 1353
1	MS1152	Steven Glover	Org. 1353

1	MS0899	Technical Library	9536 (electronic copy)

1	MS0161	Legal Technology Transfer Center	11500

Sandia National Laboratories